SUBMITTED TO ApJ Supplements
Preprint typeset using LaTeX style emulateapj v. 03/07/07

arXiv:1402.3029v1 [astro-ph.GA] 13 Feb 2014

STAR CLUSTERS IN M33: UPDATED $UBVRI$ PHOTOMETRY, AGES, METALLICITIES, AND MASSES

Zhou Fan[1] and Richard de Grijs[2,3]

submitted to ApJ Supplements

ABSTRACT

The photometric characterization of M33 star clusters is far from complete. In this paper, we present homogeneous $UBVRI$ photometry of 708 star clusters and cluster candidates in M33 based on archival images from the Local Group Galaxies Survey, which covers 0.8 deg^2 along the galaxy's major axis. Our photometry includes 387, 563, 616, 580, and 478 objects in the $UBVRI$ bands, respectively, of which 276, 405, 430, 457, and 363 do not have previously published $UBVRI$ photometry. Our photometry is consistent with previous measurements (where available) in all filters. We adopted Sloan Digital Sky Survey *ugriz* photometry for complementary purposes, as well as Two Micron All-Sky Survey near-infrared JHK photometry where available. We fitted the spectral-energy distributions of 671 star clusters and candidates to derive their ages, metallicities, and masses based on the updated PARSEC simple stellar populations synthesis models. The results of our χ^2 minimization routines show that only 205 of the 671 clusters (31%) are older than 2 Gyr, which represents a much smaller fraction of the cluster population than that in M31 (56%), suggesting that M33 is dominated by young star clusters (< 1 Gyr). We investigate the mass distributions of the star clusters—both open and globular clusters—in M33, M31, the Milky Way, and the Large Magellanic Cloud. Their mean values are $\log(M_{\rm cl}/M_\odot) = 4.25$, 5.43, 2.72, and 4.18, respectively. The fraction of open to globular clusters is highest in the Milky Way and lowest in M31. Our comparisons of the cluster ages, masses, and metallicities show that our results are basically in agreement with previous studies (where objects in common are available); differences can be traced back to differences in the models adopted, the fitting methods used, and stochastic sampling effects.

Subject headings: catalogs — galaxies: individual (M33) — galaxies: star clusters — globular clusters: general — star clusters: general

1. INTRODUCTION

Since star clusters represent an important component of the galaxies they are associated with, studies of star clusters' stellar populations and age distributions can provide clues to the formation and evolution of their host galaxies. In addition, since populous star clusters are much more luminous than individual stars, they are usually much easier to observe and study.

At a distance of 847 ± 60 kpc—equivalent to a distance modulus of $(m - M)_0 = 24.64 \pm 0.15$ mag (Galleti et al. 2004)—M33 (also known as the Triangulum Galaxy) is the third largest spiral galaxy in the Local Group of galaxies. Since the galaxy is seen relatively face-on, under an inclination of $i = 56^\circ \pm 1^\circ$ (Zaritsky et al. 1989), it is eminently suitable for studies of its star cluster system. At present, the most comprehensive and widely used star cluster catalog is that of Sarajedini & Mancone (2007), which combines data on almost all M33 star clusters published in the literature, including information on their photometry, ages, metallicities, and masses. The latest version[4] (henceforth SM10) includes 595 star clusters and candidates. Park & Lee (2007) found 104 star clusters in *Hubble Space Telescope* (*HST*)/Wide Field and Planetary Camera-2 (WFPC2) archival images, including 32 new objects based on new *HST* observations. Although their observations improved the spatial coverage of the M33 disk, this catalog is still incomplete for the entire disk. These authors found two different star cluster populations on the basis of their sample's color–magnitude diagram (CMD), including a large number of blue clusters and a smaller number of red objects. They also suggested that relatively more red clusters are found in the galaxy's outer regions.

Subsequently, Zloczewski et al. (2008) published a list of 4780 extended sources, including 3554 new cluster candidates observed with the MegaCam instrument on the 3.6 m Canada–France–Hawai'i Telescope (CFHT). However, ∼60% of these clusters are not considered genuine owing to possible misidentifications (San Roman et al. 2009, 2010). Based on *HST*/Advanced Camera for Surveys (ACS)–Wide Field Channel (WFC) observations, San Roman et al. (2009) presented photometry of 161 M33 star clusters, of which 115 were newly identified. Based on their CMDs, they suggested that these clusters' ages were between 0.01 and 1 Gyr, whereas their masses range from $5 \times 10^3 M_\odot$ to $5 \times 10^4 M_\odot$. However these authors also point out that, since their photometry is generally not sufficiently deep to detect the main-sequence turnoff (MSTO), very few of their sample clusters are older than 1 Gyr. Using MegaCam on the CFHT, San Roman et al. (2010) identified 2990 extended sources in M33, 599 of which were new cluster candidates and 204 were previously known clusters.

Electronic address: zfan@bao.ac.cn, grijs@pku.edu.cn
[1] Key Laboratory of Optical Astronomy, National Astronomical Observatories, Chinese Academy of Sciences, 20A Datun Road, Chaoyang District, Beijing 100012, China
[2] Kavli Institute for Astronomy and Astrophysics, Peking University, Yi He Yuan Lu 5, Hai Dian District, Beijing 100871, China
[3] Department of Astronomy, Peking University, Yi He Yuan Lu 5, Hai Dian District, Beijing 100871, China
[4] http://www.mancone.net/m33_catalog/, updated in December 2010.

Based on CMD analysis, these authors suggested that the majority of the clusters have young to intermediate ages, although their sample also includes some old objects. They suggested that a possible M31–M33 interaction some 3.4 Gyr ago may have triggered an epoch of star (cluster) formation in M33.

Comparison of observational spectral-energy distributions (SEDs) with theoretical stellar population synthesis models by application of χ^2 minimization is a widely used technique to estimate ages, metallicities, reddening values, and masses of extragalactic star clusters. This technique has been applied to the cluster systems in, e.g., M31 (Jiang et al. 2003; Fan et al. 2006, 2010; Ma et al. 2007, 2009; Wang et al. 2010), M33 (Ma et al. 2001, 2002a,b,c, 2004a,b), the Large Magellanic Cloud (LMC; e.g., de Grijs & Anders 2006; Popescu et al. 2012; de Grijs et al. 2013), M82 (de Grijs et al. 2003a; Lim et al. 2013), NGC 3310 and 6745 (de Grijs et al. 2003b), as well as for stellar population synthesis model comparisons (de Grijs et al. 2005; Fan & de Grijs 2012).

In this paper, we first obtain photometry for all M33 star clusters in our sample (see Section 2.1 for definition) based on archival images from the Local Group Galaxies Survey (LGGS; Massey et al. 2006). Using photometry in the $UBVRI, ugriz$ (Sloan Digital Sky Survey; SDSS) bands and Two Micron All-Sky Survey (2MASS) JHK magnitudes (Skrutskie et al. 2006)[5] when available, the ages and masses of the star clusters in our sample are estimated by comparison of their observed SEDs with updated PARSEC (version 1.1) isochrones (Bressan et al. 2012). This paper is organized as follows. Section 2 describes the sample selection and $UBVRI$ photometry. In Section 3.1 we describe the simple stellar population (SSP) models used, as well as our method to estimate the cluster ages and metallicities. In Section 3.2 we present the clusters' mass estimates, and we summarize and conclude the paper in Section 4.

2. DATA

2.1. *Sample*

Our sample star clusters are mainly selected from San Roman et al. (2010), whose database is based on observations with the CFHT/MegaCam camera. Their catalog covering the M33 area contains 2990 objects, including background galaxies, confirmed star clusters, and cluster candidates, as well as unknown objects. The catalog provides the positions and $ugriz$ photometry of all objects. Since our focus is on the star clusters, galaxies and unknown objects were eliminated from the catalog, and we subsequently performed photometry for the 803 star clusters and cluster candidates in their catalog.

We used archival $UBVRI$ images from the LGGS, which covers a region of 0.8 deg^2 along the galaxy's major axis. The images we used consisted of three separate but overlapping fields with a scale from $0.261''$ pixel^{-1} at the center to $0.258''$ pixel^{-1} in the corners of each image. The field of view of each mosaic image is 36×36 arcmin^2. The observations were taken with the Kitt Peak National Observatory 4 m telescope between August 2000 and September 2002. The median seeing of the LGGS images is $\sim 1''$. Although Ma (2012) inspected the images and obtained $UBVRI$ photometry for all star clusters and unknown objects in Sarajedini & Mancone (2007) based on archival LGGS images, there are still hundreds of star clusters from San Roman et al. (2010) in this field which do not have published $UBVRI$ photometry. Therefore, here we only perform photometry of the clusters in the LGGS images following the identifications of San Roman et al. (2010). We employed the latest version of SExtractor[6] (Bertin & Arnouts 1996) to find the sources in the images and match them to the coordinates of our 803 sample star clusters and candidates. Eventually, we detected 588 clusters and candidates with quality FLAGS = 0, which indicates that there are no problems associated with these objects (i.e., no contamination by nearby sources or saturation effects) in the LGGS images.

To supplement these data, we also include 120 confirmed star clusters from the updated (2010) version of Sarajedini & Mancone (2007, SM10), which were not included in San Roman et al. (2010). Thus, the number of clusters in our final sample is 708.

Figure 1 shows the spatial distribution of all sample clusters and candidates in the M33 field. The three data frames represent the field of view of the Massey et al. (2006) data, and the large square outline covers the observed field of San Roman et al. (2010). The large green ellipse delineates D_{25}, i.e., it corresponds to the $\mu_B = 25$ mag arcsec^{-2} isophote (Boissier et al. 2007). The yellow solid bullets and green open circles are, respectively, the confirmed star clusters and cluster candidates from San Roman et al. (2010). The combined total number of clusters and cluster candidates is 588. These latter clusters have been cross-identified in the Massey et al. (2006) image, which we will focus on here; we do not consider clusters outside of the boundaries of the Massey et al. (2006) image. The orange symbols represent the 120 star clusters identified by SM10 but not included in San Roman et al. (2010). It is clear that most star clusters and candidates are associated with and projected onto the galaxy's disk (i.e. inside the galaxy's D_{25}).

2.2. *Integrated photometry*

Prior to this work, Massey et al. (2006) compiled point-spread-function (PSF) photometry for 146,622 stars (point sources) in the M33 fields, with photometric uncertainties of $< 10\%$ at $UBVRI \sim 23$ mag. However, there are no relevant discussions of the extended sources (e.g., star clusters and galaxies) in the published LGGS papers. Recently, Ma (2012) derived aperture photometry of 392 star clusters and unknown objects in the catalog of Sarajedini & Mancone (2007) in the $UBVRI$ bands. However, there are still several hundred M33 star clusters and cluster candidates identified by San Roman et al. (2010) which lack LGGS photometry in the $UBVRI$ bands.

To obtain additional photometric information for the star clusters, we carried out photometric measurements of our sample M33 clusters and candidates. SExtractor was applied to the LGGS images in all of the $UBVRI$ bands to derive supplementary and homogeneous photometry. The SExtractor code pro-

[5] http://www.ipac.caltech.edu/2mass/

[6] http://www.astromatic.net/software/sextractor; version 2.8.6 was updated on 5 October 2009.

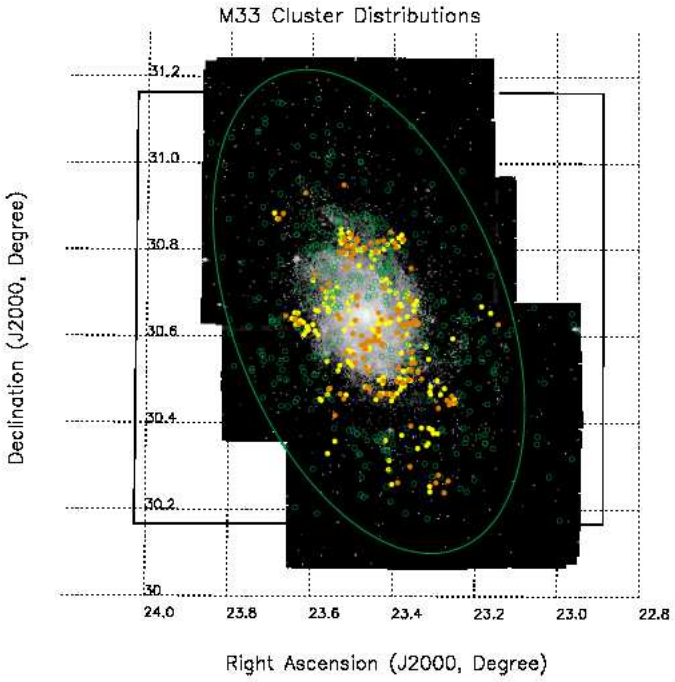

FIG. 1.— Spatial distribution of our star clusters and cluster candidates. The yellow solid bullets (confirmed clusters) and green open circles (candidate clusters) are from San Roman et al. (2010); we determined their cross-identifications in the Massey et al. (2006) image. The orange symbols represent the clusters identified by SM10 but not included in San Roman et al. (2010). The three data frames are the fields of view of Massey et al. (2006), whereas the large square outline covers the observed field of San Roman et al. (2010).

vides isophotal magnitudes corrected for the flux missed by isophotal-magnitude determination, MAG_ISOCOR. This approach works well for stars but poorly for elliptical (galaxy) profiles with broader wings. SExtractor also delivers automatic aperture photometry measurements of galaxies based on the first-moment algorithm of Kron (1980), MAG_AUTO. The MAG_BEST magnitudes can be automatically mapped onto MAG_AUTO if neighbors cannot bias the photometry by more than 10%. In all other cases, MAG_BEST is set to equal MAG_ISOCOR, because the latter measurements are not significantly affected by nearby sources. Thus, we adopted the MAG_BEST magnitudes as our final instrumental magnitudes. As a consequence, we do not need to choose the size of the aperture used. The instrumental magnitudes were calibrated in the standard Johnson–Kron–Cousins $UBVRI$ system by comparing the published magnitudes of stars from Massey et al. (2006), who calibrated their photometry using Landolt (1992) standard stars, with our instrumental magnitudes. Since the magnitudes in Massey et al. (2006) are given in the Vega system, our photometry is also tied to that system. The calibration errors range from ~ 0.01 to ~ 0.03 mag in the $UBVRI$ bands, with more than 300 secondary standard stars available in each field. Finally, we obtained photometry for 708 objects, with 387, 563, 616, 580, and 478 sources in the individual $UBVRI$ bands, respectively, of which 276, 405, 430, 457, and 363 star clusters and candidates do not have previously published photometry.

Table 1 of Massey et al. (2006) shows that the seeing conditions under which the LGGS fields were obtained ranged from $0''.8$ to $1''.2$ in all filters; for most fields the prevailing seeing was around $1''.0$. In their table 3, these authors compared the differences in their calibrated photometry between overlapping fields using well-exposed, isolated stars and found that the median difference was several millimagnitudes. Our photometry has been calibrated relative to that of Massey et al. (2006). We compared the photometric measurements of those clusters that were located in the regions of overlap between different frames and and found differences of only a few $\times 0.01$ mag. While these differences are a little larger than those reported by Massey et al. (2006), this is not unexpected, since star clusters often have more extended and more complicated profiles than stars. For clusters with more than one photometric measurement in overlapping fields, we adopted the magnitude associated with the smallest statistical uncertainty.

Table 1 lists our new broad-band $UBVRI$ magnitudes and the corresponding photometric errors. The latter combine the errors associated with MAG_BEST with those related to the flux calibration, as

$$\sigma_i^2 = \sigma_{\mathrm{best},i}^2 + \sigma_{\mathrm{calib},i}^2, \quad (1)$$

where i represents any of the $UBVRI$ bands, whereas σ_{best} and σ_{calib} correspond to the photometric uncertainties associated with the MAG_BEST magnitudes and flux calibration, respectively.

Since SExtractor applies apertures of different sizes to obtain MAG_BEST magnitudes, depending on the size of the object of interest, we applied aperture growth-curve corrections to all photometric measurements. In fact, although the MAG_BEST values represent the optimum magnitudes in the presence of neighboring sources, they may still systematically underestimate the total flux of extended sources by about 10% (McIntosh et al. 2005; Caldwell et al. 2008). Therefore, we corrected for this 'lost' flux using the appropriate aperture corrections. We used an approximate aperture radius $r = (a^2 + b^2)^{1/2}$ for our photometry by combining half the major axis, a, and half the minor axis, b. We then calculated the aperture corrections on the basis of template growth curves (derived from the LGGS data) that were most representative of our extended star clusters. The aperture corrections are slightly different for different filters and different images: on average, they are ~ 0.36 mag for $r \leq 3$ pix, ~ 0.10 mag for $3 < r \leq 5$ pix, ~ 0.05 mag for $5 < r \leq 7$ pix, and ~ 0.02 mag for $r > 7$ pix. The maximum aperture used for our photometry is 7.19 pix ($1''.85$). We therefore used $r = 7$ pix $\approx 1''.8$ as the radius for our full sample's aperture corrections.

Many previous studies (e.g., San Roman et al. 2009, 2010; Park & Lee 2007) used a fixed aperture of $r = 2''.2$ for the photometry of all clusters and a smaller aperture, $r \approx 1''.5$, for color measurements. For comparison, based on the sizes and (elliptical) profiles of the clusters in our sample, we used apertures of $r \leq 1''.5$ for the photometry of 95% of our sample clusters. Nevertheless, the apertures adopted in both this article and previous studies result in essentially the same photometry and colors. The object names we use follow the naming convention of San Roman et al. (2010) and SM10.

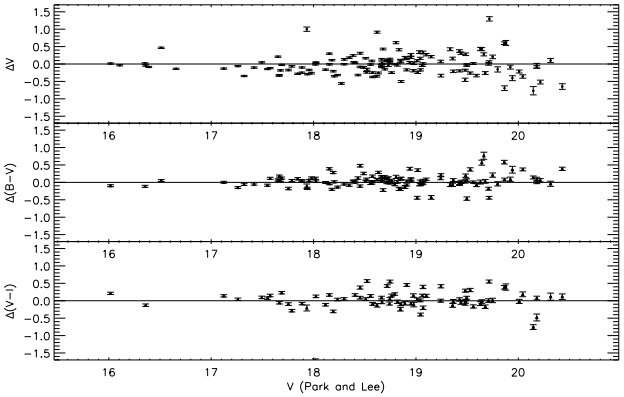

FIG. 2.— Comparisons of our photometric measurements with those of Park & Lee (2007) for all star clusters in common. The error bars represent a combination (addition in quadrature) of the uncertainties associated with our photometry and those from the literature.

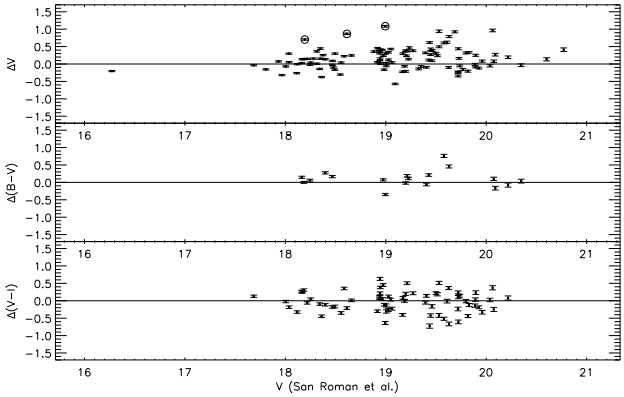

FIG. 3.— As Fig. 2 but for our photometry and that of San Roman et al. (2009). Since San Roman et al. (2009) do not provide their photometric uncertainties, the error bars only reflect the uncertainties in our photometry. The open circles are objects 105, 110, and 148 of San Roman et al. (2009).

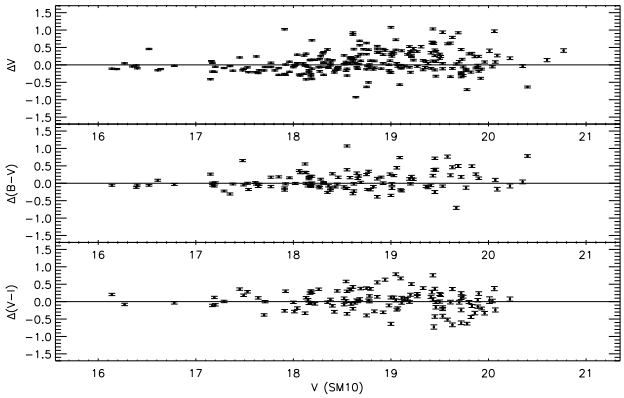

FIG. 4.— As Fig. 3 but for our photometry and that of SM10. Since SM10 do not provide their photometric uncertainties, the error bars only reflect the uncertainties associated with our photometry.

Previously, Park & Lee (2007) determined integrated BVI aperture photometry for 104 M33 star clusters using (mainly) CFHT images, as well as supplementary *HST*/WFPC2 archival images. Charge-transfer (in)efficiency (CTE) corrections were applied to the *HST* magnitudes, and all photometry has been converted to the standard Johnson–Cousins system. Figure 2 compares our photometry with that of Park & Lee (2007), which shows that there is little systematic difference: $\Delta V = 0.006 \pm 0.001$ mag (in the sense, this paper minus Park & Lee 2007), with $\sigma = 0.349$ mag. Both our $(B-V)$ and $(V-I)$ colors show good agreement with Park & Lee (2007) down to the faintest magnitudes. The differences between both sets of photometry are $\Delta(B-V) = 0.049 \pm 0.004$ mag with $\sigma = 0.189$ mag, and $\Delta(V-I) = 0.025 \pm 0.003$ mag, $\sigma = 0.302$ mag.

Figure 3 shows the difference between our photometry and that of San Roman et al. (2009), whose database includes integrated photometry of 161 star clusters in M33 based on *HST*/ACS–WFC observations. The photometric uncertainties associated with the mean offsets are defined as $\sigma/\sqrt{N}$, where σ is the standard deviation and N the number of data points. CTE corrections were applied and the photometry has been converted to the standard Johnson–Cousins system. Figure 3 shows comparisons of the respective sets of magnitudes and colors. Since San Roman et al. (2009) do not provide their photometric uncertainties, the error bars in Fig. 3 reflect our photometric uncertainties only. Our V-band magnitudes are in good agreement with those of San Roman et al. (2009) down to the faintest magnitudes: $\Delta V = 0.162 \pm 0.016$ mag (this paper minus San Roman et al. 2009), with $\sigma = 0.304$ mag. However, a few objects have magnitudes that are > 0.5 mag fainter in our database than in the tables of San Roman et al. (2009), i.e., objects 105, 110, and 148 of San Roman et al. (2009), which are marked with open circles in Fig. 3. We checked the V-band images and found that all of these objects are located close to a few fainter neighboring sources, which are treated as independent objects in our photometry but they were regarded as stars belonging to the same cluster by San Roman et al. (2009). Both our $(B-V)$ and $(V-I)$ colors show good agreement with San Roman et al. (2009). The differences between our measurements and their photometry are $\Delta(B-V) = 0.106 \pm 0.025$ mag with $\sigma = 0.233$ mag and $\Delta(V-I) = -0.065 \pm 0.008$ mag, $\sigma = 0.361$ mag.

We also compared our photometry with the measurements of SM10, who assembled their photometry from the recent literature. Figure 4 shows the relevant comparisons. Since SM10 do not provide their photometric uncertainties, the error bars only reflect the uncertainties associated with our photometry. Our photometry is generally consistent with that of SM10: $\Delta V = 0.082 \pm 0.005$ mag (in the sense of this paper minus SM10) with $\sigma = 0.322$ mag. Again, both the $(B-V)$ and $(V-I)$ colors show good agreement with SM10 down to the faintest magnitudes. The differences between our colors and their photometry are $\Delta(B-V) = 0.069 \pm 0.006$ mag with $\sigma = 0.267$ mag and $\Delta(V-I) = 0.012 \pm 0.001$ mag, $\sigma = 0.343$ mag.

We also compare our newly obtained photometric magnitudes and colors with those published by Ma (2012) in Fig. 5. The error bars shown in this figure are a combination (added in quadrature) of the uncertainties associated with our measurements and those from the literature. For all sources, the V-band offset is $\Delta V = -0.100 \pm 0.007$ mag (again, in the sense this paper minus Ma 2012), with $\sigma = 0.257$ mag. Our V-band magnitudes are in good agreement with the equivalent

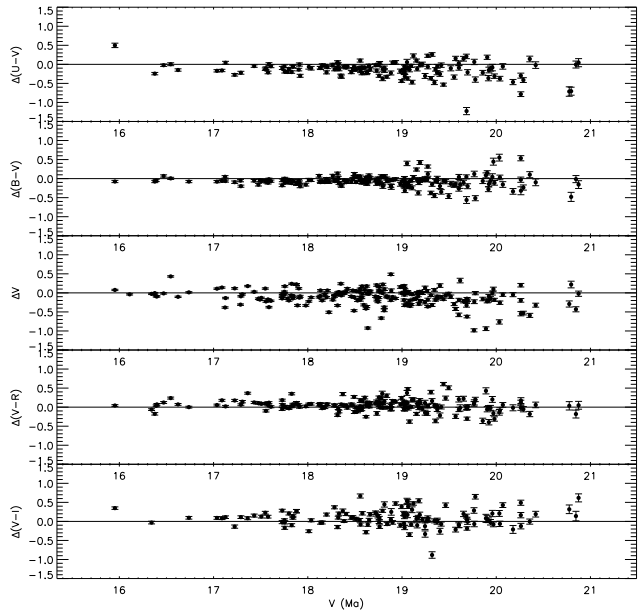

FIG. 5.— Comparison of our photometry and colors with the equivalent measurements of Ma (2012). The error bars are a combination (added in quadrature) of the uncertainties associated with our measurements and those of Ma (2012).

values of Ma (2012) for bright sources, $V < 18$ mag, while the photometry of Ma (2012) seems to be somewhat fainter than our photometry for $V > 18$ mag. In fact, Ma (2012) noted that his V-band photometry is systematically fainter than the previously published photometric measurements of Sarajedini & Mancone (2007), Park & Lee (2007), and San Roman et al. (2009), so this result is in line with our expectations. Our $(U-V)$, $(B-V)$, $(V-R)$, and $(V-I)$ colors show good agreement with the measurements of Ma (2012). The differences between our and his colors are $\Delta(U-V) = -0.151 \pm 0.013$, $\sigma = 0.244$ mag; $\Delta(B-V) = -0.068 \pm 0.005$, $\sigma = 0.154$ mag; $\Delta(V-R) = 0.049 \pm 0.004$, $\sigma = 0.157$ mag; and $\Delta(V-I) = 0.080 \pm 0.010$, $\sigma = 0.274$ mag.

Figure 6 shows the luminosity function of the M33 star clusters and candidates in our sample, which can be used to estimate the completeness of our photometry. The magnitudes are extinction-corrected absolute V-band magnitudes. We adopted a distance modulus to M33 of $(m-M)_0 = 24.64$ mag (Galleti et al. 2004). Extinction determinations for these star clusters were taken from Park & Lee (2007) and San Roman et al. (2009). For star clusters without published reddening values, we adopted an average reddening of $E(V-I) = 0.06$ mag (Sarajedini et al. 2000; San Roman et al. 2009), since for a significant number of clusters deriving individual reddening values is not possible. In fact, Sarajedini et al. (2000) found that the standard deviation associated with the average reddening value is $\Delta E(V-I) = 0.02$ mag, which shows that the scatter in reddening among most M33 star clusters is not significant. Reddening variations may introduce a maximum additional uncertainty of ~ 0.08 mag in the U band, and much smaller uncertainties in the other, redder filters, particularly in the near-infrared (NIR) bands. This is similar to the uncertainties in our photometry. We thus conclude that variations in the average reddening are unlikely to affect our fit results more significantly for clusters without prior reddening estimates than the individual reddening values determined previously for most of our other sample clusters in M33.

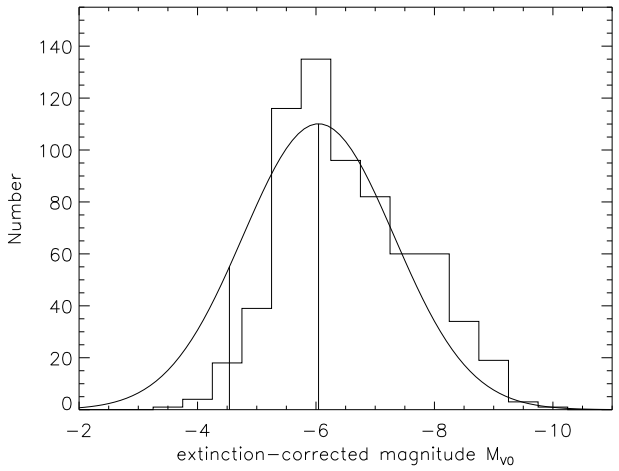

FIG. 6.— Reddening-corrected absolute V-band magnitude (M_V^0) distribution of our M33 star cluster sample. The vertical line at $M_V^0 = -4.54$ reflects our estimate of the sample's 50% completeness limit.

Using a bin size of 0.5 mag, we determined an overall limiting magnitude of $M_V^0 = -4.54$ mag, which corresponds to the half-peak height of the distribution; this follows the method adopted in our previous analysis (Fan et al. 2010) of M31 globular clusters (GCs). In addition, we found that the peak of the distribution occurs at $M_V^0 = -6.04 \pm 0.04$ mag, with $\sigma_{M_V^0} = 1.277$ mag, which we adopt as the completeness magnitude threshold. Note that a Gaussian 'fit' does not seem to actually fit the data very well. It underpredicts cluster numbers at the bright end and somewhat overpredicts them at the faint end. Therefore, we give more weight to the bright end in our fitting routine. The faint end may not be Gaussian in (true) shape but simply be depleted because of sample incompleteness.

To further explore the completeness level of the M33 star cluster sample, we show its spatial distribution in Fig. 7. The sample clusters characterized by absolute, extinction-corrected V-band magnitudes, $M_V^0 \leq -6.04$ mag, which is the peak magnitude of the distribution in Fig. 6, are shown as green points, while the purple points represent the $M_V^0 > -6.04$ mag star clusters in our sample. There is no evidence of any spatial differences between both samples. We fit Gaussian profiles to the distributions in the right ascension (R.A.) and declination (Dec) directions and determined the distribution's center coordinates: R.A. = 23.449°, with $\sigma = 0.153°$, and Dec = 30.642°, with $\sigma = 0.205°$, for the bright sources; R.A. = 23.459°($\sigma = 0.138°$) and Dec = 30.623°($\sigma = 0.192°$) for the faint objects. The two center positions are shown as the plus signs in Fig. 7.

3. SED FITS AND RESULTS

We constrain the ages, metallicities, and masses of the star clusters based on SED fitting using χ^2 minimization. We mainly used our photometry (Table 1) from the LGGS images to do so, supplemented with the SDSS *ugriz* photometry from San Roman et al. (2010). Af-

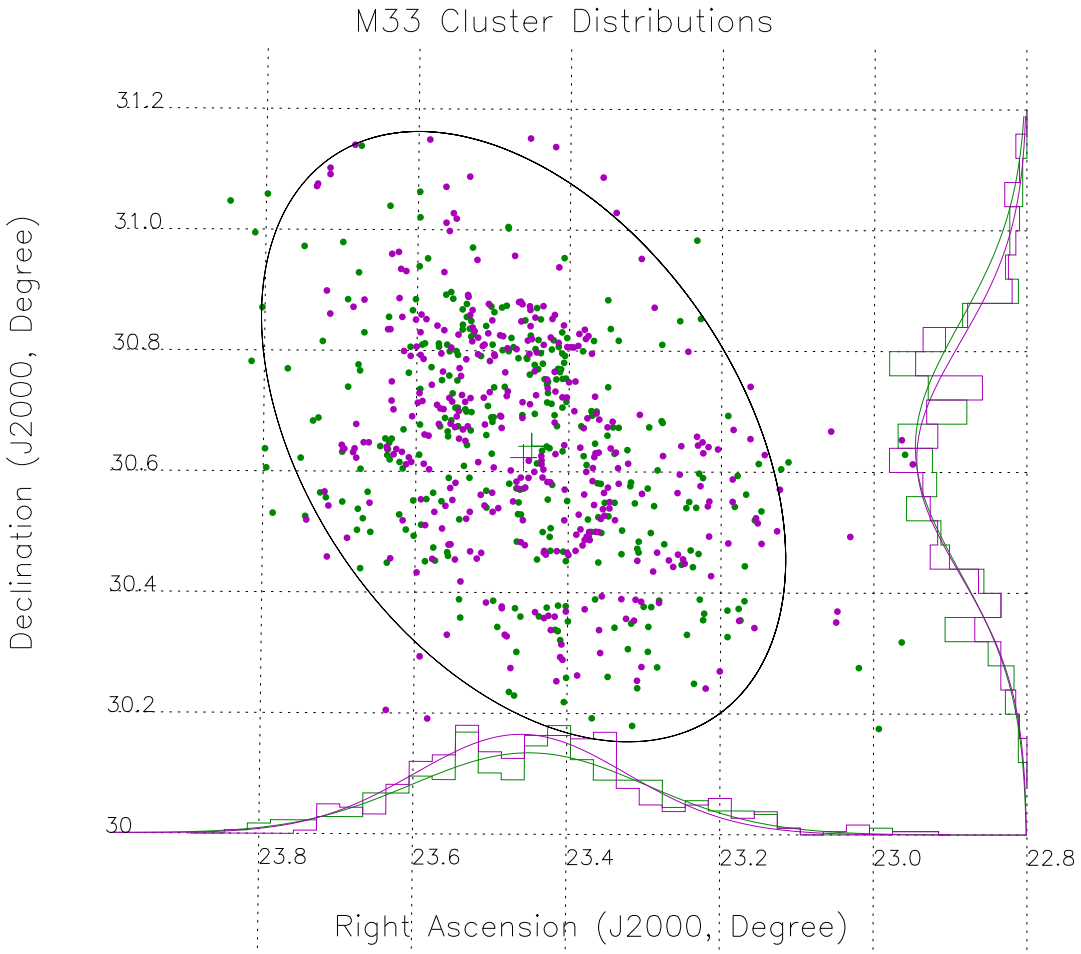

FIG. 7.— Spatial distribution of our M33 star cluster sample. The green points represent clusters with $M_V^0 \leq -6.04$ mag; the purple points are clusters with $M_V^0 > -6.04$ mag. The two plus signs represent the central positions of the Gaussian distributions for the two populations. The solid ellipse represents the galaxy's D_{25} radius.

ter elimination of those clusters for which photometry is available in too few passbands,[7] our sample is reduced to 671 star clusters and cluster candidates. We will use this subsample for SED fitting and analysis in the following sections.

3.1. *Age estimates*

As is common in relation to most ground-based observations, we can only access the *integrated* spectra and photometry of most extragalactic star clusters. Therefore, the ages, metallicities, and other physical parameters are obtained through analysis of the integrated data. As a matter of fact, a strong age–metallicity degeneracy would likely affect our analysis if only optical photometry were available (Worthey 1994; Arimoto 1996; Kaviraj et al. 2007). Anders et al. (2004) recommend to use NIR photometry if available. Inclusion of at least one NIR passband can significantly improve the accuracy of the resulting cluster parameters and partially break this degeneracy. In addition, de Grijs et al. (2005) and Wu et al. (2005) showed that NIR colors can greatly contribute to breaking the age–metallicity and age–extinction degeneracies. Therefore, we will combine our $UBVRI$ photometry with JHK photometry from 2MASS when available to disentangle the degeneracies and obtain more accurate results.

We fit the SEDs with the evolutionary tracks derived from the updated PARSEC isochrones, assuming a Chabrier (2003) lognormal stellar initial mass function (IMF).[8] These PARSEC isochrones are available for metallicities $0.0001 \leq Z \leq 0.06$ ($-2.2 \leq$ [M/H] $\leq +0.5$ dex)

[7] We only apply SED fitting to clusters with photometric measurements in ≥ 3 passbands; measurements in fewer filters lead to highly unreliable results (cf. Anders et al. 2004).

[8] http://stev.oapd.inaf.it/cgi-bin/cmd

and for stellar masses in the range $0.1 \leq M/M_{\odot} \leq 12$, with revised diffusion and overshooting for low-mass stars and improvements in the interpolation scheme. Note that, at present, the PARSEC isochrones do not include the thermally pulsing asymptotic giant-branch (TP-AGB) phase. We adopted 24 metallicities from $Z = 0.0001$ to 0.06, essentially equally spaced in in $\log Z$ space. The maximum age for a reliable interpolation in metallicity is 13.5 Gyr, or $\log(t\ \mathrm{yr}^{-1}) = 10.13$. Therefore, we adopted 71 equally spaced time steps from $\log(t\ \mathrm{yr}^{-1}) = 6.6$ (4 Myr) to $\log(t\ \mathrm{yr}^{-1}) = 10.1$ (12.6 Gyr) in steps of $\Delta \log(t\ \mathrm{yr}^{-1}) = 0.05$. The models return isochrone tables and integrated SSP magnitudes for a number of photometric systems. We adopted the SDSS *ugriz*, Johnson–Cousins *UBVRI*, and 2MASS *JHK* systems.

The magnitudes were corrected for reddening (obtained previously; see above) assuming a Cardelli et al. (1989) extinction curve. Since the wavelength ranges covered by the SDSS *ugriz* and Johnson–Cousins *UBVRI* systems are essentially the same, it is not necessary to use both for our SED fitting. We assigned priority to using the broad-band Johnson–Cousins *UBVRI* photometry, since these filters have wider bandwidths and, hence, the photometry could potentially have higher higher signal-to-noise ratios, all else being equal. Where broad-band Johnson–Cousins magnitudes were not available, the SDSS *ugriz* photometry was used. Thus, the cluster ages (t) could be determined by comparing, in the χ^2 sense, the PARSEC SSP synthesis models with the observed SEDs and adopting Z as a free parameter, i.e.

$$\chi^2_{\mathrm{min}}(t, Z) = \min \left[\sum_{i=1}^{8} \left(\frac{m^{\mathrm{obs}}_{\lambda_i} - m^{\mathrm{mod}}_{\lambda_i}}{\sigma_i} \right)^2 \right], \quad (2)$$

where $m^{\mathrm{mod}}_{\lambda_i}(t, Z)$ is the integrated magnitude in the i^{th} filter of a theoretical SSP at age t and for metallicity Z, $m^{\mathrm{obs}}_{\lambda_i}$ represents the observed, integrated magnitude in the same filter, $m_{\lambda_i} = UBVRI, ugriz, JHK$ when 2MASS data is available or $m_{\lambda_i} = UBVRI, ugriz$ when 2MASS data is not available (all magnitudes were transformed to the AB magnitude system for our SED fits). The errors, which are used as weights ($= 1/\sigma^2$) by the fitting routine, are calculated as

$$\sigma_i^2 = \sigma^2_{\mathrm{obs},i} + \sigma^2_{\mathrm{mod},i}. \quad (3)$$

Here, $\sigma_{\mathrm{obs},i}$ is the observational uncertainty; $\sigma_{\mathrm{mod},i}$ represents the uncertainty associated with the model itself, for the i^{th} filter. Following de Grijs et al. (2005), Wu et al. (2005), Fan et al. (2006), Ma et al. (2007, 2009), Fan et al. (2010), and Wang et al. (2010), we adopt $\sigma_{\mathrm{mod},i} = 0.05$ mag.

The estimated ages with 1σ errors of the M33 star clusters are listed in Table 2. We estimated the uncertainty associated with a given parameter by fixing all other parameters to their best values, then varied the parameter of interest, and recorded an error corresponding to the 1σ χ^2_{min} value.

Our newly estimated ages, compared with previous results from the literature, are plotted in Fig. 8. The top panels are comparisons of SM10 and our results, and the middle panels are those for our estimates and the results of San Roman et al. (2009). The latter authors compare MSTO photometry in the observed CMD with Girardi et al. (2000) theoretical isochrones assuming a metal abundance $Z = 0.004$, which is the mean of the disk abundance gradient in M33 (cf. Kim et al. 2002; Sarajedini et al. 2006; San Roman et al. 2009). In the top panels, we note that SM10's cluster ages and masses exhibit a general one-to-one trend with respect to our results, although the scatter is relatively large. In fact, all cluster ages and masses in SM10 were taken from the Ma et al. series of articles. These latter authors derived these parameters based on SED fits based on the Bruzual & Charlot SSP synthesis models (BC96). This is a similar approach to our method, but based on different theoretical models and photometry. In this article, we use some of the most up-to-date SSP synthesis models currently available, while our photometry is based on (more recent) observations with the Kitt Peak 4 m telescope. In addition, we used NIR photometry here, which can be used successfully to partially break the well-known age–metallicity degeneracy affecting broad-band SED analyses. A comparison of the results of San Roman et al. (2009) and the newly derived parameters presented here reveals that the systematic differences, in a logarithmic sense, in the ages, masses, and metallicities between our estimates and those of SM10 (i.e., Ma et al.) are -0.23 ± 0.77 dex, -0.32 ± 0.73 dex, and 0.08 ± 1.49 dex, respectively. This scatter is partially caused by the different metallicities adopted and partially because of stochastic sampling effects (see, e.g., Anders et al. 2013). However, the ages from San Roman et al. (2009) are systematically younger for clusters we determine as > 1 Gyr old, while they are systematically older than our estimates for objects we return as < 0.1 Gyr old. This may be partially caused by the different analysis methods or by application of different SSP models with different IMFs.

To check if our method introduces any biases, we also compare the fit results for San Roman et al. (2009) and those of SM10. This comparison shows the same trends as seen in the comparisons of San Roman et al. (2009) and our results, which indicates that the CMD fitting method of San Roman et al. (2009) may be affected by a systematic bias (see the bottom panels of Fig. 8). Since San Roman et al. (2009) adopted a single metal abundance for their CMD fits, we do not show a comparison of their metallicities with those of SM10. In fact, as San Roman et al. (2009) point out, the *isochrone-derived* ages for clusters younger than ~ 1 Gyr exhibit very little sensitivity to the assumed metal abundance. This implies that any metallicity difference between our results and those of San Roman et al. (2009) will likely have insignificant effects on the final cluster parameters derived, since almost all clusters in the sample of San Roman et al. (2009) are younger than 1 Gyr. Even if San Roman et al. (2009) had allowed their metal abundances to vary, their fit results would unlikey be affected significantly. Note that this is rather different in comparison with SED fits. In addition, we adopted the extinction values of San Roman et al. (2009).

Park et al. (2009) compared cluster ages derived from resolved CMDs with those from integrated photometry and found that ages derived from resolved CMDs cover a relatively smaller range—$7.0 \lesssim \log(t\ \mathrm{yr}^{-1}) \lesssim 8.5$—than those estimated based on integrated colors and SEDs

(see, e.g., Chandar et al. 1999, 2002; Ma et al. 2001, 2002a,b,c, 2004a,b). In addition, Santos & Frogel (1997) found that stochastic sampling effects can strongly affect the integrated $VJHK$ magnitudes of star clusters with ages $7.5 < \log(t\ \mathrm{yr}^{-1}) < 9.25$, in particular for less massive clusters (Buzzoni 1989; Barmby & Jalilian 2012; Silva-Villa & Larsen 2011).

In fact, Silva-Villa & Larsen (2011) discussed the effects of stochastic sampling on CMD fits; such effects are particularly prominent for low-mass star clusters. Since star clusters are composed of finite numbers of stars, stochastic sampling of the stellar IMF can significantly affect the derived integrated cluster parameters, such as their ages, metallicities, and masses. Recently, Anders et al. (2013) quantified the effects of stochastic sampling of stellar IMFs based on a set of GALEV SSP models for a wide range of (input) masses, metallicities, foreground extinction values, and photometric uncertainties for their model star clusters. They derive the accuracy of the integrated parameter determination in different age ranges based on performing fully sampled integrated-SED fits. For low-mass ($\sim 10^3 M_\odot$) clusters that are older than 10 Myr, the dispersion in $\log(t\ \mathrm{yr}^{-1})$ could be as much as $\sim$ 1–2 dex, while the dispersion in $\log(M_{\rm cl}/M_\odot)$ could be of the same order for [Fe/H] = 0.0 dex, foreground $E(BV) = 0.0$ mag, and assuming photometric uncertainties of 0.1 mag for all $UBVRIJHK$ magnitudes. In addition, using a variety of metallicities and different combinations of photometric passbands, stochastic sampling effects can even lead to differences of $\Delta \log(t\ \mathrm{yr}^{-1}) > 1$ dex. The offset between the estimates of SM10 and San Roman et al. (2009) can thus be understood easily. This type of effect could also partially explain the offsets in the derived parameters between SM10 and our determinations, as well as those between SM10 and San Roman et al. (2009).

We emphasize that San Roman et al. (2009) also point out that, since their photometry is generally not deep enough to detect the MSTO, few of their clusters are returned as older than 1 Gyr. The middle panel in the central row of Fig. 8 shows a comparison of the mass estimates of San Roman et al. (2009) with our new determinations. We note that the masses derived by San Roman et al. (2009) range from $5 \times 10^3 M_\odot$ to $5 \times 10^4 M_\odot$, while our estimates cover the range from $\sim 10^2 M_\odot$ to $\sim 10^6 M_\odot$. This difference can largely be traced back to the differences in our derived ages.

The left-hand panels in the top and second rows of Fig. 9 show the age distribution of our sample clusters in M33, as well as the distribution of a representative sample of M31 star clusters (Fan & de Grijs 2012), for a bin size of 0.3 dex. To allow a reasonable comparison, the parameters, such as age, metallicity, and mass of the M31 star clusters were also all derived based on the PARSEC models, using the photometric data from Fan & de Grijs (2012). We also plot the age distribution of the Milky Way star cluster sample, which is composed of both GCs and open clusters (OCs). In addition, the age estimates of LMC star clusters taken from Baumgardt et al. (2013) are also plotted in this diagram, for comparison. We note that the M33 star clusters in our sample exhibit two peaks, at ages of $\sim$ 10 Myr and $\sim$ 1 Gyr. The mean ages of the cluster samples are $\log(t\ \mathrm{yr}^{-1}) = 8.68$, 9.17, 8.46, and 8.48 for M33, M31, MW, and the LMC, respectively. For M33, the clusters with ages in excess of 10 Gyr were most likely created during the epoch when the galaxy formed, while the young star clusters might have been created in a number of mergers during the last few Gyr or by the postulated recent galactic encounter with M31 a few Gyr ago, suggested by McConnachie et al. (2009). The age distribution of the star clusters in M31 is dominated by clusters with ages between 1 Gyr and the *WMAP9* age of 13.77 ± 0.06 Gyr (Bennett et al. 2013). The age distribution of the Milky Way star clusters is based on the combination of that of the OCs collected in Dias et al. (2002)—the *New Catalog of Optically Visible Open Clusters and Candidates*; version 3.3—and the GCs, for which we assumed the *WMAP9* age. The mean age of the Milky Way's OCs is similar to that of the M33 and LMC clusters. This latter similarity implies that both galaxies have recently gone through one or more periods of active star (cluster) formation. It is clear that there is a much higher fraction of young star clusters in M33 (30.6% are older than 2 Gyr) than in M31, where 55.8% of the clusters are older than 2 Gyr.

The middle panels of Fig. 9, from the top to the third row, show the metallicity distributions of star clusters in M33, M31, and the Milky Way for a bin size of Δ[Fe/H] = 0.25 dex. The mean values of the three distributions are $\overline{\rm [Fe/H]} = -1.01$, -0.43, and -0.19 dex. The metallicity distribution of the M33 star clusters comes from our SSP fits based on the PARSEC models, while the metallicity distribution of the M31 star clusters is from the data of Fan & de Grijs (2012), also based on the PARSEC models. The metallicity distribution of the Milky Way GCs has been plotted based on the GC catalog of Harris (2010) and that of the OCs is based on the (Dias et al. 2002) catalog, which was most recently updated in 2013 and includes 201 Milky Way OCs with metallicity measurements. We computed the weighted metallicity of the two cluster samples using the numbers of GCs and OCs as weights, which is therefore dominated by the metallicity distribution of the OCs.

3.2. *Masses of the M33 star clusters*

We calculated the clusters' theoretical mass-to-light ratios (M/L_V) using the PARSEC models, luminosities based on conversion of the V-band fluxes, and a distance modulus of $(m-M)_0 = 24.64$ mag. The resulting masses are listed in Table 2. Figure 9 (right column) shows the mass distribution of the M33 star clusters in our sample, as well as the masses of the M31 and Milky Way clusters. The masses of the Galactic GCs were calculated by Gnedin & Ostriker (1997), while those of 650 OCs with mass estimates are from Piskunov et al. (2008). As before, these Galactic cluster mass estimates were combined, using as weights the total numbers of clusters of different types. For comparison, we also include the LMC star cluster data from Baumgardt et al. (2013). The bin size is $\Delta \log(M_{\rm cl}/M_\odot) = 0.3$ dex. The mean mass of the M33 clusters is $\log(M_{\rm cl}/M_\odot) = 4.25$ ($1.78 \times 10^4 M_\odot$) while the mean values for the M31 star clusters, the combined sample of Galactic star clusters, and the LMC clusters are $\log(M_{\rm cl}/M_\odot) = 5.43$ ($2.69 \times 10^5 M_\odot$), $\log(M_{\rm cl}/M_\odot) = 2.72$ ($5.24 \times 10^2 M_\odot$), and $\log(M_{\rm cl}/M_\odot) = 4.18$ ($1.51 \times 10^4 M_\odot$), respectively. Figure 9 shows that the mean mass of the star clusters in M33, which is similar to that of the LMC clusters, is

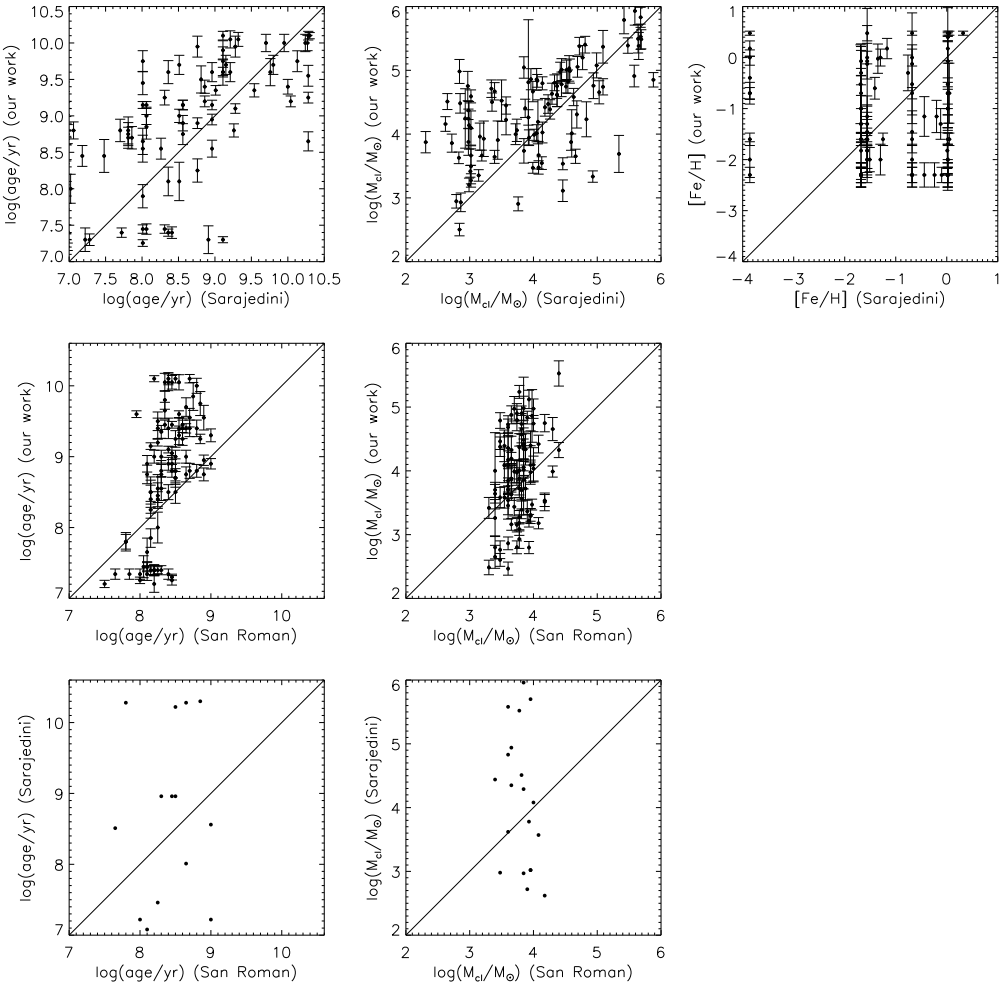

FIG. 8.— Comparisons of our age, metallicity, and mass estimates with those of (top) SM10 and (middle) San Roman et al. (2009). We also compare the parameter estimates of SM10 and San Roman et al. (2009) in the bottom row.

much lower than the equivalent masses in M31 and the Milky Way, suggesting that the M33 cluster population on the whole is dominated by lower-mass clusters.

The mass–metallicity relation (MMR) for star clusters in the 'blue sequence' (which is known as the 'blue tilt') has been discussed for many external galaxies, e.g., for a sample of six giant elliptical galaxies (Harris 2009a), M87 (Peng et al. 2009; Harris 2009b), the Sombrero galaxy (Harris et al. 2010), and M31 (Fan et al. 2009). Self-enrichment was considered a reasonable explanation by both Bailin & Harris (2009) and Strader & Smith (2008), who suggested that the level of star formation is controlled by supernova feedback, and the efficiency scaling is proportional to the proto-cloud mass. Since we have derived the masses and metallicities of the M33 clusters, we can investigate their MMR. In Fig. 10, we plot cluster masses as a function of metallicity for our sample star clusters. The filled triangles with associated error bars represent the mean values and σ's for each bin. The bin size is 0.5 dex in metallicity. For low metallicities, [Fe/H] < -0.8 dex, the cluster masses seem to decrease with metallicity, while for [Fe/H] ≥ -0.8 dex, the cluster masses increase with increasing metallicity.

Figure 11 shows the extinction-corrected absolute magnitudes as a function of age for our sample star clusters. The solid lines represent theoretical isochrones from the updated PARSEC models for masses of $10^3, 10^4, 10^5$, and $10^6 M_\odot$, for a metallicity of $Z = 0.004$. The masses of most star clusters and candidates are between $10^3 M_\odot$ and $10^5 M_\odot$. The less massive clusters, $M_{\rm cl} < 10^3 M_\odot$, tend to be young ($< 2$ Gyr) while clusters with $M_{\rm cl} > 10^5 M_\odot$ are generally old (> 2 Gyr).

The age–metallicity relations of extragalactic star clusters have been studied by many authors (e.g., de Grijs & Anders 2006; Wang et al. 2010; Fan et al. 2010). Figure 12 shows the age-versus-mass estimates of our M33 sample clusters, as well as the so-called 'fading line,' which is roughly equivalent to the $\sim 50\%$ completeness limit. The theoretical line is based on the PARSEC SSP models for a metallicity of $Z = 0.004$. For the detection limit, an absolute magnitude of $M_V \approx -5$ mag is estimated from Fig. 6. Indeed, most star clusters lie above the line. The small number of clusters found below the fading line may be due to either a possibly variable photometric completeness level or underestimated extinction. A few faint, young (< 20 Myr-old) clusters could be young OCs. Note that there are three overdensity regions in this figure, at (i) $\log(t\ {\rm yr}^{-1}) \approx 7.3$ (20 Myr), (ii) $\log(t\ {\rm yr}^{-1}) \approx 9$ (1 Gyr), and (iii) the *WMAP9* age (~ 13.7 Gyr); the latter represents the subset of the

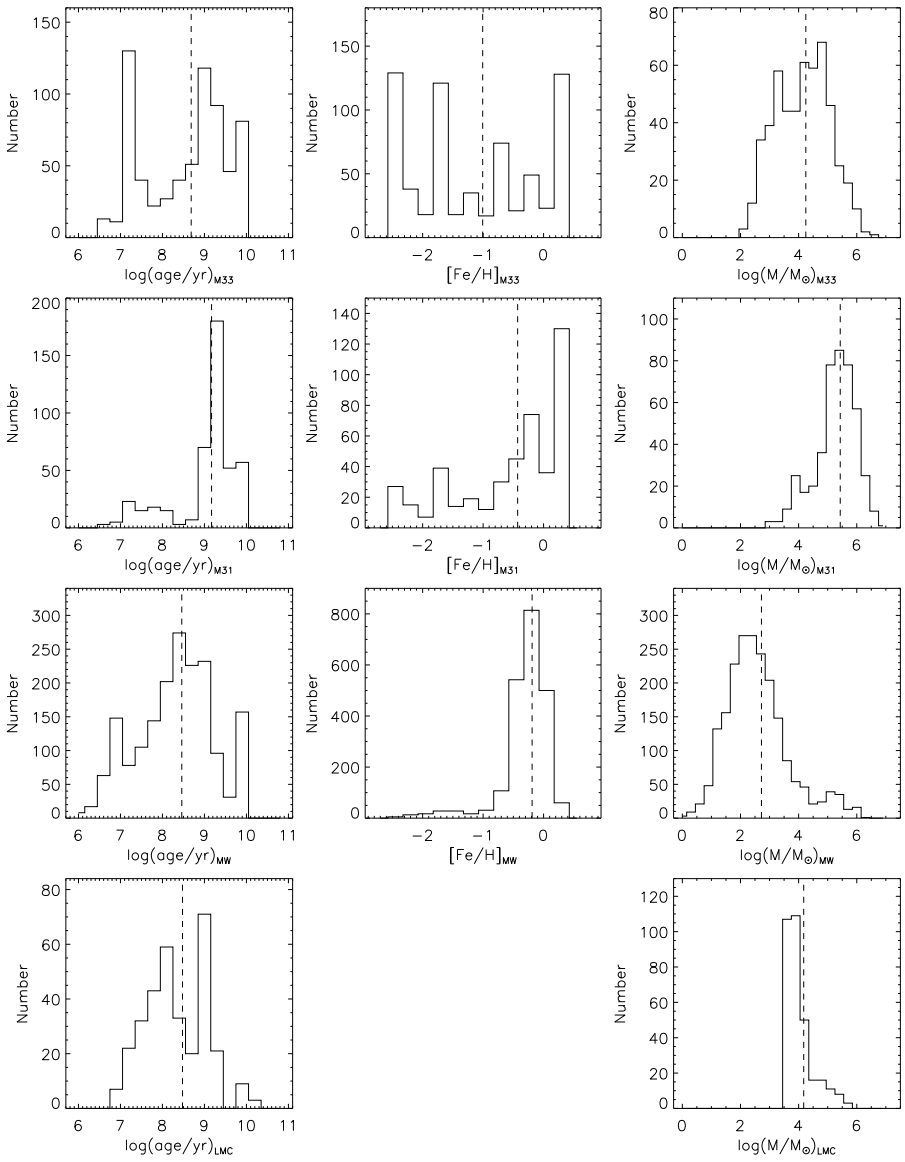

FIG. 9.— Estimated age, mass, and metallicity distributions of the star clusters and candidates in M33, M31, and the Milky Way based on the PARSEC models. The vertical dashed lines represent the mean values of the distributions. The photometric data of the M33 clusters comes from this paper, while the SEDs of the M31 globular-like clusters were analyzed by Fan & de Grijs (2012). The Milky Way star clusters are composed of GCs and OCs, for which the distributions are based on Harris (2010), the updated catalog of Dias et al. (2002), and Gnedin & Ostriker (1997). The distributions of the LMC star clusters are based on Baumgardt et al. (2013).

cluster population that seems to have formed during the time of the galaxy's formation.

4. SUMMARY

We have obtained $UBVRI$ photometry for 708 star clusters and cluster candidates in M33, which were selected from San Roman et al. (2010), including 387, 563, 616, 580, and 478 objects in the $UBVRI$ bands, respectively, of which 276, 405, 430, 457, and 363 did not have previously published $UBVRI$ photometry. The SExTRACTOR code was applied to derive the photometry from LGGS archival images, which cover 0.8 deg^2 along the major axis of M33.

We compared our photometry with previous measurements, which showed that our photometry is generally consistent with previous measurements in all filters. The ages, metallicities, and masses of our sample clusters were derived by comparison of their observed SEDs with PARSEC SSP synthesis models. The fits show that only 205 of the 671 clusters (30.55%) are older than 2 Gyr, which is a much smaller fraction than that derived for the M31 globular-like clusters (55.80%), suggesting that the M33 cluster population is dominated by young star clusters (< 1 Gyr). We also note that the mean mass of the M33 star clusters is $1.78 \times 10^4 M_\odot$, which is much less massive than that of the M31 sample ($2.69 \times 10^5 M_\odot$) and similar to that of LMC cluster population ($1.51 \times 10^4 M_\odot$), but higher than that of Milky Way star clusters (including both GCs and OCs: $5.24 \times 10^2 M_\odot$). This may be related to the fact that the mass of M33 is lower that that of M31, and the gravitational potential is not large enough to produce as many GCs as in M31. Instead, the star-formation history of M33 may be similar to that of the LMC. As for the Milky

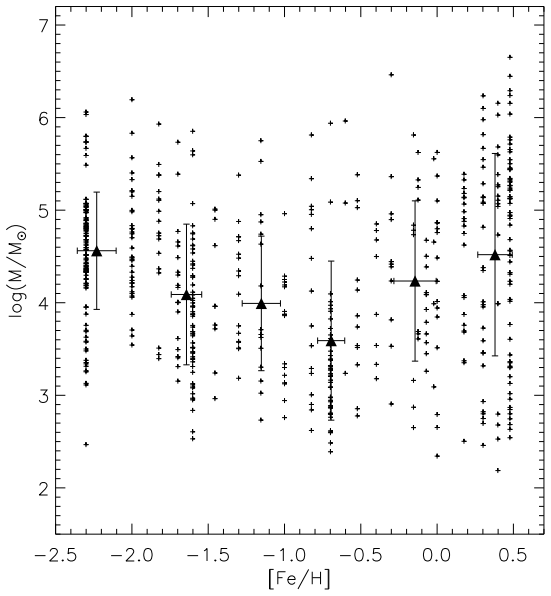

FIG. 10.— Masses versus metallicities for the M33 star clusters. We divided the metallicities into 6 bins, each with a size of 0.5 dex. The filled triangles with error bars represent the mean values and σ's for each bin.

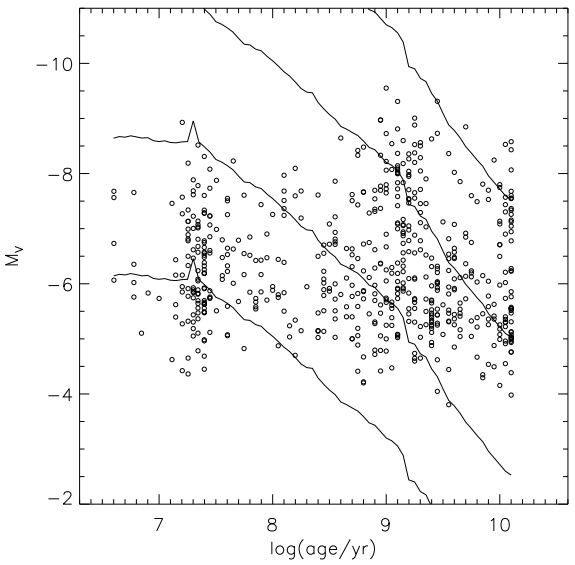

FIG. 11.— Extinction-corrected absolute magnitude as a function of cluster age. The solid lines are the expected relations for SSPs from the PARSEC model with $Z = 0.004$ and masses of $10^3, 10^4, 10^5$, and $10^6 M_\odot$ (from bottom to top).

Way, the recent few Gyr have seen the galaxy undergo quiescent evolution (a low star-formation rate).

On the other hand, the mean metallicity of the M33 clusters ([Fe/H] = −1.01 dex) is much lower than that of the M31 star clusters ([Fe/H] = −0.43 dex) and also of the Milky Way star clusters ([Fe/H] = −0.19 dex), suggesting that its star-formation history has been rather different from those of either M31 or the Milky Way. Based on the cluster mass distributions we also found that the mean mass of star clusters in M33 is similar to that in the LMC but much lower than that in M31 and higher than that in the Milky Way, indicating that M31

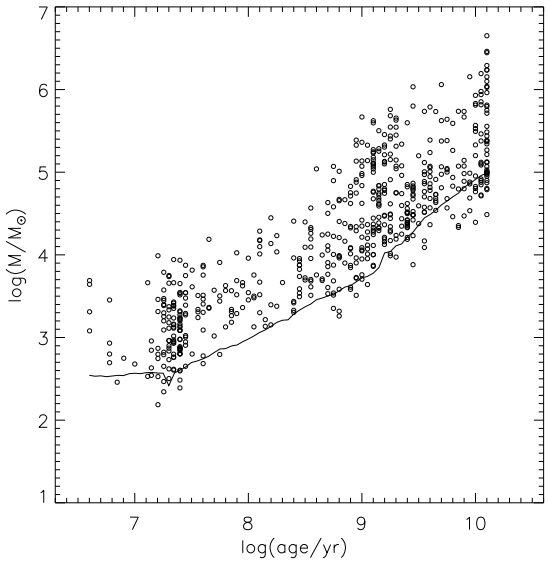

FIG. 12.— Mass as a function of age for the M33 star clusters. We also show the fading ('completeness') limit for $M_V \approx -5$ mag from Fig. 6, based on the PARSEC SSP models for a metallicity $Z = 0.004$.

underwent more violent star formation than either M33 or the LMC. We also note that stochastic sampling effects can significantly affect our SED fit results for low-mass clusters (i.e., $M_{\rm cl} \leq 10^3 M_\odot$), potentially leading to large differences in integrated cluster ages, metallicities, and masses (Anders et al. 2013). The effects of stochasticity in the clusters' stellar mass functions become weaker with increasing cluster mass. However, even for the highest-mass clusters, $M_{\rm cl} \simeq 2 \times 10^5 M_\odot$, the uncertainties in the derived logarithmic ages are 0.05–0.25 dex; the equivalent uncertainties pertaining to the derived masses are 0.09–0.17 dex. Although these uncertainties are sometimes significant, obtaining accurate, high-resolution spectroscopic observations for statistically large samples of extragalactic star clusters is often prohibitive, particularly if observing time on significantly oversubscribed (large) telescopes is sought. Broad-band imaging and parameter determination based on sophisticated SED fits is the realistic yet a poor man's alternative approach.

The broad-band SED uncertainties can be further reduced for specific age ranges, e.g., for young clusters that exhibit Hα emission, which places additional constraints on the most likely age range. At present, a number of teams are working on quantifying the effects of stochastic sampling; although the underlying message is that such effects may have significant implications in terms of the precision of the derived physical parameters, we argue that a proper understanding of one's uncertainties is of the utmost importance. One should keep these issues in mind when dealing with physical cluster parameters based on broad-band observations.

This publication makes use of data products from the Two Micron All Sky Survey, which is a joint project of the University of Massachusetts and the Infrared Processing and Analysis Center/California Institute of Technology, funded by the National Aeronautics and Space

Administration and the U.S. National Science Foundation. This research is supported by the National Natural Science Foundation of China (NFSC) through grants 11003021, 11043006, 11073001, 11373003, and 11373010. ZF also acknowledges a Young Researcher Grant from the National Astronomical Observatories, Chinese Academy of Sciences, while RdG acknowledges research support from the Royal Netherlands Academy of Arts and Sciences (KNAW) under its Visiting Professors Programme.

REFERENCES

Anders, P., Bissantz, N., Fritze-v. Alvensleben, U., & de Grijs, R. 2004, MNRAS, 347, 196
Anders, P., Kotulla, R., de Grijs, R., Wicker, J. 2013, ApJ, 778, 138
Arimoto, N. 1996, in: From Stars to Galaxies, Leitherer C., Fritze–v. Alvensleben U., Huchra J., eds., ASP Conf. Ser., (ASP: San Francisco), 98, p. 287
Bailin, J., Harris, W. E. 2009, ApJ, 695, 1082
Barmby, P., & Jalilian, F. F. 2012, AJ, 143, 87
Baumgardt, H., Parmentier, G., Anders, P., & Grebel, E. K. 2013, MNRAS, 430, 676
Bennett, C. L., et al. 2013, ApJS, 208, 20
Bertin, E., & Arnouts, S. 1996, A&AS, 317, 393
Boissier, S., et al. 2007, ApJS, 173, 524
Bressan, A., Marigo, P., Girardi, L., Salasnich, B., Dal Cero, C., Rubele, S., & Nanni, A. 2012, MNRAS, 427, 127
Buzzoni, A. 1989, ApJS, 71, 817
Caldwell, J. A. R., et al. 2008, ApJS, 174, 136
Caldwell, N., Schiavon, R., Morrison, H., Rose, J. A., & Harding, P. 2011, AJ, 141, 61
Cardelli, J. A., Clayton, G. C., & Mathis, J. S. 1989, ApJ, 345, 245
Chabrier, G. 2003, PASP, 115, 763
Chandar, R., Bianchi, L., & Ford, H. C. 1999, ApJ, 517, 668
Chandar, R., Bianchi, L., Ford, H. C., & Sarajedini, A. 2002, ApJ, 564, 712
De Angeli, F., et al. 2005, AJ, 130, 116
de Grijs, R., Bastian, N., & Lamers, H. J. G. L. M. 2003a, MNRAS, 340, 197
de Grijs, R., Anders, P., Bastian, N., Lynds, R., Lamers, H. J. G. L. M., & O'Neil, E. J. 2003b, MNRAS, 343, 1285
de Grijs, R., et al. 2005, MNRAS, 359, 874
de Grijs, R., & Anders, P. 2006, MNRAS, 366, 295
de Grijs, R., Goodwin, S. P., & Anders, P. 2013, MNRAS, 436, 136
Dias, W. S., Alessi, B. S., Moitinho, A., & Lépine, J. R. D. 2002, A&A, 389, 871
Fan, Z., Ma, J., de Grijs, R., Yang, Y., & Zhou, X. 2006, MNRAS, 371, 1648
Fan, Z., Ma, J., & Zhou, X. 2009, RAA, 9, 993
Fan, Z., de Grijs, R., & Zhou, X. 2010, ApJ, 725, 200
Fan, Z., & de Grijs, R. 2012, MNRAS, 424, 2009
Freedman, W. L., et al. 2001, ApJ, 553, 47
Girardi, L., Bressan, A., Bertelli, G., & Chiosi, C. 2000, A&AS, 141, 371
Galleti, S., Bellazzini, M., & Ferraro, F. R. 2004, A&A, 423, 925
Gnedin, O. Y., & Ostriker, J. P. 1997, ApJ, 474, 223
Harris, W. E. 2010, *A New Catalog of Globular Clusters in the Milky Way*, arXiv:1012.3224
Harris, W. E. 2009a, ApJ, 699, 254
Harris, W. E. 2009b, ApJ, 703, 939
Harris, W. E., Spitler, L. R., Forbes, D. A., & Bailin, J. 2010, MNRAS, 401, 1965
Jiang, L., Ma, J., Zhou, X., Chen, J., Wu, H., & Jiang, Z. 2003, AJ, 125, 727
Kaviraj, S., Rey, S. C., Rich, R. M., Lee, Y. W., Yoon, S. J., & Yi, S. K. 2007, MNRAS, 381, 74
Kim, M., Kim, E., Lee, M. G., Sarajedini, A., & Geisler, D. 2002, AJ, 123, 244
Kron, R. G. 1980, ApJS, 43, 305
Landolt, A. U. 1992, AJ, 104, 340
Ma, J., Zhuo, X., Wu, H., Chen, J., Jiang, Z., Zhu, J., & Xue, S. 2001, AJ, 122, 1796
Lim, S., Hwang, N., & Lee, M. G. 2013, ApJ, 766, 20
Ma, J., Zhou, X., Chen, J. S., Wu, H., Jiang, Z. J., Xue, S. J., & Zhu, J. 2002a, A&A, 385, 404
Ma, J., Zhou, X., Chen, J., Wu, H., Jiang, Z., Xue, S., & Zhu, J. 2002b, AJ, 123, 3141
Ma, J., Zhou, X., Chen, J., Wu, H., Kong, X., Jiang, Z., Zhu, J., & Xue, S. 2002c, AcA, 52, 453
Ma, J., Zhou, X., & Chen, J. 2004a, A&A, 413, 563
Ma, J., Zhou, X., & Chen, J.-S. 2004b, ChJAA, 4, 125
Ma, J., et al. 2007, ApJ, 659, 359
Ma, J., et al. 2009, AJ, 137, 4884
Ma, J. 2012, AJ, 144, 41
Massey, P., Olsen, K. A. G., Hodge, P. W., Strong, S. B., Jacoby, G. H., Schlingman, W., & Smith, R. C. 2006, AJ, 131, 2478
McConnachie, A. W., et al. 2009, Nature, 461, 66
McIntosh, D. H., et al. 2005, ApJ, 632, 191
Park, W.-K., & Lee, M. G. 2007, AJ, 134, 2168
Park, W.-K., Park, H.-S., & Lee, M. G. 2009, ApJ, 700, 103
Peng, E. W., et al. 2009, ApJ, 703, 42
Piskunov, A. E., Schilbach, E., Kharchenko, N. V., Roser, S., & Scholz, R.-D. 2008, A&A, 477, 165
Popescu, B., Hanson, M. M., & Elmegreen, B. G. 2012, ApJ, 751, 122
Sarajedini, A., Geisler, D., Schommer, R., & Harding, P. 2000, AJ, 120, 2437
Sarajedini, A., Barker, M. K., Geisler, D., Harding, P., & Schommer, R. 2006, AJ, 132, 1361
Sarajedini, A., Mancone, C. L. 2007, AJ, 134, 447
San Roman, I., Sarajedini, A., Garnett, D. R., & Holtzman, J. A. 2009, ApJ, 699, 839
San Roman, I., Sarajedini, A., & Aparicio, A. 2010, ApJ, 720, 1674
Santos, J. F. C., & Frogel, J. A. 1997, ApJ, 479, 764
Silva-Villa, E., & Larsen, S. S. 2011, A&A, 529, 25
Skrutskie, M. F., et al. 2006, AJ, 131, 1163
Strader, J., & Smith, G. H. 2008, AJ, 136, 1828
VandenBerg, D. A., Bolte, M., & Stetson, P. B. 1996, ARA&A, 34, 461
Wang, S., Fan, Z., Ma, J., de Grijs, R., & Zhou, X. 2010, AJ, 139, 1438
Worthey, G. 1994, ApJS, 95, 107
Wu, H., Shao, Z. Y., Mo, H. J., Xia, X. Y., & Deng, Z. G. 2005, ApJ, 622, 244
Xin, Y., Deng, L. C., de Grijs, R., & Kroupa, P. 2011, MNRAS, 411, 761
Zaritsky, D., Elston, R., & Hill, J. M. 1989, AJ, 97, 97
Zloczewski, K., Kaluzny, J., Hartman, J. 2008, AcA, 58, 23

TABLE 1
NEW $UBVRI$ PHOTOMETRY OF M33 CLUSTERS.

Our ID	SR ID	SM ID	U mag	B mag	V mag	R mag	I mag
1	163		19.353 ± 0.033	18.127 ± 0.020	...	...	...
2	197		19.898 ± 0.035	18.751 ± 0.021	...	17.691 ± 0.019	17.606 ± 0.029
3	203		19.951 ± 0.034	20.596 ± 0.028	19.954 ± 0.027	19.634 ± 0.027	19.204 ± 0.035
4	204		19.448 ± 0.033	19.523 ± 0.021	18.856 ± 0.020	18.384 ± 0.018	17.797 ± 0.029
5	284		19.945 ± 0.034	18.686 ± 0.020	17.539 ± 0.018	16.742 ± 0.017	...
6	316		19.890 ± 0.034	18.702 ± 0.020	17.367 ± 0.018	16.427 ± 0.017	...
7	346		20.331 ± 0.038	20.078 ± 0.025	19.400 ± 0.023	18.935 ± 0.021	18.310 ± 0.030
8	394		17.709 ± 0.032	17.406 ± 0.019	16.998 ± 0.018	16.214 ± 0.017	15.852 ± 0.028
9	405		20.673 ± 0.044	20.493 ± 0.034	...	...	...
10	425		21.152 ± 0.050	20.518 ± 0.031	19.286 ± 0.021	18.401 ± 0.019	17.606 ± 0.029
11	578		17.610 ± 0.032	17.740 ± 0.019	17.184 ± 0.018	16.823 ± 0.017	16.433 ± 0.028
12	608		19.377 ± 0.032	20.425 ± 0.040	...	...	...
13	612		...	...	...	18.663 ± 0.020	...
14	621		19.903 ± 0.035	19.729 ± 0.023	18.604 ± 0.020	17.881 ± 0.018	17.161 ± 0.028
15	649		17.505 ± 0.025	17.526 ± 0.023	16.650 ± 0.018	16.167 ± 0.017	...
16	651		19.446 ± 0.034	19.568 ± 0.023	19.334 ± 0.022	18.898 ± 0.022	18.472 ± 0.032
17	658		18.616 ± 0.032	19.711 ± 0.022	19.574 ± 0.023	19.045 ± 0.024	19.417 ± 0.038
18	660		19.854 ± 0.032	19.786 ± 0.031	19.247 ± 0.022	18.885 ± 0.022	18.323 ± 0.030
19	665		18.852 ± 0.026	19.217 ± 0.020	18.980 ± 0.020	...	...
20	667		19.849 ± 0.036	20.302 ± 0.040	19.804 ± 0.030	19.855 ± 0.035	19.680 ± 0.047
21	668		19.490 ± 0.033	18.469 ± 0.020	17.232 ± 0.018	16.342 ± 0.017	15.227 ± 0.028
22	682	6	20.054 ± 0.035	20.166 ± 0.026	19.535 ± 0.027	19.087 ± 0.027	18.806 ± 0.041
23	683		19.754 ± 0.059	20.067 ± 0.038	18.916 ± 0.022	18.155 ± 0.018	17.414 ± 0.031
24	689		...	...	20.338 ± 0.038	19.927 ± 0.035	19.505 ± 0.043
25	693		19.777 ± 0.034	19.989 ± 0.024	19.775 ± 0.025	19.999 ± 0.031	19.225 ± 0.039
26	695		17.491 ± 0.032	16.764 ± 0.019	15.826 ± 0.018	15.290 ± 0.017	14.725 ± 0.028
27	708		...	19.620 ± 0.023	19.646 ± 0.025	19.379 ± 0.024	19.212 ± 0.040
28	714		...	...	17.262 ± 0.018	16.447 ± 0.017	15.828 ± 0.028
29	716		...	19.509 ± 0.021	19.128 ± 0.020	18.663 ± 0.019	18.831 ± 0.034
30	722		17.654 ± 0.032	17.740 ± 0.019	17.400 ± 0.018	17.111 ± 0.017	...
31	729		18.246 ± 0.032	18.309 ± 0.020	17.728 ± 0.018	17.354 ± 0.017	17.062 ± 0.030
32	732	10	...	18.990 ± 0.028	18.117 ± 0.021	17.397 ± 0.019	...
33	734		17.825 ± 0.032	17.716 ± 0.019	17.060 ± 0.018	16.659 ± 0.017	16.249 ± 0.028
34	735		...	18.776 ± 0.020	18.753 ± 0.020	18.193 ± 0.019	18.580 ± 0.036
35	752		...	...	...	...	19.492 ± 0.042
36	755		17.061 ± 0.032	17.613 ± 0.019	17.493 ± 0.018	17.784 ± 0.017	...
37	759		18.156 ± 0.032	17.968 ± 0.019	17.248 ± 0.018	16.827 ± 0.017	16.036 ± 0.028
38	760		17.829 ± 0.025	19.085 ± 0.025	18.479 ± 0.019	18.586 ± 0.018	18.719 ± 0.036
39	785		17.206 ± 0.032	17.126 ± 0.019	16.466 ± 0.018	16.070 ± 0.017	...
40	791		19.447 ± 0.033	19.554 ± 0.022	19.182 ± 0.021	18.867 ± 0.020	18.143 ± 0.030
41	805		16.430 ± 0.032	16.409 ± 0.019	15.859 ± 0.018	15.526 ± 0.017	...
42	810		18.215 ± 0.032	19.885 ± 0.023	19.729 ± 0.026	18.994 ± 0.024	19.772 ± 0.046
43	811		18.851 ± 0.033	18.941 ± 0.020	18.559 ± 0.019	18.230 ± 0.018	17.703 ± 0.029
44	814		18.689 ± 0.026	18.780 ± 0.024	18.295 ± 0.019	17.906 ± 0.018	17.534 ± 0.030
45	817		...	...	17.578 ± 0.018	17.406 ± 0.017	17.302 ± 0.028
46	823		...	19.010 ± 0.020	18.728 ± 0.020	18.537 ± 0.019	18.260 ± 0.029
47	826		18.575 ± 0.032	18.191 ± 0.020	17.415 ± 0.018	16.925 ± 0.017	16.420 ± 0.028
48	830		18.132 ± 0.032	18.087 ± 0.020	17.464 ± 0.018	17.070 ± 0.017	16.655 ± 0.028
49	835		...	18.588 ± 0.025	18.334 ± 0.019	17.872 ± 0.019	17.860 ± 0.029
50	837		...	19.143 ± 0.025	17.887 ± 0.018	17.178 ± 0.017	16.170 ± 0.028
51	840		18.425 ± 0.026	18.851 ± 0.020	18.449 ± 0.019	17.978 ± 0.018	17.363 ± 0.028
52	846		...	18.497 ± 0.024	17.746 ± 0.018	17.325 ± 0.017	16.559 ± 0.028
53	847		...	...	...	...	17.931 ± 0.034
54	849		21.274 ± 0.071	20.777 ± 0.048	19.285 ± 0.024	18.373 ± 0.019	17.512 ± 0.031
55	851		...	...	...	...	19.058 ± 0.041
56	852		18.563 ± 0.026	19.210 ± 0.021	19.289 ± 0.021	19.037 ± 0.023	19.190 ± 0.035
57	856		...	...	...	...	17.650 ± 0.031
58	858		18.499 ± 0.026	19.503 ± 0.021	19.140 ± 0.021	18.761 ± 0.023	...
59	861		...	...	...	17.190 ± 0.016	17.374 ± 0.031
60	863		17.422 ± 0.055	17.842 ± 0.021	17.302 ± 0.022	16.908 ± 0.027	15.948 ± 0.070
61	871		18.149 ± 0.032	18.106 ± 0.019	17.782 ± 0.018	17.546 ± 0.018	17.211 ± 0.028
62	875		20.306 ± 0.037	20.825 ± 0.035	19.898 ± 0.030	19.207 ± 0.026	18.616 ± 0.033
63	883		...	...	...	...	18.789 ± 0.035
64	889		17.616 ± 0.032	17.643 ± 0.019	17.024 ± 0.018	16.621 ± 0.017	...
65	891		19.363 ± 0.033	18.220 ± 0.020	17.121 ± 0.018	...	...
66	893		19.320 ± 0.028	19.486 ± 0.027	18.914 ± 0.023	18.836 ± 0.023	18.632 ± 0.037
67	895		18.420 ± 0.026	18.387 ± 0.020	18.129 ± 0.019	17.961 ± 0.018	17.682 ± 0.028
68	902	486	20.178 ± 0.037	20.117 ± 0.028	19.682 ± 0.028	19.334 ± 0.026	17.790 ± 0.030
69	904	31	20.438 ± 0.037	20.418 ± 0.028	20.024 ± 0.027	19.591 ± 0.027	18.767 ± 0.036
70	908		20.042 ± 0.036	19.996 ± 0.026	19.608 ± 0.026	19.613 ± 0.027	18.818 ± 0.041
71	912	34	20.211 ± 0.036	20.407 ± 0.028	19.765 ± 0.027	19.373 ± 0.026	18.634 ± 0.032
72	914		20.035 ± 0.038	20.123 ± 0.039	19.778 ± 0.036	19.563 ± 0.036	19.331 ± 0.047
73	919		...	17.697 ± 0.019	17.606 ± 0.018	17.564 ± 0.017	17.085 ± 0.028
74	930	493	19.142 ± 0.028	19.523 ± 0.029	18.988 ± 0.026	...	...
75	936		...	...	19.068 ± 0.026	18.533 ± 0.020	17.670 ± 0.029

TABLE 1 — *Continued*

Our ID	SR ID	SM ID	U mag	B mag	V mag	R mag	I mag
76	939		19.351 ± 0.028	19.226 ± 0.026	18.645 ± 0.020	18.337 ± 0.028	···
77	940		17.694 ± 0.025	17.625 ± 0.023	16.978 ± 0.017	16.558 ± 0.015	16.161 ± 0.030
78	941		18.771 ± 0.026	18.922 ± 0.025	18.469 ± 0.019	18.056 ± 0.017	17.507 ± 0.031
79	946		···	18.968 ± 0.020	18.950 ± 0.020	18.290 ± 0.020	18.833 ± 0.036
80	947		···	19.007 ± 0.020	19.031 ± 0.020	18.460 ± 0.020	18.984 ± 0.037
81	953		17.928 ± 0.032	17.804 ± 0.019	17.135 ± 0.018	16.735 ± 0.017	16.344 ± 0.028
82	955		18.858 ± 0.032	19.359 ± 0.021	19.137 ± 0.021	18.884 ± 0.022	18.487 ± 0.032
83	956	40	19.650 ± 0.034	19.649 ± 0.023	19.017 ± 0.021	18.549 ± 0.020	18.045 ± 0.030
84	960		···	···	18.356 ± 0.019	···	···
85	962		18.486 ± 0.026	17.629 ± 0.023	16.253 ± 0.017	15.229 ± 0.015	···
86	968	496	17.843 ± 0.032	17.976 ± 0.019	17.651 ± 0.018	17.500 ± 0.016	···
87	972	42	···	···	18.372 ± 0.020	18.050 ± 0.018	17.323 ± 0.029
88	980		18.149 ± 0.032	18.018 ± 0.020	17.377 ± 0.018	16.987 ± 0.017	16.569 ± 0.028
89	981		18.184 ± 0.032	18.292 ± 0.020	17.899 ± 0.019	18.128 ± 0.017	···
90	983		···	18.847 ± 0.020	18.767 ± 0.020	···	18.786 ± 0.032
91	986		···	16.339 ± 0.019	16.187 ± 0.018	16.055 ± 0.017	15.863 ± 0.028
92	1001	499	20.210 ± 0.040	20.064 ± 0.029	19.613 ± 0.029	19.483 ± 0.027	18.873 ± 0.033
93	1009		18.230 ± 0.032	17.916 ± 0.019	16.791 ± 0.018	16.666 ± 0.017	15.805 ± 0.028
94	1012		···	19.222 ± 0.028	18.641 ± 0.021	18.491 ± 0.021	18.132 ± 0.034
95	1013	500	···	18.874 ± 0.025	18.822 ± 0.020	18.953 ± 0.022	18.932 ± 0.034
96	1020		19.848 ± 0.035	19.335 ± 0.030	18.249 ± 0.019	17.441 ± 0.016	16.650 ± 0.030
97	1021		···	···	18.780 ± 0.020	···	···
98	1022	45	20.008 ± 0.035	···	···	···	···
99	1024	501	19.625 ± 0.035	19.863 ± 0.024	19.470 ± 0.023	18.857 ± 0.022	18.594 ± 0.031
100	1028	502	···	21.034 ± 0.043	20.411 ± 0.039	19.873 ± 0.037	19.388 ± 0.045
101	1029	503	···	20.766 ± 0.032	20.153 ± 0.035	19.871 ± 0.037	19.632 ± 0.047
102	1030		17.105 ± 0.032	18.441 ± 0.020	18.024 ± 0.019	17.321 ± 0.018	···
103	1031	49	19.330 ± 0.033	19.120 ± 0.021	18.292 ± 0.019	17.753 ± 0.018	17.128 ± 0.028
104	1041	504	19.904 ± 0.036	19.516 ± 0.033	19.187 ± 0.026	18.681 ± 0.022	···
105	1049	52	20.060 ± 0.037	19.958 ± 0.026	19.771 ± 0.024	19.201 ± 0.023	18.364 ± 0.032
106	1052	505	···	···	···	19.209 ± 0.026	···
107	1059		18.419 ± 0.032	18.398 ± 0.020	17.755 ± 0.018	17.362 ± 0.017	16.953 ± 0.028
108	1066	53	18.416 ± 0.032	18.530 ± 0.020	18.223 ± 0.019	17.958 ± 0.018	···
109	1074		19.866 ± 0.035	19.838 ± 0.024	19.432 ± 0.023	18.719 ± 0.023	18.444 ± 0.033
110	1080	54	20.312 ± 0.036	20.049 ± 0.024	19.459 ± 0.023	18.993 ± 0.023	18.450 ± 0.032
111	1083		19.393 ± 0.033	18.216 ± 0.020	17.154 ± 0.018	16.062 ± 0.017	···
112	1087		···	19.597 ± 0.027	19.100 ± 0.022	···	···
113	1088		19.655 ± 0.032	···	···	18.307 ± 0.019	17.566 ± 0.029
114	1090		20.059 ± 0.036	20.012 ± 0.025	18.800 ± 0.020	18.065 ± 0.018	17.192 ± 0.028
115	1102	57	19.637 ± 0.028	19.179 ± 0.021	18.559 ± 0.019	18.196 ± 0.017	···
116	1103		17.165 ± 0.032	17.491 ± 0.019	17.321 ± 0.018	17.150 ± 0.017	16.900 ± 0.028
117	1111		17.106 ± 0.025	17.545 ± 0.019	17.494 ± 0.019	17.330 ± 0.018	···
118	1112		16.945 ± 0.025	17.474 ± 0.023	17.229 ± 0.017	16.840 ± 0.017	16.548 ± 0.030
119	1114		18.966 ± 0.027	19.275 ± 0.026	18.925 ± 0.020	18.597 ± 0.019	18.211 ± 0.033
120	1115		17.058 ± 0.025	17.483 ± 0.023	16.469 ± 0.017	16.438 ± 0.015	···
121	1122	508	···	18.563 ± 0.020	18.326 ± 0.019	18.181 ± 0.018	17.590 ± 0.029
122	1124	511	18.744 ± 0.026	19.114 ± 0.025	18.808 ± 0.020	18.534 ± 0.019	17.903 ± 0.030
123	1125		21.023 ± 0.068	20.655 ± 0.039	19.575 ± 0.028	18.781 ± 0.029	17.804 ± 0.070
124	1126		20.122 ± 0.035	20.201 ± 0.024	19.703 ± 0.023	19.152 ± 0.022	18.045 ± 0.029
125	1129	63	19.791 ± 0.032	19.524 ± 0.031	19.146 ± 0.026	19.063 ± 0.023	18.738 ± 0.037
126	1133	66	18.089 ± 0.025	18.406 ± 0.024	···	···	···
127	1134	68	18.619 ± 0.027	18.872 ± 0.025	18.611 ± 0.020	···	···
128	1138		17.549 ± 0.025	17.622 ± 0.023	17.035 ± 0.017	16.285 ± 0.015	16.268 ± 0.030
129	1139		17.189 ± 0.032	17.501 ± 0.019	17.213 ± 0.018	16.918 ± 0.017	···
130	1143		20.304 ± 0.037	20.276 ± 0.027	19.473 ± 0.027	19.174 ± 0.027	18.600 ± 0.034
131	1144		···	···	···	···	18.189 ± 0.033
132	1146		···	19.083 ± 0.025	18.908 ± 0.020	18.656 ± 0.018	18.096 ± 0.031
133	1147		19.864 ± 0.034	19.892 ± 0.033	19.868 ± 0.030	19.344 ± 0.032	···
134	1148	74	19.308 ± 0.029	19.229 ± 0.029	19.026 ± 0.025	18.629 ± 0.023	18.410 ± 0.036
135	1149	515	19.487 ± 0.029	19.407 ± 0.028	19.238 ± 0.023	···	···
136	1150		19.500 ± 0.032	19.755 ± 0.033	19.431 ± 0.030	19.169 ± 0.030	19.063 ± 0.042
137	1152	75	20.117 ± 0.037	20.059 ± 0.026	19.715 ± 0.024	19.365 ± 0.024	18.684 ± 0.036
138	1154		···	19.115 ± 0.028	18.580 ± 0.022	18.057 ± 0.019	···
139	1161	77	19.041 ± 0.033	18.942 ± 0.020	18.289 ± 0.019	17.690 ± 0.016	···
140	1162		20.110 ± 0.058	20.823 ± 0.040	20.383 ± 0.041	20.219 ± 0.046	19.482 ± 0.078
141	1163		17.954 ± 0.032	18.423 ± 0.020	18.273 ± 0.019	18.010 ± 0.018	17.567 ± 0.032
142	1166		19.898 ± 0.036	19.895 ± 0.025	19.641 ± 0.027	19.357 ± 0.028	···
143	1169		···	···	···	18.462 ± 0.021	···
144	1170	523	···	18.127 ± 0.020	17.852 ± 0.019	18.040 ± 0.017	···
145	1175	86	···	19.082 ± 0.025	18.623 ± 0.019	18.235 ± 0.019	···
146	1179	87	19.205 ± 0.027	19.239 ± 0.026	18.529 ± 0.019	17.913 ± 0.017	···
147	1180		···	19.250 ± 0.026	18.778 ± 0.022	···	···
148	1181	524	19.213 ± 0.033	19.240 ± 0.021	···	18.385 ± 0.019	17.626 ± 0.029
149	1182		···	···	···	···	19.282 ± 0.046
150	1184		16.526 ± 0.025	16.822 ± 0.023	16.522 ± 0.018	16.406 ± 0.017	15.865 ± 0.028
151	1185	525	18.731 ± 0.033	18.551 ± 0.020	17.934 ± 0.018	17.520 ± 0.017	17.184 ± 0.030

TABLE 1 — *Continued*

Our ID	SR ID	SM ID	U mag	B mag	V mag	R mag	I mag
152	1188		18.645 ± 0.026	17.493 ± 0.023	16.587 ± 0.017	15.688 ± 0.015	···
153	1190		18.295 ± 0.032	18.528 ± 0.020	18.352 ± 0.019	18.235 ± 0.018	17.615 ± 0.029
154	1196		18.717 ± 0.032	18.535 ± 0.020	17.856 ± 0.018	17.421 ± 0.017	17.003 ± 0.028
155	1197		18.888 ± 0.026	17.706 ± 0.023	16.544 ± 0.017	15.749 ± 0.015	15.309 ± 0.070
156	1199	93	···	17.698 ± 0.024	17.316 ± 0.018	···	···
157	1200		···	···	19.240 ± 0.027	19.253 ± 0.031	19.060 ± 0.044
158	1203	95	···	17.681 ± 0.024	16.977 ± 0.017	···	···
159	1204		19.000 ± 0.033	19.584 ± 0.022	19.192 ± 0.024	18.937 ± 0.022	18.536 ± 0.030
160	1207		15.792 ± 0.025	16.671 ± 0.023	16.643 ± 0.017	16.657 ± 0.015	16.580 ± 0.030
161	1208		···	20.018 ± 0.033	20.181 ± 0.034	20.001 ± 0.036	19.863 ± 0.049
162	1214	526	19.623 ± 0.033	19.542 ± 0.028	19.374 ± 0.021	19.076 ± 0.020	···
163	1215	98	···	18.347 ± 0.024	18.007 ± 0.019	17.801 ± 0.018	19.255 ± 0.041
164	1219	528	19.330 ± 0.028	19.634 ± 0.030	···	···	···
165	1224		···	19.015 ± 0.026	18.394 ± 0.020	17.853 ± 0.018	···
166	1226		···	19.615 ± 0.029	19.375 ± 0.024	19.181 ± 0.025	···
167	1230	102	18.766 ± 0.033	18.583 ± 0.020	17.916 ± 0.019	17.439 ± 0.018	17.057 ± 0.031
168	1232	531	···	18.569 ± 0.024	18.365 ± 0.018	18.153 ± 0.017	17.759 ± 0.031
169	1233	103	19.154 ± 0.028	19.086 ± 0.026	18.541 ± 0.020	18.158 ± 0.018	17.676 ± 0.032
170	1235	106	19.038 ± 0.027	19.114 ± 0.025	18.695 ± 0.020	18.383 ± 0.019	···
171	1237	109	19.436 ± 0.030	19.558 ± 0.030	19.228 ± 0.026	18.915 ± 0.025	18.642 ± 0.037
172	1239	110	···	18.092 ± 0.025	17.648 ± 0.019	17.267 ± 0.016	···
173	1241	532	18.835 ± 0.026	18.926 ± 0.025	18.534 ± 0.019	18.281 ± 0.018	17.755 ± 0.029
174	1244		19.325 ± 0.030	19.845 ± 0.033	19.055 ± 0.026	18.588 ± 0.024	18.067 ± 0.035
175	1249	114	18.560 ± 0.032	18.928 ± 0.020	18.792 ± 0.020	18.722 ± 0.019	18.613 ± 0.033
176	1251	533	···	···	···	19.738 ± 0.031	19.465 ± 0.037
177	1255	117	19.396 ± 0.028	19.187 ± 0.026	18.631 ± 0.020	18.058 ± 0.018	···
178	1258	121	19.286 ± 0.029	19.160 ± 0.027	18.580 ± 0.021	18.188 ± 0.019	17.641 ± 0.032
179	1262	122	18.797 ± 0.027	18.800 ± 0.025	18.369 ± 0.020	17.983 ± 0.018	17.487 ± 0.031
180	1265	537	18.201 ± 0.025	18.458 ± 0.020	18.306 ± 0.019	18.224 ± 0.018	17.731 ± 0.029
181	1268	124	18.993 ± 0.027	···	18.434 ± 0.019	···	···
182	1271		17.777 ± 0.025	18.155 ± 0.024	17.834 ± 0.018	17.412 ± 0.017	···
183	1273	126	···	···	17.713 ± 0.019	···	17.090 ± 0.031
184	1275		···	···	19.152 ± 0.022	···	18.510 ± 0.038
185	1276		16.576 ± 0.025	17.239 ± 0.023	17.098 ± 0.017	16.683 ± 0.015	16.568 ± 0.030
186	1282		19.770 ± 0.034	19.948 ± 0.023	19.575 ± 0.022	19.243 ± 0.021	18.810 ± 0.030
187	1283	539	19.808 ± 0.034	20.061 ± 0.026	19.543 ± 0.027	19.166 ± 0.027	···
188	1286		···	19.410 ± 0.025	19.223 ± 0.027	18.889 ± 0.023	···
189	1289	541	21.306 ± 0.053	21.209 ± 0.045	20.736 ± 0.046	···	···
190	1290		19.540 ± 0.029	···	19.165 ± 0.026	18.896 ± 0.026	19.123 ± 0.039
191	1295		17.375 ± 0.025	17.026 ± 0.019	16.729 ± 0.018	16.567 ± 0.017	15.958 ± 0.028
192	1296		···	···	18.409 ± 0.019	18.277 ± 0.017	···
193	1297	136	18.762 ± 0.027	18.888 ± 0.025	18.444 ± 0.019	18.148 ± 0.018	17.655 ± 0.031
194	1300		18.794 ± 0.026	19.595 ± 0.028	19.527 ± 0.025	19.473 ± 0.028	19.273 ± 0.043
195	1302		18.015 ± 0.026	19.372 ± 0.025	19.273 ± 0.021	18.595 ± 0.020	···
196	1303	138	18.891 ± 0.027	19.119 ± 0.026	18.675 ± 0.020	18.302 ± 0.018	17.889 ± 0.032
197	1305		···	···	···	···	16.185 ± 0.030
198	1306		17.885 ± 0.032	17.436 ± 0.019	17.111 ± 0.018	16.347 ± 0.017	15.929 ± 0.028
199	1307		19.987 ± 0.036	19.877 ± 0.036	19.363 ± 0.030	···	···
200	1311		···	17.080 ± 0.023	16.738 ± 0.018	···	···
201	1312		···	···	16.106 ± 0.017	15.661 ± 0.017	15.294 ± 0.028
202	1315		18.997 ± 0.027	19.086 ± 0.027	18.781 ± 0.022	18.643 ± 0.022	18.511 ± 0.035
203	1317		18.893 ± 0.033	18.173 ± 0.020	17.288 ± 0.018	16.748 ± 0.017	16.256 ± 0.028
204	1319	141	···	···	17.649 ± 0.018	17.221 ± 0.017	16.710 ± 0.028
205	1320		20.473 ± 0.044	20.335 ± 0.042	19.790 ± 0.036	19.174 ± 0.031	18.375 ± 0.037
206	1322		17.945 ± 0.025	17.848 ± 0.023	17.136 ± 0.017	16.685 ± 0.015	16.630 ± 0.030
207	1323	543	20.276 ± 0.038	20.226 ± 0.028	19.879 ± 0.029	19.608 ± 0.030	19.373 ± 0.037
208	1324	143	···	···	···	16.608 ± 0.015	16.821 ± 0.070
209	1328	146	···	18.890 ± 0.026	18.548 ± 0.021	18.441 ± 0.029	···
210	1329		19.310 ± 0.028	19.567 ± 0.028	19.330 ± 0.024	19.182 ± 0.023	18.894 ± 0.037
211	1330	147	19.431 ± 0.028	19.386 ± 0.026	18.657 ± 0.020	18.069 ± 0.017	···
212	1331	544	20.122 ± 0.036	20.233 ± 0.027	19.809 ± 0.027	19.350 ± 0.025	18.516 ± 0.030
213	1332		···	···	18.513 ± 0.020	18.281 ± 0.019	17.913 ± 0.030
214	1333		17.032 ± 0.025	17.052 ± 0.023	16.233 ± 0.017	15.376 ± 0.015	···
215	1334		···	···	···	19.031 ± 0.023	···
216	1335		19.649 ± 0.034	19.567 ± 0.032	19.421 ± 0.025	18.920 ± 0.023	18.264 ± 0.033
217	1336		18.769 ± 0.026	18.976 ± 0.025	18.520 ± 0.020	17.943 ± 0.018	···
218	1339		17.620 ± 0.025	18.333 ± 0.019	18.053 ± 0.018	17.792 ± 0.017	16.972 ± 0.028
219	1342		···	···	17.051 ± 0.018	···	···
220	1348		19.937 ± 0.031	19.941 ± 0.032	19.693 ± 0.030	19.538 ± 0.031	19.181 ± 0.042
221	1349		19.289 ± 0.033	18.620 ± 0.020	17.890 ± 0.019	17.419 ± 0.017	16.975 ± 0.028
222	1352		19.519 ± 0.030	19.890 ± 0.033	19.595 ± 0.031	19.386 ± 0.031	19.168 ± 0.043
223	1355	151	19.037 ± 0.027	18.957 ± 0.025	18.626 ± 0.020	18.371 ± 0.019	17.979 ± 0.032
224	1356		18.462 ± 0.026	18.878 ± 0.025	18.665 ± 0.020	···	···
225	1358		19.085 ± 0.033	20.049 ± 0.023	19.447 ± 0.021	18.221 ± 0.018	···
226	1359		···	···	17.915 ± 0.018	17.196 ± 0.017	15.992 ± 0.028
227	1367	155	···	20.209 ± 0.035	19.270 ± 0.023	19.091 ± 0.024	18.414 ± 0.033

TABLE 1 — *Continued*

Our ID	SR ID	SM ID	U mag	B mag	V mag	R mag	I mag
228	1368		18.119 ± 0.025	17.800 ± 0.023	16.997 ± 0.017	16.503 ± 0.015	16.021 ± 0.030
229	1369	547	18.315 ± 0.026	18.608 ± 0.024	18.333 ± 0.018	18.062 ± 0.017	···
230	1374	156	16.683 ± 0.025	17.299 ± 0.023	17.146 ± 0.017	16.977 ± 0.015	16.668 ± 0.030
231	1376		···	···	···	18.800 ± 0.021	19.253 ± 0.036
232	1377		···	···	17.562 ± 0.022	···	17.096 ± 0.031
233	1378		···	19.531 ± 0.027	18.904 ± 0.020	18.244 ± 0.017	18.332 ± 0.032
234	1379		17.783 ± 0.055	17.884 ± 0.021	17.342 ± 0.022	16.957 ± 0.027	15.994 ± 0.070
235	1380		19.662 ± 0.036	19.676 ± 0.034	19.295 ± 0.027	18.813 ± 0.032	···
236	1381		18.001 ± 0.025	18.706 ± 0.024	18.685 ± 0.020	18.583 ± 0.019	18.606 ± 0.033
237	1384		···	19.504 ± 0.021	17.931 ± 0.019	17.342 ± 0.017	16.607 ± 0.030
238	1385		···	···	18.035 ± 0.019	17.992 ± 0.018	17.906 ± 0.029
239	1387		19.176 ± 0.028	19.270 ± 0.026	18.934 ± 0.021	18.589 ± 0.018	18.057 ± 0.031
240	1389	162	18.893 ± 0.033	19.415 ± 0.021	19.213 ± 0.022	18.861 ± 0.024	18.140 ± 0.034
241	1392	163	···	19.035 ± 0.027	18.951 ± 0.024	18.532 ± 0.025	18.981 ± 0.041
242	1393	165	19.019 ± 0.028	19.045 ± 0.026	18.704 ± 0.021	18.435 ± 0.020	18.189 ± 0.034
243	1396	550	18.029 ± 0.026	18.125 ± 0.020	···	···	···
244	1403		···	18.035 ± 0.023	17.698 ± 0.018	18.068 ± 0.018	20.139 ± 0.049
245	1404	551	···	19.346 ± 0.026	···	···	···
246	1409		···	···	···	···	18.082 ± 0.030
247	1411		···	···	18.052 ± 0.019	···	···
248	1412	168	···	18.072 ± 0.024	17.715 ± 0.019	···	···
249	1413		···	···	19.087 ± 0.026	19.112 ± 0.026	···
250	1414		···	···	20.409 ± 0.031	···	···
251	1418		···	···	17.268 ± 0.017	17.194 ± 0.016	···
252	1419	555	···	19.022 ± 0.025	18.675 ± 0.020	19.573 ± 0.032	···
253	1421		···	18.694 ± 0.026	18.819 ± 0.022	18.349 ± 0.021	18.009 ± 0.034
254	1422		···	17.323 ± 0.023	17.282 ± 0.022	···	···
255	1426		···	···	···	17.575 ± 0.016	17.472 ± 0.028
256	1429	556	19.902 ± 0.034	19.548 ± 0.023	19.297 ± 0.021	18.736 ± 0.019	···
257	1432		18.727 ± 0.026	19.093 ± 0.026	18.726 ± 0.020	18.404 ± 0.018	17.776 ± 0.032
258	1435	558	···	···	20.797 ± 0.043	···	···
259	1437	174	···	18.505 ± 0.024	18.190 ± 0.019	17.955 ± 0.017	17.254 ± 0.029
260	1438		18.053 ± 0.025	19.280 ± 0.025	19.007 ± 0.021	18.691 ± 0.018	18.684 ± 0.036
261	1442		···	···	···	19.191 ± 0.029	18.555 ± 0.037
262	1443		18.977 ± 0.027	19.236 ± 0.026	18.870 ± 0.021	18.390 ± 0.019	···
263	1444	560	···	···	18.896 ± 0.019	···	···
264	1448	564	···	19.243 ± 0.028	19.479 ± 0.021	18.966 ± 0.021	18.873 ± 0.031
265	1457		···	···	···	···	17.472 ± 0.029
266	1458	178	···	···	···	15.565 ± 0.027	14.973 ± 0.030
267	1460		17.620 ± 0.025	17.686 ± 0.023	16.929 ± 0.017	16.755 ± 0.015	16.197 ± 0.030
268	1466	181	18.751 ± 0.026	18.756 ± 0.020	18.446 ± 0.019	18.261 ± 0.018	···
269	1467		20.106 ± 0.038	20.247 ± 0.034	19.577 ± 0.032	···	···
270	1469		···	19.496 ± 0.029	19.322 ± 0.024	19.060 ± 0.024	···
271	1472	567	···	···	···	···	18.476 ± 0.032
272	1475		19.112 ± 0.033	···	···	···	18.170 ± 0.032
273	1476		···	···	···	···	18.459 ± 0.036
274	1477		18.180 ± 0.025	19.031 ± 0.025	19.059 ± 0.020	19.050 ± 0.020	18.803 ± 0.036
275	1479		19.535 ± 0.033	19.608 ± 0.032	19.110 ± 0.026	18.853 ± 0.024	···
276	1481		···	18.930 ± 0.022	18.920 ± 0.024	18.818 ± 0.029	18.375 ± 0.032
277	1485		···	19.051 ± 0.025	19.021 ± 0.021	18.639 ± 0.021	18.186 ± 0.034
278	1486		···	19.497 ± 0.028	19.216 ± 0.024	18.866 ± 0.023	18.484 ± 0.037
279	1487	184	···	···	18.828 ± 0.021	18.214 ± 0.018	17.656 ± 0.031
280	1496		···	···	···	19.483 ± 0.036	···
281	1501		···	19.662 ± 0.034	19.111 ± 0.029	···	···
282	1503		···	17.245 ± 0.023	16.863 ± 0.017	16.690 ± 0.015	···
283	1504		18.236 ± 0.026	18.328 ± 0.024	17.961 ± 0.018	17.670 ± 0.016	17.336 ± 0.031
284	1506		···	19.276 ± 0.030	19.027 ± 0.026	18.995 ± 0.025	···
285	1507	186	19.426 ± 0.028	19.389 ± 0.026	18.801 ± 0.019	18.367 ± 0.017	···
286	1510	573	···	18.995 ± 0.024	18.244 ± 0.018	···	···
287	1511		···	19.758 ± 0.030	19.448 ± 0.026	19.153 ± 0.024	18.711 ± 0.035
288	1513	187	20.142 ± 0.036	20.461 ± 0.039	20.064 ± 0.035	19.783 ± 0.032	18.971 ± 0.038
289	1514		17.662 ± 0.055	17.823 ± 0.021	17.278 ± 0.022	16.871 ± 0.027	15.885 ± 0.070
290	1522	190	18.027 ± 0.025	18.269 ± 0.024	18.050 ± 0.018	17.800 ± 0.028	···
291	1524		···	18.420 ± 0.024	18.260 ± 0.018	18.077 ± 0.016	17.591 ± 0.031
292	1525	191	18.644 ± 0.026	18.604 ± 0.024	17.986 ± 0.019	17.917 ± 0.017	17.472 ± 0.031
293	1533		20.296 ± 0.040	20.152 ± 0.038	19.525 ± 0.032	19.182 ± 0.031	18.967 ± 0.043
294	1534	192	19.579 ± 0.030	19.624 ± 0.029	···	···	···
295	1540		17.088 ± 0.025	17.455 ± 0.023	17.225 ± 0.017	17.092 ± 0.027	···
296	1541		···	18.859 ± 0.025	19.073 ± 0.024	18.115 ± 0.017	18.917 ± 0.034
297	1543		···	···	18.306 ± 0.021	···	···
298	1545		17.719 ± 0.032	17.500 ± 0.019	16.808 ± 0.018	16.747 ± 0.017	15.953 ± 0.028
299	1547	199	···	17.875 ± 0.024	17.562 ± 0.018	···	···
300	1548		20.862 ± 0.047	20.744 ± 0.045	19.876 ± 0.030	19.233 ± 0.025	18.626 ± 0.036
301	1552	201	18.505 ± 0.032	18.882 ± 0.024	18.378 ± 0.019	18.314 ± 0.017	···
302	1553		19.199 ± 0.028	19.198 ± 0.026	18.706 ± 0.021	18.321 ± 0.019	17.784 ± 0.032
303	1557		17.221 ± 0.025	17.189 ± 0.023	16.767 ± 0.017	16.529 ± 0.015	16.243 ± 0.030

TABLE 1 — *Continued*

Our ID	SR ID	SM ID	U mag	B mag	V mag	R mag	I mag
304	1558		···	···	···	···	18.307 ± 0.034
305	1563		19.918 ± 0.036	···	···	···	···
306	1564		17.819 ± 0.025	18.433 ± 0.024	17.818 ± 0.018	17.369 ± 0.016	17.077 ± 0.030
307	1565		17.390 ± 0.025	18.890 ± 0.025	18.749 ± 0.020	18.044 ± 0.028	···
308	1566	206	17.986 ± 0.032	17.837 ± 0.019	17.200 ± 0.017	16.620 ± 0.015	16.075 ± 0.030
309	1569		18.224 ± 0.032	18.541 ± 0.020	18.359 ± 0.019	18.259 ± 0.018	18.023 ± 0.029
310	1570		18.749 ± 0.032	17.772 ± 0.019	16.785 ± 0.018	16.402 ± 0.017	···
311	1580		18.626 ± 0.026	18.668 ± 0.024	17.986 ± 0.018	17.570 ± 0.016	17.182 ± 0.030
312	1582	214	17.543 ± 0.025	17.948 ± 0.023	17.663 ± 0.017	17.353 ± 0.016	16.883 ± 0.030
313	1584		18.912 ± 0.032	17.760 ± 0.019	17.179 ± 0.018	16.570 ± 0.017	16.012 ± 0.028
314	1587		21.180 ± 0.050	20.716 ± 0.034	19.667 ± 0.023	18.940 ± 0.021	18.175 ± 0.029
315	1589		20.340 ± 0.037	20.323 ± 0.037	19.981 ± 0.032	19.612 ± 0.031	18.995 ± 0.040
316	1599		18.015 ± 0.032	···	···	19.027 ± 0.020	18.701 ± 0.031
317	1601	222	16.523 ± 0.025	···	16.519 ± 0.017	16.239 ± 0.015	···
318	1603		17.154 ± 0.025	17.544 ± 0.023	17.221 ± 0.017	16.996 ± 0.015	16.726 ± 0.030
319	1605		17.141 ± 0.055	···	16.883 ± 0.022	16.681 ± 0.027	16.183 ± 0.070
320	1606		···	···	19.535 ± 0.029	18.848 ± 0.030	17.853 ± 0.071
321	1607		17.942 ± 0.025	17.264 ± 0.023	16.331 ± 0.017	15.715 ± 0.015	14.980 ± 0.070
322	1609		···	···	···	18.810 ± 0.022	19.067 ± 0.038
323	1610		···	19.410 ± 0.022	18.994 ± 0.021	18.560 ± 0.020	18.794 ± 0.035
324	1614		···	19.214 ± 0.023	19.093 ± 0.021	18.493 ± 0.020	18.247 ± 0.034
325	1617	229	18.977 ± 0.056	19.529 ± 0.027	18.764 ± 0.022	18.314 ± 0.020	17.782 ± 0.032
326	1619		···	19.236 ± 0.023	18.886 ± 0.023	···	···
327	1625		···	19.820 ± 0.025	19.366 ± 0.027	18.823 ± 0.023	19.085 ± 0.040
328	1626		···	19.771 ± 0.023	19.492 ± 0.025	19.159 ± 0.026	19.381 ± 0.040
329	1628	235	19.615 ± 0.031	19.324 ± 0.029	18.876 ± 0.023	18.743 ± 0.019	18.114 ± 0.031
330	1633		18.101 ± 0.025	18.265 ± 0.024	18.021 ± 0.018	17.831 ± 0.016	···
331	1640		20.702 ± 0.042	20.351 ± 0.030	19.803 ± 0.029	19.348 ± 0.027	18.722 ± 0.032
332	1657		···	17.043 ± 0.019	16.946 ± 0.018	16.895 ± 0.015	16.732 ± 0.028
333	1664		···	···	17.701 ± 0.018	17.327 ± 0.016	···
334	1665	257	···	···	17.540 ± 0.017	17.150 ± 0.015	17.473 ± 0.030
335	1666		···	18.082 ± 0.024	18.100 ± 0.018	17.913 ± 0.018	···
336	1667	587	19.484 ± 0.029	19.830 ± 0.023	19.654 ± 0.024	···	18.105 ± 0.033
337	1669	260	···	···	16.070 ± 0.017	···	···
338	1670		···	···	18.502 ± 0.023	···	19.996 ± 0.044
339	1672	261	17.128 ± 0.055	16.613 ± 0.023	16.030 ± 0.017	15.684 ± 0.015	15.084 ± 0.028
340	1673	262	···	19.189 ± 0.027	18.888 ± 0.022	18.546 ± 0.020	17.642 ± 0.032
341	1676		19.037 ± 0.027	19.167 ± 0.026	18.748 ± 0.020	18.398 ± 0.018	···
342	1679	264	18.815 ± 0.027	18.802 ± 0.022	···	···	···
343	1684		···	···	16.400 ± 0.017	15.624 ± 0.015	14.838 ± 0.070
344	1686		16.796 ± 0.055	18.500 ± 0.024	18.333 ± 0.019	···	18.082 ± 0.033
345	1696		19.387 ± 0.028	19.622 ± 0.028	18.892 ± 0.023	18.837 ± 0.022	18.130 ± 0.033
346	1697		17.785 ± 0.025	18.151 ± 0.024	17.929 ± 0.018	17.772 ± 0.016	17.550 ± 0.031
347	1698		17.848 ± 0.032	···	···	17.876 ± 0.018	17.313 ± 0.028
348	1699	270	···	18.056 ± 0.024	···	···	···
349	1702	271	···	18.888 ± 0.026	18.329 ± 0.020	18.070 ± 0.019	···
350	1703	588	20.252 ± 0.042	20.665 ± 0.027	20.080 ± 0.024	19.433 ± 0.025	19.698 ± 0.037
351	1704	273	···	···	16.305 ± 0.017	15.756 ± 0.015	···
352	1707	274	17.845 ± 0.026	19.146 ± 0.026	···	···	19.305 ± 0.044
353	1709	589	19.967 ± 0.035	19.615 ± 0.022	18.905 ± 0.020	18.282 ± 0.019	17.706 ± 0.032
354	1710	275	18.250 ± 0.032	17.959 ± 0.019	16.977 ± 0.018	16.124 ± 0.017	···
355	1717		···	16.990 ± 0.023	16.303 ± 0.017	15.812 ± 0.015	···
356	1721	590	17.720 ± 0.032	···	···	···	···
357	1724	289	17.627 ± 0.026	17.732 ± 0.024	17.331 ± 0.018	17.121 ± 0.016	···
358	1727	291	···	18.017 ± 0.024	17.721 ± 0.018	17.417 ± 0.017	17.045 ± 0.030
359	1733	298	···	17.630 ± 0.024	17.582 ± 0.022	17.549 ± 0.027	17.285 ± 0.031
360	1735		16.867 ± 0.025	16.744 ± 0.023	16.022 ± 0.017	15.211 ± 0.015	···
361	1740	302	18.421 ± 0.026	18.896 ± 0.025	18.833 ± 0.020	···	···
362	1741		···	18.647 ± 0.024	18.390 ± 0.020	18.467 ± 0.019	18.424 ± 0.034
363	1742	303	16.349 ± 0.025	17.587 ± 0.023	17.342 ± 0.018	16.750 ± 0.016	17.416 ± 0.031
364	1743		20.666 ± 0.062	20.647 ± 0.039	19.588 ± 0.030	19.158 ± 0.031	19.095 ± 0.035
365	1745		···	···	18.021 ± 0.018	···	18.142 ± 0.032
366	1749		19.428 ± 0.028	19.768 ± 0.022	19.259 ± 0.022	···	···
367	1750	306	18.851 ± 0.027	18.791 ± 0.025	18.321 ± 0.019	···	···
368	1751	308	17.705 ± 0.025	18.188 ± 0.024	18.067 ± 0.018	17.575 ± 0.016	17.629 ± 0.031
369	1752	307	19.284 ± 0.029	19.431 ± 0.029	19.155 ± 0.025	19.048 ± 0.024	18.834 ± 0.037
370	1753		19.530 ± 0.029	19.672 ± 0.029	19.280 ± 0.026	19.017 ± 0.024	19.017 ± 0.038
371	1754		17.621 ± 0.025	18.078 ± 0.023	17.765 ± 0.018	17.558 ± 0.017	···
372	1756		19.483 ± 0.031	19.535 ± 0.030	19.001 ± 0.024	18.935 ± 0.021	···
373	1757	312	···	18.546 ± 0.023	18.353 ± 0.024	···	···
374	1761		21.056 ± 0.065	20.474 ± 0.032	19.389 ± 0.026	18.791 ± 0.029	18.007 ± 0.071
375	1763		19.545 ± 0.028	19.746 ± 0.028	19.356 ± 0.022	19.209 ± 0.023	···
376	1764		20.838 ± 0.065	20.957 ± 0.045	20.282 ± 0.042	19.588 ± 0.033	19.051 ± 0.041
377	1765	316	17.262 ± 0.025	17.204 ± 0.023	16.370 ± 0.017	16.009 ± 0.027	···
378	1766	594	19.345 ± 0.030	19.444 ± 0.029	18.976 ± 0.024	18.512 ± 0.021	17.842 ± 0.032
379	1767		19.833 ± 0.029	19.862 ± 0.027	19.278 ± 0.022	18.806 ± 0.030	···

TABLE 1 — *Continued*

Our ID	SR ID	SM ID	U mag	B mag	V mag	R mag	I mag
380	1770		···	19.278 ± 0.024	19.342 ± 0.025	···	18.444 ± 0.035
381	1773		···	···	···	18.864 ± 0.028	18.566 ± 0.040
382	1774		···	18.998 ± 0.026	18.598 ± 0.022	···	···
383	1776		···	···	17.150 ± 0.017	16.936 ± 0.015	16.664 ± 0.030
384	1779		···	···	···	16.131 ± 0.027	···
385	1781	322	19.290 ± 0.028	19.385 ± 0.026	18.910 ± 0.021	18.468 ± 0.020	17.904 ± 0.033
386	1784		···	···	17.759 ± 0.018	17.553 ± 0.016	···
387	1787		···	···	···	15.197 ± 0.027	···
388	1794		18.940 ± 0.027	19.086 ± 0.025	18.812 ± 0.020	18.441 ± 0.019	17.778 ± 0.033
389	1796	327	···	18.506 ± 0.020	18.204 ± 0.020	18.288 ± 0.019	17.986 ± 0.033
390	1798		18.692 ± 0.026	17.835 ± 0.023	16.852 ± 0.017	16.178 ± 0.015	15.976 ± 0.030
391	1799		16.260 ± 0.025	16.281 ± 0.023	15.523 ± 0.017	···	···
392	1800		19.062 ± 0.027	19.466 ± 0.028	19.277 ± 0.024	19.101 ± 0.024	18.706 ± 0.037
393	1802		···	17.583 ± 0.024	17.323 ± 0.018	17.077 ± 0.016	···
394	1803		19.903 ± 0.035	20.013 ± 0.025	19.180 ± 0.021	18.402 ± 0.019	17.767 ± 0.031
395	1806		20.214 ± 0.037	20.146 ± 0.026	19.810 ± 0.027	19.450 ± 0.029	19.187 ± 0.037
396	1811		···	···	18.675 ± 0.020	···	···
397	1812		···	17.126 ± 0.023	17.154 ± 0.022	17.215 ± 0.027	17.129 ± 0.030
398	1817		···	···	···	18.671 ± 0.024	18.805 ± 0.039
399	1819	333	18.223 ± 0.032	18.193 ± 0.024	17.709 ± 0.018	17.294 ± 0.016	···
400	1820		15.666 ± 0.025	16.111 ± 0.023	15.520 ± 0.017	15.144 ± 0.015	···
401	1821		···	18.830 ± 0.025	18.646 ± 0.020	18.036 ± 0.017	···
402	1822		···	17.638 ± 0.023	17.233 ± 0.017	16.822 ± 0.015	···
403	1823		19.681 ± 0.030	19.611 ± 0.028	19.015 ± 0.022	18.578 ± 0.020	18.410 ± 0.033
404	1824	335	···	18.453 ± 0.024	18.099 ± 0.018	17.750 ± 0.017	17.245 ± 0.031
405	1827		···	19.487 ± 0.028	19.468 ± 0.023	19.099 ± 0.025	19.087 ± 0.038
406	1829		16.485 ± 0.025	16.862 ± 0.023	16.456 ± 0.018	16.130 ± 0.017	···
407	1830		18.500 ± 0.026	19.136 ± 0.025	18.606 ± 0.019	18.337 ± 0.018	18.258 ± 0.032
408	1833	338	···	···	19.535 ± 0.025	19.333 ± 0.025	19.096 ± 0.038
409	1836		···	18.117 ± 0.024	18.042 ± 0.018	17.833 ± 0.018	17.763 ± 0.029
410	1837		21.178 ± 0.066	19.902 ± 0.030	19.831 ± 0.033	19.596 ± 0.036	19.126 ± 0.074
411	1841		···	18.652 ± 0.024	18.507 ± 0.019	18.455 ± 0.019	18.453 ± 0.034
412	1843		17.586 ± 0.025	18.515 ± 0.024	18.397 ± 0.019	18.506 ± 0.018	···
413	1844		···	···	···	19.709 ± 0.033	19.276 ± 0.045
414	1845		18.861 ± 0.027	19.136 ± 0.024	···	···	···
415	1846		20.746 ± 0.061	20.903 ± 0.038	19.824 ± 0.032	19.143 ± 0.031	18.335 ± 0.071
416	1849	596	17.851 ± 0.032	18.288 ± 0.020	18.089 ± 0.019	17.864 ± 0.018	17.655 ± 0.031
417	1850		19.318 ± 0.028	19.521 ± 0.027	19.170 ± 0.022	18.835 ± 0.021	···
418	1855		···	17.958 ± 0.023	17.519 ± 0.018	17.350 ± 0.017	17.031 ± 0.028
419	1856		···	···	18.978 ± 0.023	19.090 ± 0.024	18.283 ± 0.035
420	1857		17.434 ± 0.032	18.894 ± 0.020	18.982 ± 0.019	18.977 ± 0.019	···
421	1859		···	17.002 ± 0.021	16.955 ± 0.022	16.786 ± 0.027	···
422	1866		···	···	18.377 ± 0.019	17.793 ± 0.018	17.678 ± 0.030
423	1867		17.963 ± 0.025	18.695 ± 0.020	18.404 ± 0.019	18.409 ± 0.019	18.504 ± 0.030
424	1868		···	···	18.154 ± 0.023	···	···
425	1870		17.702 ± 0.026	18.082 ± 0.024	17.828 ± 0.023	···	···
426	1872	345	18.686 ± 0.032	18.695 ± 0.020	18.366 ± 0.019	18.072 ± 0.018	17.527 ± 0.028
427	1874	346	18.412 ± 0.032	18.843 ± 0.020	18.200 ± 0.019	17.386 ± 0.017	16.527 ± 0.030
428	1875	347	18.724 ± 0.026	18.759 ± 0.025	···	···	···
429	1877		21.224 ± 0.070	···	···	···	···
430	1880	350	18.415 ± 0.032	18.256 ± 0.020	17.785 ± 0.019	17.534 ± 0.017	···
431	1887		17.287 ± 0.025	16.799 ± 0.023	15.951 ± 0.017	15.408 ± 0.027	···
432	1888	351	18.429 ± 0.032	18.321 ± 0.020	17.954 ± 0.019	17.740 ± 0.018	17.411 ± 0.031
433	1892		···	19.457 ± 0.026	19.189 ± 0.022	18.948 ± 0.021	18.483 ± 0.034
434	1896	353	17.620 ± 0.025	17.807 ± 0.023	17.458 ± 0.018	17.131 ± 0.016	16.795 ± 0.031
435	1897		18.366 ± 0.055	18.425 ± 0.022	17.706 ± 0.022	17.175 ± 0.027	16.131 ± 0.070
436	1899		···	···	···	···	18.139 ± 0.071
437	1900		19.091 ± 0.027	19.257 ± 0.026	18.934 ± 0.021	18.648 ± 0.021	18.303 ± 0.034
438	1901	355	17.670 ± 0.025	17.979 ± 0.024	17.635 ± 0.018	···	···
439	1904		18.846 ± 0.026	19.148 ± 0.021	18.985 ± 0.021	18.912 ± 0.021	···
440	1905		···	···	···	18.239 ± 0.028	17.236 ± 0.030
441	1909		···	18.679 ± 0.022	18.508 ± 0.018	18.172 ± 0.017	17.544 ± 0.031
442	1911		···	17.514 ± 0.019	16.630 ± 0.018	16.023 ± 0.017	···
443	1912		18.568 ± 0.026	18.924 ± 0.024	18.591 ± 0.019	···	···
444	1915		18.830 ± 0.026	18.762 ± 0.025	18.272 ± 0.019	17.910 ± 0.017	···
445	1918		19.513 ± 0.031	19.952 ± 0.033	19.379 ± 0.029	19.299 ± 0.028	18.627 ± 0.038
446	1919	360	19.639 ± 0.032	19.892 ± 0.030	18.984 ± 0.020	18.554 ± 0.019	···
447	1921		19.548 ± 0.030	19.880 ± 0.032	19.512 ± 0.029	19.539 ± 0.032	20.552 ± 0.046
448	1922		20.011 ± 0.034	20.029 ± 0.034	19.511 ± 0.029	19.177 ± 0.027	···
449	1923		···	···	18.747 ± 0.022	18.330 ± 0.019	18.733 ± 0.038
450	1931		···	19.333 ± 0.026	19.169 ± 0.021	18.636 ± 0.021	18.385 ± 0.034
451	1932	598	20.372 ± 0.038	20.411 ± 0.030	19.985 ± 0.032	19.686 ± 0.034	19.306 ± 0.039
452	1937		18.137 ± 0.025	18.826 ± 0.024	18.451 ± 0.019	18.341 ± 0.019	18.220 ± 0.029
453	1939		19.966 ± 0.036	19.989 ± 0.026	19.610 ± 0.026	18.920 ± 0.024	···
454	1941		···	19.415 ± 0.026	18.859 ± 0.021	18.658 ± 0.020	18.490 ± 0.034
455	1944	599	20.242 ± 0.035	20.381 ± 0.026	19.892 ± 0.026	19.369 ± 0.025	···

TABLE 1 — *Continued*

Our ID	SR ID	SM ID	U mag	B mag	V mag	R mag	I mag
456	1950		···	···	17.845 ± 0.018	···	···
457	1953		···	16.979 ± 0.023	16.752 ± 0.017	16.573 ± 0.015	16.188 ± 0.030
458	1955		17.745 ± 0.032	17.372 ± 0.019	17.110 ± 0.018	16.383 ± 0.017	···
459	1957	371	16.901 ± 0.025	17.141 ± 0.019	···	···	···
460	1959	372	18.786 ± 0.026	18.769 ± 0.020	18.438 ± 0.019	18.166 ± 0.018	17.701 ± 0.029
461	1961		19.609 ± 0.056	18.595 ± 0.022	17.528 ± 0.022	16.723 ± 0.027	15.493 ± 0.070
462	1962		···	···	···	···	18.468 ± 0.037
463	1965		17.519 ± 0.025	17.477 ± 0.023	16.757 ± 0.017	16.311 ± 0.015	15.885 ± 0.030
464	1967		···	21.400 ± 0.049	19.522 ± 0.026	18.743 ± 0.020	17.829 ± 0.029
465	1970		16.327 ± 0.032	16.647 ± 0.019	16.413 ± 0.018	16.242 ± 0.017	16.276 ± 0.030
466	1973		20.108 ± 0.037	19.954 ± 0.035	19.397 ± 0.028	18.947 ± 0.025	18.469 ± 0.035
467	1976	375	19.988 ± 0.036	19.924 ± 0.033	19.417 ± 0.028	···	···
468	1977		···	···	···	···	18.195 ± 0.034
469	1978	376	···	18.625 ± 0.025	18.278 ± 0.020	···	···
470	1980		···	19.411 ± 0.029	19.396 ± 0.027	···	18.876 ± 0.039
471	1982		19.370 ± 0.027	18.205 ± 0.024	16.766 ± 0.017	15.660 ± 0.015	···
472	1984		19.225 ± 0.033	19.201 ± 0.021	18.786 ± 0.021	18.373 ± 0.020	17.708 ± 0.030
473	1985		18.183 ± 0.032	17.650 ± 0.019	16.832 ± 0.018	16.685 ± 0.017	15.864 ± 0.028
474	1987		···	···	···	···	17.590 ± 0.031
475	1988		17.242 ± 0.025	17.832 ± 0.023	16.971 ± 0.017	16.662 ± 0.015	16.689 ± 0.030
476	1993		19.792 ± 0.031	19.978 ± 0.032	19.523 ± 0.026	19.116 ± 0.024	···
477	1995		17.276 ± 0.032	17.439 ± 0.019	16.690 ± 0.018	16.226 ± 0.017	15.687 ± 0.028
478	1996		18.854 ± 0.028	19.134 ± 0.027	18.795 ± 0.023	···	···
479	1997		16.497 ± 0.025	17.326 ± 0.023	17.216 ± 0.017	17.114 ± 0.015	17.005 ± 0.030
480	1998		18.489 ± 0.026	17.389 ± 0.023	16.270 ± 0.017	15.485 ± 0.015	···
481	1999	382	19.250 ± 0.028	19.373 ± 0.021	19.058 ± 0.020	18.760 ± 0.020	17.989 ± 0.030
482	2000	383	19.326 ± 0.030	19.537 ± 0.030	19.258 ± 0.025	···	···
483	2001		17.661 ± 0.055	17.713 ± 0.021	17.134 ± 0.022	16.710 ± 0.027	···
484	2002		19.875 ± 0.036	19.568 ± 0.032	···	···	···
485	2003		···	···	17.467 ± 0.022	16.790 ± 0.027	···
486	2004		18.055 ± 0.032	18.077 ± 0.019	17.760 ± 0.018	17.515 ± 0.018	17.123 ± 0.028
487	2005		19.505 ± 0.028	19.653 ± 0.028	18.966 ± 0.023	18.934 ± 0.031	···
488	2011		19.581 ± 0.029	19.674 ± 0.029	19.280 ± 0.025	19.002 ± 0.024	18.644 ± 0.036
489	2013		20.180 ± 0.061	20.486 ± 0.038	19.525 ± 0.029	18.832 ± 0.022	18.107 ± 0.032
490	2016		18.934 ± 0.028	18.887 ± 0.026	18.082 ± 0.019	17.475 ± 0.017	16.822 ± 0.031
491	2018		21.332 ± 0.052	21.351 ± 0.045	20.074 ± 0.029	19.072 ± 0.023	18.214 ± 0.030
492	2020		16.075 ± 0.025	17.050 ± 0.019	16.604 ± 0.017	16.727 ± 0.017	16.670 ± 0.030
493	2023		···	17.989 ± 0.024	17.376 ± 0.018	16.877 ± 0.016	16.403 ± 0.030
494	2024		19.191 ± 0.028	19.233 ± 0.027	18.628 ± 0.019	18.007 ± 0.017	17.368 ± 0.031
495	2026	388	18.171 ± 0.026	18.398 ± 0.024	···	···	···
496	2029		···	19.669 ± 0.033	19.585 ± 0.032	···	···
497	2030		20.592 ± 0.044	20.446 ± 0.042	20.036 ± 0.038	19.680 ± 0.037	19.446 ± 0.047
498	2033	389	18.111 ± 0.026	18.428 ± 0.020	18.145 ± 0.019	17.790 ± 0.018	···
499	2035		···	···	18.367 ± 0.020	···	···
500	2042		19.064 ± 0.033	19.325 ± 0.021	19.436 ± 0.021	19.728 ± 0.036	···
501	2043	392	17.923 ± 0.026	18.089 ± 0.024	···	···	···
502	2046		18.376 ± 0.026	18.307 ± 0.024	17.800 ± 0.018	17.493 ± 0.017	16.921 ± 0.028
503	2047		18.472 ± 0.032	18.838 ± 0.020	18.639 ± 0.019	18.458 ± 0.018	17.813 ± 0.029
504	2048		···	18.994 ± 0.027	19.154 ± 0.027	19.123 ± 0.027	18.744 ± 0.040
505	2050	395	15.613 ± 0.025	16.016 ± 0.023	···	···	···
506	2054	396	18.983 ± 0.033	19.073 ± 0.020	18.792 ± 0.020	18.478 ± 0.020	18.387 ± 0.033
507	2057		20.708 ± 0.039	21.319 ± 0.057	20.677 ± 0.044	19.943 ± 0.033	···
508	2058		18.745 ± 0.032	19.188 ± 0.020	18.959 ± 0.020	···	···
509	2061		19.118 ± 0.027	19.405 ± 0.026	18.974 ± 0.021	18.815 ± 0.022	18.670 ± 0.036
510	2063		19.011 ± 0.028	18.829 ± 0.025	18.084 ± 0.023	···	···
511	2066		···	18.528 ± 0.024	17.777 ± 0.018	17.439 ± 0.016	17.136 ± 0.030
512	2072		18.902 ± 0.026	17.833 ± 0.023	16.566 ± 0.017	15.667 ± 0.015	···
513	2075	402	17.753 ± 0.032	17.680 ± 0.019	16.991 ± 0.018	16.462 ± 0.017	15.861 ± 0.028
514	2086		···	18.456 ± 0.024	18.173 ± 0.019	17.904 ± 0.017	17.507 ± 0.031
515	2092	406	19.852 ± 0.032	21.405 ± 0.036	20.462 ± 0.029	19.933 ± 0.026	19.136 ± 0.035
516	2094		···	20.400 ± 0.028	18.595 ± 0.019	17.385 ± 0.017	16.243 ± 0.030
517	2095		···	17.891 ± 0.023	17.603 ± 0.017	17.317 ± 0.016	···
518	2096		19.404 ± 0.028	19.216 ± 0.027	19.044 ± 0.023	18.855 ± 0.023	18.622 ± 0.036
519	2101		17.469 ± 0.025	19.062 ± 0.025	18.608 ± 0.020	17.899 ± 0.018	18.444 ± 0.036
520	2103		···	16.026 ± 0.019	15.281 ± 0.018	14.873 ± 0.017	···
521	2106		19.816 ± 0.030	19.640 ± 0.028	18.831 ± 0.020	18.301 ± 0.018	17.691 ± 0.031
522	2107		18.897 ± 0.026	19.136 ± 0.020	18.718 ± 0.020	18.650 ± 0.019	18.455 ± 0.030
523	2110		···	18.231 ± 0.019	17.305 ± 0.018	16.368 ± 0.017	···
524	2113		20.475 ± 0.063	20.349 ± 0.036	19.618 ± 0.028	18.814 ± 0.029	17.835 ± 0.070
525	2114		···	20.095 ± 0.036	20.208 ± 0.032	20.458 ± 0.038	···
526	2115	409	19.566 ± 0.032	19.443 ± 0.030	19.109 ± 0.024	18.547 ± 0.021	···
527	2116		19.316 ± 0.028	19.958 ± 0.032	19.728 ± 0.030	19.461 ± 0.032	19.015 ± 0.042
528	2119	410	18.060 ± 0.025	18.361 ± 0.020	···	···	···
529	2121		···	···	···	19.410 ± 0.035	···
530	2126	413	···	18.431 ± 0.022	···	···	···
531	2132	416	19.592 ± 0.033	19.553 ± 0.022	18.790 ± 0.020	18.168 ± 0.019	17.567 ± 0.029

TABLE 1 — *Continued*

Our ID	SR ID	SM ID	U mag	B mag	V mag	R mag	I mag
532	2136		···	···	20.164 ± 0.042	19.590 ± 0.036	19.219 ± 0.045
533	2145		17.243 ± 0.025	17.549 ± 0.023	16.499 ± 0.017	16.089 ± 0.015	16.104 ± 0.030
534	2149		19.036 ± 0.027	20.018 ± 0.034	20.049 ± 0.035	19.520 ± 0.033	···
535	2156		···	···	···	19.757 ± 0.040	18.791 ± 0.040
536	2174		17.098 ± 0.025	17.501 ± 0.023	16.834 ± 0.017	16.628 ± 0.015	16.412 ± 0.030
537	2176		···	···	···	···	18.745 ± 0.039
538	2177		17.517 ± 0.025	17.846 ± 0.024	17.600 ± 0.018	17.455 ± 0.017	17.025 ± 0.031
539	2181		17.907 ± 0.025	17.566 ± 0.023	16.771 ± 0.017	16.280 ± 0.015	16.217 ± 0.030
540	2185		19.239 ± 0.028	19.342 ± 0.027	19.012 ± 0.022	18.735 ± 0.022	18.437 ± 0.035
541	2189		···	···	17.942 ± 0.018	17.434 ± 0.015	16.621 ± 0.030
542	2193		···	20.318 ± 0.031	20.008 ± 0.037	···	···
543	2194		17.975 ± 0.025	17.910 ± 0.023	17.125 ± 0.017	16.616 ± 0.015	···
544	2198		···	18.656 ± 0.024	18.576 ± 0.018	18.250 ± 0.017	18.168 ± 0.032
545	2199		19.302 ± 0.028	19.557 ± 0.029	19.128 ± 0.024	18.797 ± 0.022	18.263 ± 0.034
546	2202		19.614 ± 0.029	20.734 ± 0.046	20.389 ± 0.042	19.188 ± 0.028	19.604 ± 0.050
547	2206		17.701 ± 0.025	18.130 ± 0.024	17.862 ± 0.018	···	···
548	2210		18.927 ± 0.026	19.940 ± 0.031	19.958 ± 0.031	19.231 ± 0.029	19.936 ± 0.055
549	2214		19.434 ± 0.028	19.461 ± 0.027	19.140 ± 0.022	18.804 ± 0.020	18.307 ± 0.034
550	2219		···	19.422 ± 0.027	19.164 ± 0.025	19.201 ± 0.027	19.295 ± 0.044
551	2221		20.285 ± 0.061	19.951 ± 0.031	18.811 ± 0.025	17.871 ± 0.028	16.868 ± 0.070
552	2222	428	18.180 ± 0.026	18.146 ± 0.024	17.406 ± 0.018	16.843 ± 0.016	16.299 ± 0.030
553	2231		17.449 ± 0.025	17.195 ± 0.023	16.306 ± 0.017	15.720 ± 0.015	···
554	2232		18.668 ± 0.027	18.550 ± 0.025	17.697 ± 0.019	17.072 ± 0.016	16.517 ± 0.030
555	2236	432	20.179 ± 0.036	20.307 ± 0.037	19.792 ± 0.033	19.439 ± 0.032	19.258 ± 0.044
556	2239		···	···	19.211 ± 0.023	···	18.745 ± 0.039
557	2243		···	18.971 ± 0.026	19.099 ± 0.023	18.877 ± 0.024	19.063 ± 0.041
558	2245		16.511 ± 0.025	16.669 ± 0.023	16.102 ± 0.017	···	15.395 ± 0.030
559	2249		17.905 ± 0.025	···	18.943 ± 0.021	18.505 ± 0.018	18.425 ± 0.036
560	2250		19.716 ± 0.032	19.890 ± 0.033	19.507 ± 0.028	19.053 ± 0.024	18.415 ± 0.033
561	2252		···	20.824 ± 0.042	20.212 ± 0.040	19.573 ± 0.037	18.910 ± 0.074
562	2284		16.759 ± 0.025	16.986 ± 0.023	16.290 ± 0.017	15.490 ± 0.015	15.493 ± 0.030
563	2285		19.382 ± 0.028	19.584 ± 0.027	19.323 ± 0.023	19.071 ± 0.023	18.792 ± 0.036
564	2286		18.104 ± 0.025	18.851 ± 0.024	18.823 ± 0.019	18.847 ± 0.019	18.880 ± 0.034
565	2290		18.167 ± 0.055	18.034 ± 0.021	17.278 ± 0.022	16.722 ± 0.027	15.686 ± 0.070
566	2291		···	···	···	19.239 ± 0.033	19.300 ± 0.077
567	2295		17.688 ± 0.025	17.353 ± 0.023	16.475 ± 0.017	15.563 ± 0.015	15.500 ± 0.030
568	2298		18.220 ± 0.026	19.404 ± 0.027	19.096 ± 0.021	18.684 ± 0.020	18.898 ± 0.040
569	2300		18.440 ± 0.026	18.576 ± 0.024	18.015 ± 0.018	17.645 ± 0.016	17.295 ± 0.030
570	2311		19.704 ± 0.034	19.839 ± 0.035	19.681 ± 0.033	19.422 ± 0.033	19.137 ± 0.044
571	2313		20.119 ± 0.036	19.049 ± 0.025	17.724 ± 0.018	16.968 ± 0.015	16.386 ± 0.030
572	2321		···	···	···	···	18.646 ± 0.036
573	2330		18.622 ± 0.055	18.258 ± 0.021	17.396 ± 0.022	16.738 ± 0.027	···
574	2333		19.584 ± 0.056	18.802 ± 0.022	17.495 ± 0.022	16.462 ± 0.027	···
575	2336		18.351 ± 0.026	18.667 ± 0.024	18.404 ± 0.018	17.874 ± 0.017	17.635 ± 0.031
576	2354		17.635 ± 0.025	18.952 ± 0.025	18.991 ± 0.021	18.698 ± 0.021	18.714 ± 0.038
577	2356		···	19.077 ± 0.027	19.323 ± 0.025	···	···
578	2367		20.403 ± 0.060	21.194 ± 0.050	20.538 ± 0.047	20.085 ± 0.044	19.392 ± 0.077
579	2373		···	···	···	18.521 ± 0.021	18.706 ± 0.038
580	2407		19.015 ± 0.027	19.136 ± 0.026	18.684 ± 0.020	18.082 ± 0.018	···
581	2420		19.333 ± 0.027	18.419 ± 0.024	17.286 ± 0.017	15.530 ± 0.015	···
582	2439		17.581 ± 0.025	···	16.611 ± 0.017	16.130 ± 0.015	16.068 ± 0.030
583	2442		···	···	19.842 ± 0.037	19.316 ± 0.033	18.769 ± 0.040
584	2443		19.599 ± 0.056	18.906 ± 0.022	17.678 ± 0.022	16.722 ± 0.027	···
585	2460		18.285 ± 0.026	18.275 ± 0.021	19.122 ± 0.019	16.709 ± 0.015	16.319 ± 0.030
586	2478		···	···	19.710 ± 0.032	18.990 ± 0.030	18.008 ± 0.071
587	2483		19.699 ± 0.029	18.759 ± 0.022	17.572 ± 0.022	16.276 ± 0.015	15.711 ± 0.070
588	2541		···	21.095 ± 0.048	19.846 ± 0.030	18.678 ± 0.029	17.670 ± 0.070
589	3		20.841 ± 0.045	20.666 ± 0.033	20.096 ± 0.031	19.726 ± 0.031	19.294 ± 0.039
590	61		19.786 ± 0.032	19.812 ± 0.031	19.097 ± 0.022	18.738 ± 0.023	18.080 ± 0.034
591	71		19.819 ± 0.034	19.631 ± 0.022	18.951 ± 0.022	18.355 ± 0.020	17.659 ± 0.030
592	76		19.191 ± 0.034	20.053 ± 0.024	19.781 ± 0.025	19.798 ± 0.026	19.307 ± 0.035
593	78		···	18.994 ± 0.026	18.691 ± 0.021	18.403 ± 0.020	···
594	81		···	19.249 ± 0.027	18.740 ± 0.022	···	···
595	83		19.844 ± 0.033	19.805 ± 0.031	19.515 ± 0.028	19.302 ± 0.028	18.861 ± 0.038
596	88		···	19.564 ± 0.026	19.398 ± 0.021	18.892 ± 0.020	18.480 ± 0.030
597	100		20.776 ± 0.051	20.798 ± 0.050	20.415 ± 0.048	20.390 ± 0.050	19.772 ± 0.082
598	118		19.691 ± 0.032	···	···	···	···
599	120		···	20.237 ± 0.027	19.715 ± 0.026	19.035 ± 0.024	18.546 ± 0.035
600	123		···	···	18.999 ± 0.023	18.844 ± 0.022	18.749 ± 0.037
601	127		···	19.348 ± 0.031	19.105 ± 0.025	18.707 ± 0.022	18.023 ± 0.033
602	130		19.457 ± 0.033	···	···	···	···
603	142		18.607 ± 0.028	19.892 ± 0.037	19.473 ± 0.028	18.348 ± 0.021	···
604	159		···	19.485 ± 0.029	···	···	···
605	161		18.834 ± 0.026	19.207 ± 0.025	18.922 ± 0.019	18.598 ± 0.018	18.160 ± 0.031
606	166		···	21.540 ± 0.056	20.069 ± 0.036	19.498 ± 0.023	18.576 ± 0.032
607	179		···	···	18.781 ± 0.024	18.545 ± 0.021	18.053 ± 0.033

TABLE 1 — *Continued*

Our ID	SR ID	SM ID	U mag	B mag	V mag	R mag	I mag
608	182		19.855 ± 0.033	19.836 ± 0.031	19.205 ± 0.023	18.721 ± 0.019	18.228 ± 0.032
609	189		20.348 ± 0.040	20.349 ± 0.041	19.832 ± 0.034	19.817 ± 0.036	···
610	193		20.315 ± 0.040	···	20.483 ± 0.047	19.944 ± 0.033	19.170 ± 0.037
611	196		21.612 ± 0.046	21.320 ± 0.036	20.852 ± 0.035	20.459 ± 0.045	19.602 ± 0.045
612	204		18.490 ± 0.027	19.124 ± 0.027	19.072 ± 0.023	18.790 ± 0.023	18.562 ± 0.035
613	207		19.018 ± 0.027	19.225 ± 0.027	19.244 ± 0.020	18.624 ± 0.020	···
614	208		19.971 ± 0.034	19.784 ± 0.021	19.369 ± 0.020	19.083 ± 0.020	18.455 ± 0.033
615	210		19.414 ± 0.032	19.869 ± 0.035	19.758 ± 0.034	19.575 ± 0.035	···
616	212		···	19.796 ± 0.031	19.315 ± 0.022	18.968 ± 0.021	18.239 ± 0.030
617	217		···	19.202 ± 0.028	18.943 ± 0.023	18.674 ± 0.021	18.112 ± 0.032
618	232		20.020 ± 0.034	19.897 ± 0.033	···	18.788 ± 0.029	···
619	233		···	19.036 ± 0.026	18.556 ± 0.020	18.008 ± 0.018	17.411 ± 0.031
620	236		19.495 ± 0.029	19.816 ± 0.028	19.378 ± 0.021	19.241 ± 0.022	19.164 ± 0.036
621	238		19.380 ± 0.028	19.293 ± 0.026	18.792 ± 0.020	18.480 ± 0.018	18.127 ± 0.031
622	240		19.433 ± 0.028	19.545 ± 0.027	19.170 ± 0.021	19.135 ± 0.029	···
623	242		···	···	···	···	18.509 ± 0.035
624	247		17.858 ± 0.055	···	···	···	···
625	253		20.236 ± 0.037	20.849 ± 0.047	21.014 ± 0.051	···	···
626	254		19.796 ± 0.033	20.152 ± 0.034	19.797 ± 0.029	19.685 ± 0.032	···
627	256		19.896 ± 0.035	20.277 ± 0.040	20.131 ± 0.041	19.987 ± 0.043	19.882 ± 0.078
628	265		···	18.422 ± 0.025	···	···	···
629	266		20.614 ± 0.038	20.667 ± 0.041	19.953 ± 0.029	19.473 ± 0.030	19.027 ± 0.042
630	279		20.272 ± 0.032	19.564 ± 0.026	17.786 ± 0.018	16.584 ± 0.015	15.842 ± 0.030
631	282		18.676 ± 0.027	18.917 ± 0.026	···	···	···
632	287		18.727 ± 0.026	19.070 ± 0.027	19.000 ± 0.024	18.830 ± 0.025	19.610 ± 0.051
633	292		···	18.833 ± 0.023	18.514 ± 0.020	18.084 ± 0.019	17.612 ± 0.032
634	293		···	18.860 ± 0.024	19.559 ± 0.032	19.072 ± 0.029	18.661 ± 0.039
635	294		19.126 ± 0.031	19.770 ± 0.033	19.359 ± 0.029	···	···
636	296		19.549 ± 0.030	19.503 ± 0.028	19.017 ± 0.023	18.604 ± 0.021	···
637	310		···	···	20.483 ± 0.036	19.704 ± 0.033	···
638	311		···	20.644 ± 0.047	19.940 ± 0.034	19.494 ± 0.034	···
639	320		···	···	16.315 ± 0.017	16.308 ± 0.015	16.026 ± 0.030
640	342		18.605 ± 0.027	19.206 ± 0.026	19.080 ± 0.023	18.999 ± 0.024	19.031 ± 0.039
641	361		19.718 ± 0.031	20.010 ± 0.033	19.696 ± 0.030	19.673 ± 0.035	···
642	377		···	18.530 ± 0.022	18.266 ± 0.020	18.074 ± 0.019	···
643	393		20.046 ± 0.033	19.803 ± 0.033	19.433 ± 0.029	19.123 ± 0.028	18.780 ± 0.040
644	405		19.520 ± 0.028	19.940 ± 0.023	19.684 ± 0.025	19.798 ± 0.026	19.592 ± 0.039
645	411		19.712 ± 0.034	19.634 ± 0.032	19.136 ± 0.026	18.718 ± 0.024	18.569 ± 0.033
646	412		19.884 ± 0.036	20.083 ± 0.038	19.418 ± 0.031	18.970 ± 0.023	18.523 ± 0.032
647	419		17.901 ± 0.025	18.697 ± 0.024	···	···	···
648	422		19.806 ± 0.033	19.472 ± 0.032	19.305 ± 0.028	18.800 ± 0.024	17.906 ± 0.032
649	426		···	···	···	···	19.345 ± 0.046
650	452		19.918 ± 0.032	20.131 ± 0.032	19.750 ± 0.027	19.454 ± 0.027	19.151 ± 0.043
651	466		···	···	···	19.016 ± 0.026	···
652	468		19.500 ± 0.029	19.666 ± 0.029	19.214 ± 0.023	18.769 ± 0.022	···
653	469		20.336 ± 0.040	20.035 ± 0.036	19.642 ± 0.028	18.807 ± 0.024	···
654	485		20.988 ± 0.045	20.692 ± 0.033	20.042 ± 0.031	19.531 ± 0.030	19.465 ± 0.040
655	487		20.046 ± 0.035	20.368 ± 0.027	20.146 ± 0.029	19.871 ± 0.034	19.455 ± 0.043
656	488		···	19.556 ± 0.033	19.609 ± 0.032	···	···
657	489		20.330 ± 0.038	20.444 ± 0.026	19.809 ± 0.025	···	18.561 ± 0.034
658	490		20.964 ± 0.047	20.753 ± 0.038	20.314 ± 0.039	···	···
659	491		20.208 ± 0.038	20.326 ± 0.029	20.115 ± 0.029	19.880 ± 0.028	19.437 ± 0.034
660	492		19.950 ± 0.036	19.867 ± 0.025	19.457 ± 0.025	···	···
661	494		···	···	21.182 ± 0.051	20.757 ± 0.049	···
662	495		20.235 ± 0.035	20.250 ± 0.024	19.554 ± 0.025	19.304 ± 0.026	19.127 ± 0.042
663	498		···	···	···	···	19.616 ± 0.043
664	506		19.046 ± 0.033	19.241 ± 0.022	18.966 ± 0.021	18.799 ± 0.021	18.432 ± 0.030
665	509		20.201 ± 0.038	20.228 ± 0.026	19.275 ± 0.028	···	···
666	513		21.223 ± 0.055	···	19.698 ± 0.032	19.397 ± 0.030	···
667	514		···	19.881 ± 0.023	19.479 ± 0.022	19.110 ± 0.023	18.395 ± 0.033
668	516		19.521 ± 0.032	19.629 ± 0.032	···	···	17.646 ± 0.032
669	517		···	21.652 ± 0.041	21.027 ± 0.038	20.499 ± 0.041	19.623 ± 0.046
670	518		20.656 ± 0.043	20.638 ± 0.036	20.359 ± 0.038	20.209 ± 0.042	···
671	519		19.584 ± 0.034	19.970 ± 0.025	19.470 ± 0.027	19.584 ± 0.031	19.549 ± 0.045
672	520		···	21.084 ± 0.055	20.235 ± 0.032	19.832 ± 0.031	19.319 ± 0.042
673	521		20.706 ± 0.037	20.752 ± 0.027	19.872 ± 0.035	19.342 ± 0.030	···
674	522		···	19.687 ± 0.032	20.469 ± 0.036	20.601 ± 0.035	20.279 ± 0.042
675	527		19.654 ± 0.034	19.860 ± 0.023	19.443 ± 0.023	18.999 ± 0.026	···
676	529		19.885 ± 0.036	20.040 ± 0.026	19.752 ± 0.028	19.298 ± 0.029	18.768 ± 0.037
677	530		···	···	···	19.016 ± 0.026	···
678	534		···	···	···	18.624 ± 0.024	18.441 ± 0.036
679	535		19.754 ± 0.034	19.954 ± 0.024	19.808 ± 0.026	19.711 ± 0.030	19.487 ± 0.041
680	536		18.967 ± 0.033	19.470 ± 0.021	19.361 ± 0.021	19.090 ± 0.022	18.300 ± 0.033
681	538		···	18.687 ± 0.025	···	···	···
682	540		20.432 ± 0.036	20.244 ± 0.025	19.582 ± 0.024	19.043 ± 0.023	18.118 ± 0.031
683	542		···	20.778 ± 0.036	20.446 ± 0.037	19.059 ± 0.023	18.358 ± 0.035

TABLE 1 — *Continued*

Our ID	SR ID	SM ID	U mag	B mag	V mag	R mag	I mag
684	546		20.437 ± 0.042	20.011 ± 0.029	19.311 ± 0.024	18.656 ± 0.024	17.809 ± 0.032
685	549		19.542 ± 0.028	20.161 ± 0.023	19.714 ± 0.026	19.927 ± 0.033	19.503 ± 0.041
686	552		···	21.270 ± 0.035	20.185 ± 0.028	19.538 ± 0.025	19.353 ± 0.034
687	553		19.084 ± 0.055	···	18.503 ± 0.019	···	···
688	554		19.655 ± 0.035	19.810 ± 0.024	19.366 ± 0.024	18.962 ± 0.026	···
689	557		18.199 ± 0.032	18.339 ± 0.020	18.114 ± 0.019	17.986 ± 0.016	17.746 ± 0.031
690	559		···	19.520 ± 0.028	19.105 ± 0.023	18.677 ± 0.021	18.405 ± 0.034
691	561		20.324 ± 0.035	20.242 ± 0.025	20.160 ± 0.029	20.167 ± 0.030	19.858 ± 0.044
692	562		19.307 ± 0.030	20.207 ± 0.035	19.849 ± 0.026	19.288 ± 0.025	···
693	563		19.162 ± 0.033	19.106 ± 0.026	18.791 ± 0.024	···	···
694	568		···	···	···	17.740 ± 0.016	···
695	569		20.313 ± 0.036	20.596 ± 0.027	20.164 ± 0.026	19.678 ± 0.024	19.069 ± 0.035
696	574		19.536 ± 0.034	19.109 ± 0.022	18.522 ± 0.021	18.595 ± 0.022	···
697	575		20.092 ± 0.036	19.875 ± 0.024	19.582 ± 0.024	19.273 ± 0.025	18.754 ± 0.036
698	577		21.263 ± 0.041	21.078 ± 0.031	20.612 ± 0.029	20.294 ± 0.029	···
699	578		21.131 ± 0.041	20.899 ± 0.031	20.420 ± 0.030	20.028 ± 0.029	20.127 ± 0.044
700	579		20.450 ± 0.036	20.350 ± 0.026	20.054 ± 0.026	19.804 ± 0.027	19.933 ± 0.056
701	583		···	···	···	17.417 ± 0.017	16.649 ± 0.030
702	584		···	···	···	18.941 ± 0.025	19.477 ± 0.047
703	586		18.030 ± 0.026	18.682 ± 0.025	18.595 ± 0.021	18.538 ± 0.019	18.365 ± 0.032
704	591		19.267 ± 0.033	19.417 ± 0.022	19.356 ± 0.025	19.202 ± 0.023	18.216 ± 0.036
705	592		19.726 ± 0.031	19.889 ± 0.025	19.497 ± 0.026	19.292 ± 0.027	18.578 ± 0.038
706	593		···	19.678 ± 0.029	19.123 ± 0.024	18.797 ± 0.022	18.454 ± 0.031
707	595		19.800 ± 0.034	20.052 ± 0.024	19.528 ± 0.026	19.219 ± 0.027	18.827 ± 0.036
708	597		20.193 ± 0.039	19.919 ± 0.027	19.376 ± 0.026	19.703 ± 0.033	18.264 ± 0.034

[a] 'SR' and 'SM' refer to the IDs of San Roman et al. (2010) and SM10, respectively.

TABLE 2
AGES, METALLICITIES AND MASSES OF THE M33 STAR CLUSTERS.

Object	Age (Gyr)	[Fe/H] (dex)	$\log(M_{cl})$ $[M_\odot]$
SR1001	2.510 ± 0.775	-2.301 ± 0.150	4.184 ± 0.144
SR1009	1.580 ± 0.260	0.477 ± 0.088	5.154 ± 0.175
SR1012	1.120 ± 0.259	-1.602 ± 0.122	4.148 ± 0.129
SR1013	0.006 ± 0.002	0.301 ± 1.049	2.688 ± 0.112
SR1020	1.580 ± 0.185	-0.824 ± 0.150	4.025 ± 0.100
SR1021	0.022 ± 0.008	-1.602 ± 0.122	3.032 ± 0.081
SR1022	3.160 ± 1.810	-2.301 ± 0.238	4.683 ± 0.244
SR1024	3.980 ± 1.400	-2.301 ± 0.150	4.565 ± 0.004
SR1028	2.000 ± 0.465	-0.699 ± 0.301	3.914 ± 0.059
SR1029	1.000 ± 0.233	-1.456 ± 0.412	3.666 ± 0.093
SR1030	0.022 ± 0.002	-1.602 ± 0.122	3.230 ± 0.186
SR1031	10.000 ± 2.760	-1.155 ± 0.316	5.516 ± 0.010
SR1041	0.631 ± 0.146	0.301 ± 0.238	3.896 ± 0.084
SR1049	12.600 ± 1.845	-2.301 ± 0.150	4.837 ± 0.032
SR1052	0.020 ± 0.002	-1.602 ± 0.122	2.674 ± 0.124
SR1059	3.980 ± 1.555	-1.699 ± 0.199	5.257 ± 0.131
SR1066	0.355 ± 0.169	-0.699 ± 0.850	4.051 ± 0.043
SR1074	11.200 ± 3.145	-2.301 ± 0.238	4.920 ± 0.001
SR1080	2.820 ± 1.250	-1.301 ± 0.301	4.508 ± 0.016
SR1083	12.600 ± 0.700	0.477 ± 0.040	6.177 ± 0.113
SR1087	1.260 ± 0.145	-1.602 ± 0.122	4.108 ± 0.006
SR1088	3.550 ± 0.410	-0.071 ± 0.051	4.874 ± 0.179
SR1090	6.310 ± 1.305	0.477 ± 0.040	5.205 ± 0.059
SR1102	0.794 ± 0.146	0.477 ± 0.040	4.326 ± 0.118
SR1103	0.126 ± 0.086	-1.155 ± 0.850	4.149 ± 0.033
SR1111	0.040 ± 0.013	-1.602 ± 0.122	3.765 ± 0.090
SR1112	0.025 ± 0.005	-0.699 ± 0.111	3.635 ± 0.017
SR1114	1.410 ± 0.260	-2.000 ± 0.350	4.293 ± 0.037
SR1115	3.550 ± 1.385	-2.301 ± 0.150	5.634 ± 0.102
SR1122	0.025 ± 0.004	-0.699 ± 0.111	3.176 ± 0.042
SR1124	0.025 ± 0.004	-0.699 ± 0.111	3.056 ± 0.030
SR1125	7.940 ± 0.915	0.301 ± 0.111	5.130 ± 0.013
SR1126	12.600 ± 2.330	-1.155 ± 0.228	5.002 ± 0.050
SR1129	0.316 ± 0.087	0.176 ± 0.398	3.608 ± 0.088
SR1133	0.016 ± 0.002	0.477 ± 0.040	3.018 ± 0.128
SR1134	0.126 ± 0.072	-1.301 ± 1.088	3.625 ± 0.046
SR1138	1.000 ± 0.233	0.176 ± 0.199	4.984 ± 0.002
SR1139	0.501 ± 0.213	-1.155 ± 0.228	4.544 ± 0.089
SR1143	8.910 ± 3.490	-1.824 ± 0.350	4.784 ± 0.096
SR1144	0.063 ± 0.022	-1.301 ± 0.301	3.286 ± 0.165
SR1146	0.025 ± 0.003	-0.699 ± 0.111	2.925 ± 0.054
SR1147	0.025 ± 0.004	-0.699 ± 0.111	2.583 ± 0.013
SR1148	0.501 ± 0.176	-0.523 ± 0.850	3.761 ± 0.097
SR1149	0.562 ± 0.320	-1.699 ± 0.573	3.965 ± 0.040
SR1150	0.447 ± 0.175	-1.155 ± 0.316	3.594 ± 0.115
SR1152	2.820 ± 0.870	-2.301 ± 0.150	4.375 ± 0.047
SR1154	1.000 ± 0.184	0.301 ± 0.150	4.204 ± 0.144
SR1161	10.000 ± 3.145	-1.824 ± 0.350	5.504 ± 0.010
SR1162	0.025 ± 0.004	-0.699 ± 0.111	2.316 ± 0.074
SR1163	0.025 ± 0.005	-0.699 ± 0.650	3.184 ± 0.050
SR1166	0.562 ± 0.220	-1.602 ± 0.850	3.605 ± 0.079
SR1169	1.410 ± 0.260	-1.699 ± 0.423	4.336 ± 0.635
SR1170	0.316 ± 0.150	-2.301 ± 0.150	4.274 ± 0.123
SR1175	1.260 ± 0.259	-1.602 ± 0.122	4.342 ± 0.029
SR1179	12.600 ± 1.845	-2.301 ± 0.238	5.511 ± 0.025
SR1180	0.040 ± 0.009	-1.602 ± 0.122	3.355 ± 0.110
SR1181	5.010 ± 1.765	-2.301 ± 0.150	5.066 ± 0.189
SR1182	5.620 ± 2.875	-1.602 ± 0.423	4.458 ± 0.503
SR1184	0.025 ± 0.004	-0.699 ± 0.111	3.816 ± 0.119
SR1185	1.000 ± 0.184	0.176 ± 0.199	4.576 ± 0.048
SR1188	8.910 ± 1.030	0.398 ± 0.150	6.104 ± 0.052
SR1190	0.025 ± 0.004	-0.699 ± 0.588	3.164 ± 0.039
SR1196	1.580 ± 0.295	-0.398 ± 0.262	4.674 ± 0.106
SR1197	2.000 ± 0.230	0.477 ± 0.040	5.441 ± 0.103
SR1199	0.178 ± 0.079	0.477 ± 0.040	4.123 ± 0.109
SR1200	0.040 ± 0.007	-1.602 ± 0.122	2.965 ± 0.125
SR1203	0.562 ± 0.131	-0.301 ± 0.350	4.784 ± 0.114
SR1204	0.025 ± 0.004	-0.699 ± 0.111	2.807 ± 0.060
SR1207	0.018 ± 0.008	-0.071 ± 0.051	3.735 ± 0.053
SR1208	0.018 ± 0.002	0.000 ± 0.124	2.360 ± 0.018
SR1214	0.251 ± 0.069	0.477 ± 0.150	3.410 ± 0.026
SR1215	0.018 ± 0.002	-1.602 ± 0.122	3.397 ± 0.075
SR1219	0.025 ± 0.005	-0.699 ± 0.213	2.639 ± 0.140
SR1224	1.410 ± 0.160	-1.602 ± 0.122	4.639 ± 0.049

TABLE 2 — *Continued*

Object	Age (Gyr)	[Fe/H] (dex)	$\log(M_{cl})$ $[M_\odot]$
SR1226	0.025 ± 0.005	-0.523 ± 0.335	2.807 ± 0.047
SR1230	1.260 ± 0.205	0.000 ± 0.166	4.672 ± 0.087
SR1232	0.022 ± 0.004	-0.155 ± 0.262	3.114 ± 0.047
SR1233	3.980 ± 1.400	-2.301 ± 0.238	4.993 ± 0.015
SR1235	0.562 ± 0.247	-1.000 ± 0.466	4.238 ± 0.014
SR1237	0.501 ± 0.198	-1.000 ± 0.650	3.852 ± 0.054
SR1239	0.631 ± 0.146	-0.022 ± 0.287	4.541 ± 0.115
SR1241	0.794 ± 0.245	-1.301 ± 0.228	4.337 ± 0.007
SR1244	7.940 ± 3.490	-2.000 ± 0.238	4.817 ± 0.166
SR1249	0.063 ± 0.017	-2.301 ± 0.150	3.616 ± 0.012
SR1251	0.016 ± 0.002	0.477 ± 0.040	2.919 ± 0.126
SR1255	2.240 ± 0.520	-1.155 ± 0.389	4.741 ± 0.127
SR1258	3.980 ± 1.400	-2.301 ± 0.150	5.054 ± 0.162
SR1262	1.580 ± 0.295	-2.000 ± 0.301	4.745 ± 0.101
SR1265	0.045 ± 0.026	0.477 ± 0.040	3.364 ± 0.180
SR1271	1.260 ± 0.205	-1.699 ± 0.423	4.770 ± 0.545
SR1273	0.158 ± 0.315	-0.523 ± 0.850	4.137 ± 0.373
SR1276	0.028 ± 0.008	-0.824 ± 0.423	3.688 ± 0.060
SR1282	2.240 ± 0.365	-2.301 ± 0.150	4.187 ± 0.064
SR1283	2.510 ± 0.990	-2.301 ± 0.238	4.246 ± 0.111
SR1286	1.120 ± 0.308	0.477 ± 0.040	4.001 ± 0.199
SR1289	0.631 ± 0.174	-0.071 ± 0.938	3.195 ± 0.064
SR1290	1.120 ± 0.185	-2.000 ± 0.238	4.042 ± 0.076
SR1295	1.260 ± 0.145	-2.000 ± 0.301	4.988 ± 0.162
SR1296	0.071 ± 0.032	-1.602 ± 0.122	3.459 ± 0.106
SR1297	0.020 ± 0.002	-0.398 ± 0.184	3.109 ± 0.069
SR1300	0.020 ± 0.004	-1.155 ± 0.316	2.690 ± 0.043
SR1302	0.022 ± 0.004	-0.699 ± 0.150	2.817 ± 0.019
SR1303	0.501 ± 0.176	-1.000 ± 0.301	4.214 ± 0.036
SR1305	12.600 ± 1.300	-0.602 ± 0.213	5.805 ± 0.180
SR1306	1.260 ± 0.145	0.176 ± 0.199	4.960 ± 0.105
SR1307	12.600 ± 3.490	-2.000 ± 0.301	4.976 ± 0.022
SR1311	0.158 ± 0.062	-1.602 ± 0.122	4.356 ± 0.092
SR1312	1.000 ± 0.184	-0.301 ± 0.199	5.272 ± 0.090
SR1315	1.000 ± 0.206	-2.000 ± 0.238	4.122 ± 0.092
SR1317	1.580 ± 0.260	0.477 ± 0.040	4.993 ± 0.138
SR1319	0.025 ± 0.003	-0.824 ± 0.150	3.465 ± 0.070
SR1320	4.470 ± 1.575	-1.602 ± 0.650	4.451 ± 0.088
SR1322	0.794 ± 0.146	0.176 ± 0.199	4.745 ± 0.084
SR1323	0.562 ± 0.155	-0.398 ± 0.850	3.442 ± 0.097
SR1324	1.260 ± 0.230	0.176 ± 0.199	4.887 ± 0.143
SR1328	0.355 ± 0.139	-2.301 ± 0.238	4.174 ± 0.087
SR1329	0.126 ± 0.138	-1.000 ± 0.889	3.222 ± 0.077
SR1330	10.000 ± 3.145	-2.000 ± 0.301	5.358 ± 0.028
SR1331	12.600 ± 1.845	-2.301 ± 0.238	4.771 ± 0.019
SR1332	1.410 ± 0.160	-1.699 ± 0.423	4.540 ± 0.072
SR1333	1.410 ± 0.330	0.477 ± 0.088	5.444 ± 0.058
SR1334	5.620 ± 3.420	-2.301 ± 0.238	4.680 ± 0.267
SR1335	4.470 ± 1.575	-2.301 ± 0.150	4.648 ± 0.016
SR1336	2.510 ± 0.410	-0.398 ± 0.850	4.844 ± 0.008
SR1339	0.025 ± 0.003	-0.699 ± 0.111	3.266 ± 0.056
SR1342	0.022 ± 0.002	-0.071 ± 0.150	3.510 ± 0.153
SR1348	0.251 ± 0.069	0.477 ± 0.150	3.263 ± 0.041
SR1349	1.410 ± 0.230	0.477 ± 0.088	4.764 ± 0.076
SR1352	0.141 ± 0.155	-1.000 ± 0.650	3.107 ± 0.109
SR1355	0.891 ± 0.276	-1.301 ± 0.316	4.281 ± 0.011
SR1356	0.079 ± 0.034	-1.602 ± 0.122	3.444 ± 0.074
SR1358	6.310 ± 1.035	-1.602 ± 0.122	4.879 ± 0.049
SR1359	5.010 ± 0.575	0.000 ± 0.238	5.596 ± 0.028
SR1367	1.780 ± 0.415	-1.602 ± 0.122	4.196 ± 0.082
SR1368	1.410 ± 0.260	0.398 ± 0.088	5.248 ± 0.007
SR1369	0.028 ± 0.005	-0.699 ± 0.213	3.257 ± 0.034
SR1374	0.020 ± 0.009	-1.602 ± 0.650	3.699 ± 0.039
SR1376	0.018 ± 0.004	-1.456 ± 0.951	2.996 ± 0.200
SR1377	0.016 ± 0.005	0.477 ± 0.088	3.277 ± 0.037
SR1378	1.410 ± 0.160	-1.602 ± 0.122	4.260 ± 0.034
SR1379	6.310 ± 3.365	-2.301 ± 0.150	5.599 ± 0.007
SR1380	4.470 ± 2.285	-2.301 ± 0.238	4.602 ± 0.081
SR1381	0.036 ± 0.014	-1.699 ± 0.199	3.235 ± 0.075
SR1384	11.200 ± 1.300	0.301 ± 0.111	5.734 ± 0.082
SR1385	0.036 ± 0.015	-1.155 ± 0.223	3.391 ± 0.118
SR1387	1.410 ± 0.160	-2.000 ± 0.238	4.462 ± 0.008
SR1389	0.025 ± 0.004	-0.699 ± 0.111	2.815 ± 0.048
SR1392	0.282 ± 0.145	-2.301 ± 0.150	3.760 ± 0.117
SR1393	1.120 ± 0.259	-1.824 ± 0.199	4.271 ± 0.095
SR1396	0.040 ± 0.012	-1.602 ± 0.122	3.382 ± 0.152

TABLE 2 — *Continued*

Object	Age (Gyr)	[Fe/H] (dex)	$\log(M_{cl})$ $[M_\odot]$
SR1403	0.018 ± 0.002	-2.301 ± 0.150	3.428 ± 0.148
SR1404	0.025 ± 0.004	-0.699 ± 0.111	3.101 ± 0.133
SR1409	0.040 ± 0.011	-1.602 ± 0.122	3.283 ± 0.147
SR1411	0.018 ± 0.002	-1.602 ± 0.122	3.311 ± 0.077
SR1412	0.708 ± 0.336	-2.301 ± 0.301	4.537 ± 0.129
SR1413	0.020 ± 0.002	-1.602 ± 0.122	2.728 ± 0.231
SR1414	0.016 ± 0.002	0.398 ± 0.088	2.267 ± 0.081
SR1418	0.004 ± 0.001	-1.602 ± 0.122	3.589 ± 0.054
SR1419	0.014 ± 0.002	0.477 ± 0.040	2.770 ± 0.076
SR1421	0.282 ± 0.099	-0.523 ± 0.412	3.683 ± 0.054
SR1422	0.040 ± 0.007	-1.602 ± 0.122	3.780 ± 0.092
SR1426	0.040 ± 0.009	-1.602 ± 0.122	3.445 ± 0.136
SR1429	1.580 ± 0.185	-1.602 ± 0.122	4.168 ± 0.023
SR1432	1.780 ± 0.465	-2.000 ± 0.301	4.512 ± 0.019
SR1435	2.820 ± 0.325	-1.602 ± 0.122	4.154 ± 0.273
SR1437	0.025 ± 0.004	-0.699 ± 0.111	3.258 ± 0.052
SR1438	0.022 ± 0.004	-1.000 ± 0.238	2.915 ± 0.028
SR1442	5.620 ± 1.980	-2.301 ± 0.150	4.659 ± 0.184
SR1443	2.510 ± 1.100	-2.301 ± 0.150	4.627 ± 0.006
SR1444	0.016 ± 0.005	0.398 ± 0.088	2.807 ± 0.011
SR1448	0.071 ± 0.025	-1.301 ± 0.301	3.186 ± 0.002
SR1457	0.004 ± 0.002	-1.602 ± 0.122	3.358 ± 0.214
SR1458	1.260 ± 0.145	0.301 ± 0.150	5.359 ± 0.184
SR1460	2.240 ± 0.365	-0.824 ± 0.350	5.243 ± 0.098
SR1466	0.282 ± 0.110	-0.071 ± 1.049	3.883 ± 0.044
SR1467	10.000 ± 3.490	-2.301 ± 0.238	4.757 ± 0.070
SR1469	0.282 ± 0.124	-0.523 ± 0.738	3.493 ± 0.043
SR1472	0.009 ± 0.006	0.398 ± 0.966	2.912 ± 0.344
SR1475	0.022 ± 0.002	-1.602 ± 0.122	2.781 ± 0.127
SR1476	0.079 ± 0.028	-1.602 ± 0.122	3.232 ± 0.178
SR1477	0.018 ± 0.002	0.000 ± 0.124	2.704 ± 0.089
SR1479	2.240 ± 0.790	-2.301 ± 0.238	4.329 ± 0.108
SR1481	0.018 ± 0.005	0.301 ± 0.238	2.792 ± 0.030
SR1485	0.022 ± 0.004	-1.602 ± 0.122	3.010 ± 0.007
SR1486	0.891 ± 0.206	-1.602 ± 0.122	3.963 ± 0.001
SR1487	3.980 ± 2.130	-1.602 ± 0.122	5.079 ± 0.008
SR1496	5.010 ± 1.960	0.000 ± 0.150	4.670 ± 0.763
SR1501	0.355 ± 0.082	0.176 ± 0.262	3.467 ± 0.217
SR1503	0.126 ± 0.045	-1.000 ± 0.238	4.213 ± 0.074
SR1504	1.410 ± 0.160	-1.824 ± 0.350	4.694 ± 0.030
SR1506	0.398 ± 0.093	0.176 ± 0.350	3.589 ± 0.168
SR1507	5.620 ± 3.225	-2.301 ± 0.238	5.070 ± 0.040
SR1510	0.022 ± 0.004	-0.699 ± 0.150	3.321 ± 0.067
SR1511	1.120 ± 0.259	-1.602 ± 0.122	3.931 ± 0.023
SR1513	2.510 ± 0.775	-2.301 ± 0.150	4.227 ± 0.016
SR1514	12.600 ± 3.145	-2.301 ± 0.238	5.808 ± 0.012
SR1522	0.100 ± 0.058	-1.456 ± 0.412	3.931 ± 0.028
SR1524	0.025 ± 0.005	-0.602 ± 0.335	3.222 ± 0.015
SR1525	1.410 ± 0.160	-2.301 ± 0.150	4.771 ± 0.064
SR1533	0.794 ± 0.146	0.176 ± 0.199	3.795 ± 0.078
SR1534	2.240 ± 0.790	-2.301 ± 0.238	4.360 ± 0.265
SR1540	0.056 ± 0.057	-0.699 ± 0.588	3.860 ± 0.048
SR1541	0.006 ± 0.002	0.301 ± 0.111	2.725 ± 0.030
SR1543	0.501 ± 0.116	-0.071 ± 0.287	3.891 ± 0.219
SR1545	1.260 ± 0.145	-0.125 ± 0.287	5.010 ± 0.100
SR1547	0.079 ± 0.035	-1.602 ± 0.122	3.896 ± 0.130
SR1548	12.600 ± 1.845	-0.824 ± 0.199	5.090 ± 0.086
SR1552	0.028 ± 0.004	-0.699 ± 0.301	3.213 ± 0.061
SR1553	5.620 ± 2.465	-2.301 ± 0.238	5.024 ± 0.023
SR1557	1.260 ± 0.145	-1.824 ± 0.423	5.044 ± 0.062
SR1558	0.025 ± 0.003	-0.699 ± 0.111	2.691 ± 0.127
SR1563	1.580 ± 0.370	-2.000 ± 0.350	4.015 ± 0.157
SR1564	0.022 ± 0.002	-0.699 ± 0.588	3.293 ± 0.088
SR1565	0.022 ± 0.004	-1.602 ± 0.122	3.103 ± 0.022
SR1566	10.000 ± 3.145	-1.824 ± 0.350	5.900 ± 0.030
SR1569	0.089 ± 0.032	-1.155 ± 1.088	3.582 ± 0.043
SR1570	2.000 ± 0.230	0.477 ± 0.088	5.347 ± 0.102
SR1580	5.010 ± 1.765	-1.824 ± 0.350	5.313 ± 0.064
SR1582	0.025 ± 0.004	-0.699 ± 0.111	3.529 ± 0.016
SR1584	1.780 ± 0.210	0.477 ± 0.040	5.200 ± 0.019
SR1587	4.470 ± 1.980	0.398 ± 0.150	4.700 ± 0.033
SR1589	3.980 ± 1.745	-2.301 ± 0.238	4.355 ± 0.010
SR1599	0.014 ± 0.002	0.477 ± 0.040	2.699 ± 0.127
SR1601	0.631 ± 0.268	-1.456 ± 0.301	4.955 ± 0.057
SR1603	0.251 ± 0.089	-1.602 ± 0.850	4.365 ± 0.043
SR1605	1.580 ± 0.295	-2.000 ± 0.350	5.171 ± 0.040

TABLE 2 — *Continued*

Object	Age (Gyr)	[Fe/H] (dex)	$\log(M_{cl})$ $[M_\odot]$
SR1606	11.200 ± 1.845	-0.523 ± 0.272	5.096 ± 0.006
SR1607	2.000 ± 0.230	0.477 ± 0.040	5.574 ± 0.056
SR1609	0.040 ± 0.004	-1.602 ± 0.122	2.962 ± 0.132
SR1610	0.126 ± 0.058	-1.602 ± 0.122	3.420 ± 0.097
SR1614	1.000 ± 0.308	-1.602 ± 0.122	4.067 ± 0.019
SR1617	5.620 ± 2.220	-2.301 ± 0.150	5.023 ± 0.021
SR1619	0.200 ± 0.107	-1.602 ± 0.549	3.570 ± 0.094
SR1625	0.891 ± 0.206	-1.602 ± 0.272	3.710 ± 0.193
SR1626	0.158 ± 0.056	-1.824 ± 0.350	3.285 ± 0.111
SR1628	2.240 ± 0.520	-2.301 ± 0.150	4.519 ± 0.078
SR1633	0.355 ± 0.188	-1.000 ± 0.850	4.174 ± 0.018
SR0163	2.000 ± 0.230	0.477 ± 0.040	5.146 ± 0.255
SR1640	2.000 ± 0.465	-0.301 ± 0.262	4.157 ± 0.078
SR1657	0.020 ± 0.004	-1.301 ± 0.228	3.694 ± 0.056
SR1664	0.018 ± 0.003	0.477 ± 0.040	3.264 ± 0.035
SR1665	0.013 ± 0.007	-1.602 ± 0.122	3.639 ± 0.024
SR1666	0.004 ± 0.001	-1.602 ± 0.122	3.270 ± 0.042
SR1667	10.000 ± 2.760	-2.000 ± 0.301	4.819 ± 0.016
SR1669	0.016 ± 0.002	0.398 ± 0.088	3.917 ± 0.072
SR1670	0.018 ± 0.002	-2.301 ± 0.150	3.234 ± 0.020
SR1672	0.891 ± 0.163	0.176 ± 0.150	5.351 ± 0.037
SR1673	4.470 ± 1.380	-2.301 ± 0.150	4.891 ± 0.022
SR1676	1.780 ± 0.550	-2.000 ± 0.350	4.477 ± 0.008
SR1679	1.780 ± 0.415	-2.301 ± 0.150	4.698 ± 0.145
SR1684	12.600 ± 0.700	-0.301 ± 0.199	6.443 ± 0.019
SR1686	0.018 ± 0.002	-0.022 ± 0.123	3.053 ± 0.039
SR1696	3.550 ± 1.555	-2.301 ± 0.238	4.726 ± 0.041
SR1697	0.089 ± 0.039	-0.125 ± 1.088	3.653 ± 0.012
SR1698	0.022 ± 0.002	-1.602 ± 0.122	2.915 ± 0.127
SR1699	0.112 ± 0.039	0.477 ± 0.088	3.665 ± 0.166
SR1702	1.000 ± 0.233	-1.602 ± 0.122	4.326 ± 0.094
SR1703	0.562 ± 0.131	0.000 ± 0.287	3.555 ± 0.041
SR1704	5.010 ± 1.765	-2.301 ± 0.150	6.011 ± 0.049
SR1707	0.018 ± 0.002	-2.301 ± 0.238	3.083 ± 0.144
SR1709	2.820 ± 0.460	-0.071 ± 0.350	4.659 ± 0.016
SR1710	3.980 ± 0.655	0.477 ± 0.150	5.868 ± 0.079
SR1717	11.200 ± 3.490	-2.000 ± 0.238	6.172 ± 0.022
SR1721	0.028 ± 0.005	-0.699 ± 0.423	3.282 ± 0.138
SR1724	0.631 ± 0.195	-1.301 ± 0.389	4.671 ± 0.136
SR1727	0.025 ± 0.004	-0.523 ± 0.772	3.516 ± 0.118
SR1733	0.016 ± 0.002	0.301 ± 0.111	3.461 ± 0.086
SR1735	1.260 ± 0.230	0.398 ± 0.150	5.597 ± 0.212
SR1740	0.056 ± 0.029	-1.824 ± 0.350	3.390 ± 0.051
SR1741	0.112 ± 0.031	-2.301 ± 0.150	3.673 ± 0.084
SR1742	0.006 ± 0.002	0.301 ± 0.111	3.385 ± 0.069
SR1743	1.120 ± 0.205	0.301 ± 0.150	3.923 ± 0.088
SR1745	0.018 ± 0.003	-1.602 ± 0.122	3.300 ± 0.099
SR1749	12.600 ± 2.760	-2.301 ± 0.238	5.028 ± 0.023
SR1750	2.000 ± 0.705	-2.301 ± 0.238	4.700 ± 0.048
SR1751	0.126 ± 0.045	-2.000 ± 0.301	4.102 ± 0.003
SR1752	0.355 ± 0.169	-2.301 ± 0.238	3.940 ± 0.016
SR1753	1.120 ± 0.205	-2.000 ± 0.301	4.027 ± 0.045
SR1754	0.028 ± 0.004	-0.699 ± 0.213	3.426 ± 0.051
SR1756	1.580 ± 0.370	-2.301 ± 0.238	4.304 ± 0.059
SR1757	0.040 ± 0.007	-1.602 ± 0.122	3.389 ± 0.122
SR1761	3.980 ± 1.765	0.301 ± 0.150	4.845 ± 0.029
SR1763	0.025 ± 0.005	-0.699 ± 0.111	2.792 ± 0.009
SR1764	11.200 ± 2.330	-1.301 ± 0.301	4.717 ± 0.002
SR1765	2.510 ± 0.655	-1.602 ± 0.850	5.517 ± 0.081
SR1766	12.600 ± 3.145	-2.301 ± 0.150	5.118 ± 0.002
SR1767	12.600 ± 3.490	-2.301 ± 0.238	5.054 ± 0.057
SR1770	0.025 ± 0.004	-0.699 ± 0.111	2.766 ± 0.041
SR1773	5.620 ± 2.680	-2.301 ± 0.150	4.704 ± 0.218
SR1774	0.631 ± 0.336	-2.301 ± 0.238	4.078 ± 0.130
SR1776	0.126 ± 0.060	-1.000 ± 0.738	4.137 ± 0.035
SR1779	6.310 ± 2.465	-2.301 ± 0.150	5.824 ± 0.190
SR1781	3.980 ± 1.745	-2.301 ± 0.238	4.887 ± 0.028
SR1784	0.022 ± 0.002	0.477 ± 0.040	3.296 ± 0.056
SR1787	12.600 ± 1.845	-0.301 ± 0.262	6.531 ± 0.359
SR1794	2.820 ± 0.870	-2.301 ± 0.150	4.744 ± 0.028
SR1796	0.447 ± 0.175	-2.000 ± 0.301	4.125 ± 0.116
SR1798	1.580 ± 0.295	0.477 ± 0.040	5.235 ± 0.069
SR1799	1.260 ± 0.290	-0.125 ± 0.287	5.484 ± 0.140
SR1800	0.025 ± 0.005	-0.824 ± 0.772	2.816 ± 0.026
SR1802	0.501 ± 0.116	-0.071 ± 0.350	4.387 ± 0.115
SR1803	2.510 ± 0.655	0.477 ± 0.040	4.500 ± 0.060

TABLE 2 — *Continued*

Object	Age (Gyr)	[Fe/H] (dex)	$\log(M_{cl})$ $[M_\odot]$
SR1806	1.260 ± 0.259	-1.000 ± 0.378	3.811 ± 0.051
SR1811	0.016 ± 0.105	0.477 ± 0.088	2.798 ± 0.071
SR1812	0.004 ± 0.002	-1.602 ± 1.049	3.657 ± 0.032
SR1817	0.020 ± 0.002	-1.602 ± 0.122	2.803 ± 0.124
SR1819	3.160 ± 1.690	-2.000 ± 0.350	5.181 ± 0.017
SR1820	2.820 ± 0.990	-2.301 ± 0.150	5.889 ± 0.145
SR1821	0.025 ± 0.005	-0.699 ± 0.111	3.059 ± 0.026
SR1822	5.620 ± 1.550	-1.602 ± 0.122	5.686 ± 0.046
SR1823	0.794 ± 0.146	0.176 ± 0.199	4.059 ± 0.019
SR1824	1.410 ± 0.230	-1.602 ± 0.122	4.609 ± 0.006
SR1827	0.022 ± 0.004	-1.000 ± 0.238	2.727 ± 0.031
SR1829	1.780 ± 0.465	-2.000 ± 0.350	5.377 ± 0.025
SR1830	0.282 ± 0.087	-0.699 ± 0.650	3.767 ± 0.057
SR1833	0.020 ± 0.011	-2.301 ± 0.238	3.211 ± 0.099
SR1836	0.050 ± 0.018	-1.301 ± 0.223	3.498 ± 0.074
SR1837	0.501 ± 0.116	0.477 ± 0.088	3.592 ± 0.013
SR1841	0.040 ± 0.014	-1.699 ± 0.199	3.366 ± 0.038
SR1843	0.014 ± 0.002	0.477 ± 0.040	2.862 ± 0.095
SR1844	0.018 ± 0.002	-2.301 ± 0.150	3.219 ± 0.121
SR1845	0.071 ± 0.038	0.477 ± 0.389	3.087 ± 0.295
SR1846	12.600 ± 1.845	-0.523 ± 0.650	5.023 ± 0.003
SR1849	0.063 ± 0.022	-0.071 ± 1.000	3.529 ± 0.039
SR1850	1.780 ± 0.550	-2.301 ± 0.238	4.356 ± 0.015
SR1855	0.794 ± 0.219	-1.602 ± 0.122	4.583 ± 0.039
SR1856	0.020 ± 0.002	-0.155 ± 0.262	2.792 ± 0.079
SR1857	0.016 ± 0.002	0.477 ± 0.040	2.838 ± 0.092
SR1859	0.032 ± 0.005	-0.301 ± 0.350	3.815 ± 0.320
SR1866	3.550 ± 1.385	-2.301 ± 0.150	4.946 ± 0.027
SR1867	0.079 ± 0.032	-2.301 ± 0.238	3.596 ± 0.092
SR1868	0.022 ± 0.008	-0.824 ± 0.500	3.208 ± 0.027
SR1870	0.020 ± 0.002	-0.398 ± 0.184	3.241 ± 0.092
SR1872	2.510 ± 0.580	-2.301 ± 0.150	4.812 ± 0.011
SR1874	3.980 ± 0.460	0.477 ± 0.040	5.231 ± 0.008
SR1875	0.251 ± 0.162	-0.523 ± 0.738	3.908 ± 0.369
SR1877	0.158 ± 0.081	-1.602 ± 1.111	2.601 ± 0.193
SR1880	0.355 ± 0.109	0.477 ± 0.040	4.308 ± 0.213
SR1887	1.780 ± 0.210	0.398 ± 0.238	5.614 ± 0.069
SR1888	0.794 ± 0.219	-1.824 ± 0.350	4.691 ± 0.060
SR1892	0.022 ± 0.005	-1.602 ± 0.650	2.921 ± 0.029
SR1896	0.794 ± 0.185	-1.301 ± 0.228	4.684 ± 0.028
SR1897	12.600 ± 2.330	-1.155 ± 0.316	5.793 ± 0.043
SR1899	1.780 ± 0.550	-2.000 ± 0.301	4.236 ± 0.170
SR1900	1.260 ± 0.145	-1.699 ± 0.335	4.345 ± 0.016
SR1901	0.126 ± 0.105	-0.699 ± 0.967	3.915 ± 0.097
SR1904	0.063 ± 0.027	0.477 ± 0.539	3.083 ± 0.044
SR1905	0.016 ± 0.002	0.477 ± 0.040	2.678 ± 0.178
SR1909	0.025 ± 0.003	-0.699 ± 0.111	3.136 ± 0.004
SR1911	1.780 ± 0.210	0.477 ± 0.040	5.073 ± 0.365
SR1912	3.550 ± 1.690	-2.301 ± 0.150	4.943 ± 0.056
SR1915	1.780 ± 0.550	-1.456 ± 0.500	4.612 ± 0.005
SR1918	1.580 ± 0.295	-2.000 ± 0.301	4.153 ± 0.059
SR1919	1.410 ± 0.230	-0.071 ± 0.287	4.368 ± 0.018
SR1921	0.018 ± 0.003	-0.155 ± 0.850	2.582 ± 0.069
SR1922	3.550 ± 1.690	-2.301 ± 0.238	4.485 ± 0.034
SR1923	0.282 ± 0.124	-2.000 ± 0.301	3.756 ± 0.118
SR1931	0.025 ± 0.004	-0.699 ± 0.111	2.884 ± 0.007
SR1932	1.260 ± 0.145	-1.699 ± 0.412	3.935 ± 0.066
SR1937	0.056 ± 0.020	-1.301 ± 0.223	3.463 ± 0.041
SR1939	11.200 ± 3.490	-2.301 ± 0.238	4.827 ± 0.021
SR1941	0.794 ± 0.250	-1.602 ± 0.122	4.042 ± 0.044
SR1944	5.620 ± 2.680	-2.301 ± 0.150	4.575 ± 0.007
SR1950	0.032 ± 0.013	-1.699 ± 0.199	3.589 ± 0.025
SR1953	0.028 ± 0.005	-0.398 ± 0.423	3.843 ± 0.031
SR1955	1.000 ± 0.163	-0.301 ± 0.199	4.898 ± 0.062
SR1957	0.045 ± 0.026	-1.602 ± 0.350	4.030 ± 0.203
SR1959	1.410 ± 0.160	-2.000 ± 0.301	4.586 ± 0.005
SR1961	11.200 ± 1.300	0.301 ± 0.111	5.986 ± 0.009
SR1962	0.028 ± 0.005	-1.602 ± 0.122	2.924 ± 0.135
SR1965	1.120 ± 0.205	0.176 ± 0.150	5.068 ± 0.073
SR1967	12.600 ± 0.700	0.477 ± 0.040	5.212 ± 0.132
SR1970	0.562 ± 0.176	-2.301 ± 0.150	4.970 ± 0.101
SR1973	2.820 ± 1.250	-1.301 ± 0.301	4.420 ± 0.061
SR1976	0.447 ± 0.157	-0.125 ± 1.000	3.628 ± 0.060
SR1977	0.020 ± 0.002	-1.602 ± 0.122	2.686 ± 0.124
SR1978	0.631 ± 0.336	-2.301 ± 0.238	4.313 ± 0.091
SR0197	1.260 ± 0.205	0.477 ± 0.040	4.323 ± 0.157

TABLE 2 — *Continued*

Object	Age (Gyr)	[Fe/H] (dex)	$\log(M_{cl})$ $[M_\odot]$
SR1980	0.020 ± 0.002	-1.602 ± 0.122	2.764 ± 0.072
SR1982	12.600 ± 0.700	0.477 ± 0.040	6.372 ± 0.074
SR1984	7.940 ± 3.795	-2.301 ± 0.150	5.069 ± 0.004
SR1985	1.260 ± 0.205	0.398 ± 0.150	5.177 ± 0.095
SR1987	0.004 ± 0.002	-1.602 ± 0.122	3.406 ± 0.129
SR1988	0.355 ± 0.109	0.477 ± 0.040	4.500 ± 0.066
SR1993	3.550 ± 1.690	-2.301 ± 0.150	4.493 ± 0.020
SR1995	1.260 ± 0.205	0.176 ± 0.150	5.195 ± 0.039
SR1996	2.820 ± 0.325	0.000 ± 0.238	4.810 ± 0.011
SR1997	0.020 ± 0.004	-1.155 ± 0.316	3.640 ± 0.018
SR1998	2.000 ± 0.230	0.477 ± 0.040	5.545 ± 0.110
SR1999	1.580 ± 0.260	-2.000 ± 0.238	4.459 ± 0.010
SR2000	0.028 ± 0.004	-0.699 ± 0.213	2.861 ± 0.085
SR2001	7.940 ± 3.795	-2.301 ± 0.150	5.759 ± 0.023
SR2002	3.980 ± 0.460	0.477 ± 0.040	4.914 ± 0.138
SR2003	12.600 ± 1.300	-0.602 ± 0.213	5.995 ± 0.032
SR2004	1.410 ± 0.160	-2.000 ± 0.301	4.757 ± 0.039
SR2005	1.410 ± 0.260	-1.824 ± 0.573	4.264 ± 0.058
SR2011	1.780 ± 0.415	-2.301 ± 0.150	4.243 ± 0.054
SR2013	11.200 ± 2.330	-0.699 ± 0.588	5.080 ± 0.008
SR2016	5.620 ± 2.195	-0.523 ± 0.772	5.353 ± 0.029
SR2018	12.600 ± 1.845	0.398 ± 0.088	5.002 ± 0.066
SR2020	0.045 ± 0.018	-1.699 ± 0.199	4.061 ± 0.128
SR2023	2.240 ± 0.365	-0.602 ± 0.213	5.010 ± 0.068
SR2024	2.820 ± 0.460	0.000 ± 0.150	4.861 ± 0.005
SR2026	0.020 ± 0.002	-0.155 ± 0.163	3.120 ± 0.122
SR2029	1.000 ± 0.349	-2.301 ± 0.150	3.756 ± 0.194
SR2030	0.794 ± 0.185	-0.125 ± 0.287	3.583 ± 0.026
SR2033	0.028 ± 0.004	-0.699 ± 0.150	3.332 ± 0.059
SR2035	0.020 ± 0.002	-1.602 ± 0.122	3.154 ± 0.095
SR0203	2.510 ± 0.775	-2.301 ± 0.150	4.107 ± 0.082
SR2042	0.014 ± 0.003	0.477 ± 0.040	2.498 ± 0.044
SR2043	0.251 ± 0.110	-0.523 ± 0.500	4.081 ± 0.297
SR2046	2.240 ± 0.365	-1.000 ± 0.378	4.898 ± 0.064
SR2047	0.025 ± 0.004	-0.699 ± 0.111	3.063 ± 0.024
SR2048	0.050 ± 0.021	0.477 ± 0.438	2.964 ± 0.054
SR0204	10.000 ± 3.145	-1.824 ± 0.350	5.230 ± 0.029
SR2050	0.028 ± 0.012	-1.155 ± 0.316	4.234 ± 0.178
SR2054	0.891 ± 0.349	-2.301 ± 0.238	4.325 ± 0.016
SR2057	10.000 ± 2.760	-2.000 ± 0.301	4.372 ± 0.022
SR2058	0.028 ± 0.060	-0.824 ± 0.423	2.963 ± 0.042
SR2061	0.631 ± 0.222	-1.456 ± 0.301	3.925 ± 0.038
SR2063	0.708 ± 0.164	0.301 ± 0.238	4.290 ± 0.089
SR2066	1.410 ± 0.230	-1.602 ± 0.122	4.669 ± 0.076
SR2072	1.580 ± 0.185	-0.824 ± 0.150	4.687 ± 0.112
SR2075	1.260 ± 0.230	0.176 ± 0.199	5.137 ± 0.045
SR2086	0.025 ± 0.004	-0.699 ± 0.111	3.240 ± 0.035
SR2092	7.940 ± 2.790	-2.301 ± 0.150	4.471 ± 0.145
SR2094	12.600 ± 0.700	0.477 ± 0.040	5.672 ± 0.042
SR2095	0.028 ± 0.032	-0.699 ± 0.150	3.520 ± 0.021
SR2096	0.282 ± 0.065	0.301 ± 0.301	3.536 ± 0.053
SR2101	0.040 ± 0.019	-1.155 ± 0.223	3.240 ± 0.063
SR2103	1.000 ± 0.163	0.301 ± 0.199	5.484 ± 0.183
SR2106	2.820 ± 0.460	-0.155 ± 0.262	4.730 ± 0.053
SR2107	0.708 ± 0.222	-1.699 ± 0.199	4.108 ± 0.057
SR2110	1.580 ± 0.295	0.477 ± 0.040	5.087 ± 0.036
SR2113	6.310 ± 1.765	0.477 ± 0.040	4.958 ± 0.021
SR2114	0.013 ± 0.007	-1.602 ± 0.122	2.451 ± 0.079
SR2115	3.980 ± 2.035	-2.301 ± 0.238	4.745 ± 0.035
SR2116	0.022 ± 0.004	-0.699 ± 0.650	2.568 ± 0.048
SR2119	0.045 ± 0.022	-1.602 ± 0.412	3.512 ± 0.191
SR2121	12.600 ± 1.300	-0.699 ± 0.301	4.645 ± 0.183
SR2126	0.016 ± 0.003	0.477 ± 0.088	...
SR2132	11.200 ± 2.760	-1.301 ± 0.301	5.378 ± 0.138
SR2145	0.891 ± 0.163	0.176 ± 0.199	5.024 ± 0.110
SR2149	0.022 ± 0.004	-1.602 ± 0.122	2.543 ± 0.063
SR2156	12.600 ± 0.700	0.477 ± 0.040	4.757 ± 0.176
SR2174	1.260 ± 0.205	-1.456 ± 0.412	4.905 ± 0.095
SR2176	0.028 ± 0.011	-1.155 ± 0.223	2.852 ± 0.157
SR2177	0.028 ± 0.004	-0.699 ± 0.650	3.417 ± 0.126
SR2181	1.000 ± 0.163	0.301 ± 0.199	4.967 ± 0.105
SR2185	1.260 ± 0.205	-1.699 ± 0.423	4.242 ± 0.056
SR2189	0.018 ± 0.002	0.477 ± 0.040	3.155 ± 0.046
SR2193	0.056 ± 0.042	-0.699 ± 0.588	2.720 ± 0.076
SR2194	1.580 ± 0.295	0.000 ± 0.350	5.022 ± 0.078
SR2198	0.025 ± 0.009	-1.000 ± 0.238	3.104 ± 0.020

TABLE 2 — *Continued*

Object	Age (Gyr)	[Fe/H] (dex)	$\log(M_{cl})$ $[M_\odot]$
SR2199	2.510 ± 0.990	-2.301 ± 0.150	4.442 ± 0.076
SR2202	3.550 ± 1.235	-2.301 ± 0.150	4.168 ± 0.174
SR2206	0.022 ± 0.004	-0.699 ± 0.213	3.403 ± 0.026
SR2210	0.112 ± 0.035	-2.301 ± 0.150	3.078 ± 0.051
SR2214	2.510 ± 0.690	-2.301 ± 0.150	4.523 ± 0.010
SR2219	0.071 ± 0.019	-2.301 ± 0.150	3.224 ± 0.089
SR2221	11.200 ± 1.300	0.301 ± 0.111	5.363 ± 0.102
SR2222	10.000 ± 3.145	-2.000 ± 0.301	5.715 ± 0.116
SR2231	1.780 ± 0.210	0.301 ± 0.238	5.473 ± 0.073
SR2232	10.000 ± 2.760	-0.824 ± 0.199	5.734 ± 0.077
SR2236	1.260 ± 0.290	-1.000 ± 0.427	3.821 ± 0.051
SR2239	0.014 ± 0.002	0.477 ± 0.040	2.620 ± 0.012
SR2243	0.071 ± 0.022	-2.301 ± 0.238	3.246 ± 0.095
SR2245	2.820 ± 0.990	-2.301 ± 0.150	5.743 ± 0.058
SR2249	0.020 ± 0.002	-0.824 ± 0.150	2.857 ± 0.045
SR2250	5.620 ± 1.980	-2.301 ± 0.150	4.648 ± 0.032
SR2252	2.820 ± 0.460	0.000 ± 0.166	4.186 ± 0.045
SR2284	1.120 ± 0.205	0.176 ± 0.150	5.256 ± 0.071
SR2285	0.355 ± 0.155	-0.699 ± 0.772	3.608 ± 0.005
SR2286	0.045 ± 0.026	-2.301 ± 0.150	3.262 ± 0.092
SR2290	1.780 ± 0.210	0.398 ± 0.238	5.168 ± 0.016
SR2291	0.022 ± 0.004	-1.000 ± 0.316	2.606 ± 0.133
SR2295	1.580 ± 0.260	0.477 ± 0.040	5.410 ± 0.045
SR2298	0.028 ± 0.014	-1.155 ± 0.223	3.023 ± 0.135
SR2300	3.550 ± 1.250	-2.301 ± 0.150	5.041 ± 0.076
SR2311	0.251 ± 0.110	-0.523 ± 1.000	3.270 ± 0.059
SR2313	2.000 ± 0.230	0.477 ± 0.040	4.965 ± 0.108
SR2321	0.004 ± 0.002	-1.602 ± 0.122	2.869 ± 0.205
SR2330	11.200 ± 2.330	-0.699 ± 0.588	5.957 ± 0.018
SR2333	12.600 ± 0.700	0.477 ± 0.040	6.153 ± 0.000
SR2336	1.410 ± 0.160	-1.699 ± 0.350	4.662 ± 0.005
SR2354	0.020 ± 0.002	-1.456 ± 0.223	2.931 ± 0.033
SR2356	0.032 ± 0.011	0.477 ± 0.150	2.728 ± 0.071
SR2367	7.080 ± 2.765	-2.301 ± 0.150	4.313 ± 0.019
SR2373	0.040 ± 0.007	-1.602 ± 0.122	3.066 ± 0.134
SR2407	7.080 ± 3.795	-2.301 ± 0.238	5.073 ± 0.161
SR2420	12.600 ± 0.700	0.477 ± 0.040	6.220 ± 0.017
SR2439	1.000 ± 0.233	0.301 ± 0.199	5.047 ± 0.090
SR2442	10.000 ± 2.760	-0.824 ± 0.199	4.901 ± 0.052
SR2443	12.600 ± 1.300	0.398 ± 0.150	6.024 ± 0.003
SR2460	1.780 ± 0.210	0.477 ± 0.040	4.764 ± 0.323
SR2478	12.600 ± 0.700	0.477 ± 0.040	5.153 ± 0.115
SR2483	12.600 ± 1.300	0.301 ± 0.111	6.094 ± 0.006
SR2541	12.600 ± 0.700	0.477 ± 0.040	5.182 ± 0.032
SR0284	2.000 ± 0.230	0.477 ± 0.040	5.043 ± 0.104
SR0316	1.580 ± 0.185	-0.824 ± 0.150	4.479 ± 0.673
SR0346	2.510 ± 0.410	-0.398 ± 0.850	4.457 ± 0.042
SR0394	1.260 ± 0.230	0.301 ± 0.150	4.949 ± 0.137
SR0405	1.580 ± 0.415	-2.301 ± 0.150	3.711 ± 0.161
SR0425	12.600 ± 1.300	0.398 ± 0.150	5.341 ± 0.043
SR0578	1.000 ± 0.163	-0.155 ± 0.199	4.750 ± 0.088
SR0608	3.980 ± 0.460	0.477 ± 0.040	4.661 ± 0.138
SR0612	0.050 ± 0.018	-1.602 ± 0.122	3.239 ± 0.148
SR0621	12.600 ± 1.845	-0.022 ± 0.287	5.522 ± 0.033
SR0649	1.410 ± 0.230	0.301 ± 0.238	5.232 ± 0.053
SR0651	2.240 ± 0.520	-2.301 ± 0.150	4.277 ± 0.070
SR0658	0.010 ± 0.005	0.398 ± 1.088	2.632 ± 0.047
SR0660	7.940 ± 3.795	-2.301 ± 0.150	4.867 ± 0.023
SR0665	0.079 ± 0.098	-0.824 ± 0.889	3.245 ± 0.045
SR0667	0.355 ± 0.215	-1.824 ± 0.350	3.352 ± 0.158
SR0668	12.600 ± 0.700	0.301 ± 0.111	6.166 ± 0.069
SR0682	3.550 ± 1.385	-2.301 ± 0.150	4.504 ± 0.072
SR0683	3.980 ± 0.460	0.477 ± 0.040	4.870 ± 0.076
SR0689	8.910 ± 3.795	-1.824 ± 0.350	4.504 ± 0.030
SR0693	0.040 ± 0.009	0.477 ± 0.040	2.645 ± 0.039
SR0695	1.780 ± 0.210	0.477 ± 0.040	5.564 ± 0.195
SR0708	0.020 ± 0.002	-0.824 ± 0.150	2.546 ± 0.073
SR0714	11.200 ± 1.300	-1.602 ± 0.122	5.793 ± 0.059
SR0716	0.089 ± 0.068	-1.602 ± 0.122	3.327 ± 0.035
SR0722	0.562 ± 0.220	-1.602 ± 0.850	4.480 ± 0.101
SR0729	1.260 ± 0.205	-0.398 ± 0.301	4.598 ± 0.080
SR0732	1.780 ± 0.330	0.477 ± 0.040	4.745 ± 0.164
SR0734	0.891 ± 0.163	0.176 ± 0.150	4.821 ± 0.087
SR0735	0.036 ± 0.012	-1.456 ± 0.223	3.211 ± 0.030
SR0752	0.004 ± 0.002	-1.602 ± 0.122	2.572 ± 0.235
SR0755	0.018 ± 0.002	-0.071 ± 0.051	3.282 ± 0.167

TABLE 2 — *Continued*

Object	Age (Gyr)	[Fe/H] (dex)	$\log(M_{cl})$ $[M_\odot]$
SR0759	1.260 ± 0.230	0.398 ± 0.088	5.035 ± 0.072
SR0760	0.006 ± 0.002	0.301 ± 0.111	2.836 ± 0.096
SR0785	1.260 ± 0.205	-0.125 ± 0.287	5.187 ± 0.059
SR0791	4.470 ± 1.575	-2.301 ± 0.150	4.733 ± 0.004
SR0805	0.891 ± 0.206	-0.125 ± 0.287	5.173 ± 0.155
SR0810	0.007 ± 0.002	0.301 ± 0.111	2.379 ± 0.079
SR0811	2.820 ± 0.870	-2.301 ± 0.150	4.817 ± 0.000
SR0814	3.550 ± 1.115	-2.301 ± 0.150	5.007 ± 0.001
SR0817	0.040 ± 0.038	-1.602 ± 0.122	3.668 ± 0.088
SR0823	0.447 ± 0.229	-1.602 ± 0.122	3.971 ± 0.026
SR0826	1.260 ± 0.230	0.398 ± 0.150	4.977 ± 0.063
SR0830	0.891 ± 0.103	0.176 ± 0.150	4.678 ± 0.070
SR0835	0.251 ± 0.110	-1.602 ± 0.122	3.877 ± 0.086
SR0837	12.600 ± 1.300	-0.155 ± 0.199	5.844 ± 0.031
SR0840	0.025 ± 0.004	-0.699 ± 0.111	3.100 ± 0.064
SR0846	10.000 ± 2.760	-2.000 ± 0.301	5.576 ± 0.010
SR0847	0.020 ± 0.004	-1.602 ± 0.122	2.966 ± 0.127
SR0849	12.600 ± 0.700	0.477 ± 0.040	5.403 ± 0.035
SR0851	0.013 ± 0.008	-1.602 ± 0.122	2.884 ± 0.124
SR0852	0.071 ± 0.022	-2.301 ± 0.238	3.218 ± 0.046
SR0856	0.020 ± 0.005	-0.398 ± 0.262	3.081 ± 0.138
SR0858	0.022 ± 0.005	-1.602 ± 0.122	2.868 ± 0.101
SR0861	0.040 ± 0.004	-1.602 ± 0.122	3.618 ± 0.126
SR0863	7.940 ± 3.490	-2.301 ± 0.150	5.689 ± 0.022
SR0871	1.580 ± 0.295	-2.301 ± 0.150	4.846 ± 0.005
SR0875	12.600 ± 2.330	-1.155 ± 0.316	4.791 ± 0.082
SR0883	0.063 ± 0.022	-1.602 ± 0.122	3.159 ± 0.146
SR0889	7.080 ± 4.065	-2.301 ± 0.238	5.717 ± 0.020
SR0891	2.000 ± 0.230	0.477 ± 0.040	5.219 ± 0.095
SR0893	1.260 ± 0.145	-2.000 ± 0.301	4.213 ± 0.063
SR0895	0.282 ± 0.065	0.301 ± 0.539	3.872 ± 0.083
SR0902	3.980 ± 0.460	0.477 ± 0.040	4.654 ± 0.029
SR0904	11.200 ± 3.490	-2.301 ± 0.150	4.779 ± 0.055
SR0908	2.000 ± 0.465	-2.301 ± 0.150	4.102 ± 0.089
SR0912	10.000 ± 2.760	-2.000 ± 0.301	4.735 ± 0.029
SR0914	0.891 ± 0.244	-1.456 ± 0.412	3.631 ± 0.087
SR0919	0.020 ± 0.004	0.176 ± 0.238	3.315 ± 0.057
SR0930	0.100 ± 0.065	-1.602 ± 0.122	3.310 ± 0.145
SR0936	12.600 ± 1.300	0.000 ± 0.124	5.260 ± 0.109
SR0939	1.260 ± 0.205	-0.301 ± 0.301	4.441 ± 0.003
SR0940	4.470 ± 1.900	-1.699 ± 0.423	5.718 ± 0.016
SR0941	5.010 ± 1.765	-2.301 ± 0.150	5.073 ± 0.007
SR0946	0.100 ± 0.035	-2.000 ± 0.301	3.500 ± 0.043
SR0947	0.112 ± 0.031	-2.301 ± 0.150	3.446 ± 0.053
SR0953	0.891 ± 0.163	0.176 ± 0.150	4.699 ± 0.181
SR0955	0.025 ± 0.005	-0.699 ± 0.650	2.824 ± 0.065
SR0956	5.010 ± 1.765	-2.301 ± 0.150	4.952 ± 0.023
SR0960	0.036 ± 0.017	-1.000 ± 0.816	3.246 ± 0.094
SR0962	12.600 ± 0.700	0.477 ± 0.040	6.604 ± 0.048
SR0968	0.178 ± 0.056	0.477 ± 0.040	3.958 ± 0.078
SR0972	2.000 ± 0.780	-1.602 ± 0.122	4.675 ± 0.078
SR0980	2.000 ± 0.465	-0.824 ± 0.350	4.858 ± 0.184
SR0981	0.355 ± 0.215	-2.301 ± 0.238	4.165 ± 0.165
SR0983	0.004 ± 0.003	-1.602 ± 1.389	3.022 ± 0.058
SR0986	0.398 ± 0.157	-2.301 ± 0.150	4.898 ± 0.142
SM100	0.891 ± 0.314	-1.301 ± 0.389	3.510 ± 0.162
SM120	2.510 ± 0.410	-0.301 ± 0.850	4.388 ± 1.081
SM127	5.010 ± 1.765	-2.301 ± 0.238	4.812 ± 0.981
SM142	7.940 ± 2.790	-2.301 ± 0.150	4.800 ± 0.981
SM161	0.025 ± 0.003	-0.699 ± 0.111	2.975 ± 0.090
SM166	12.600 ± 0.700	0.477 ± 0.040	5.125 ± 0.121
SM182	8.910 ± 3.490	-1.824 ± 0.350	4.988 ± 0.189
SM189	0.501 ± 0.176	-0.301 ± 0.938	3.530 ± 0.837
SM193	7.080 ± 3.365	-2.301 ± 0.150	4.354 ± 0.891
SM196	12.600 ± 2.330	-1.699 ± 0.199	4.487 ± 0.180
SM204	0.028 ± 0.004	-0.301 ± 0.441	2.906 ± 0.109
SM207	0.562 ± 0.198	-1.000 ± 0.378	3.876 ± 0.209
SM208	4.470 ± 1.380	-2.301 ± 0.238	4.654 ± 0.215
SM210	0.040 ± 0.035	-0.523 ± 1.088	2.777 ± 0.200
SM212	12.600 ± 2.760	-2.301 ± 0.238	4.982 ± 0.188
SM217	0.022 ± 0.004	-0.699 ± 0.588	2.930 ± 0.146
SM233	12.600 ± 3.145	-1.824 ± 0.350	5.381 ± 0.216
SM236	0.708 ± 0.222	-1.699 ± 0.199	3.901 ± 0.151
SM238	1.260 ± 0.205	-0.523 ± 0.772	4.245 ± 0.466
SM240	1.000 ± 0.314	-2.000 ± 0.301	4.059 ± 0.175
SM254	0.141 ± 0.138	-1.000 ± 0.938	3.135 ± 0.271

TABLE 2 — *Continued*

Object	Age (Gyr)	[Fe/H] (dex)	$\log(M_{cl})$ $[M_\odot]$
SM256	0.158 ± 0.075	-1.699 ± 0.573	3.153 ± 0.295
SM266	8.910 ± 3.490	-1.824 ± 0.350	4.688 ± 0.190
SM279	12.600 ± 0.700	0.477 ± 0.040	6.038 ± 0.242
SM287	0.008 ± 0.001	0.301 ± 0.111	2.749 ± 0.088
SM292	2.820 ± 1.235	-2.000 ± 0.301	4.833 ± 0.225
SM293	0.016 ± 0.003	0.398 ± 0.088	2.527 ± 0.094
SM296	3.550 ± 1.690	-2.000 ± 0.301	4.702 ± 0.221
SM320	0.022 ± 0.004	0.000 ± 0.150	3.943 ± 0.123
SM342	0.112 ± 0.035	-2.301 ± 0.150	3.480 ± 0.160
SM361	0.282 ± 0.192	-1.699 ± 0.573	3.494 ± 0.274
SM393	0.501 ± 0.082	0.477 ± 0.088	3.765 ± 0.189
SM003	1.780 ± 0.330	-0.824 ± 0.350	3.929 ± 0.320
SM405	0.178 ± 0.062	-2.301 ± 0.238	3.378 ± 0.133
SM411	0.794 ± 0.146	0.000 ± 0.166	4.013 ± 0.134
SM412	8.910 ± 3.490	-2.301 ± 0.150	4.858 ± 0.171
SM419	8.910 ± 3.145	-1.456 ± 0.412	...
SM422	2.510 ± 0.410	0.477 ± 0.040	4.510 ± 0.125
SM452	1.260 ± 0.145	-1.699 ± 0.412	4.004 ± 0.598
SM468	3.160 ± 1.385	-2.301 ± 0.238	4.593 ± 0.175
SM469	2.510 ± 0.410	-0.301 ± 0.301	4.417 ± 0.425
SM485	0.891 ± 0.163	0.301 ± 0.150	3.726 ± 0.146
SM487	0.025 ± 0.005	-0.699 ± 0.111	2.485 ± 0.114
SM489	12.600 ± 1.845	-1.456 ± 0.301	4.901 ± 0.116
SM491	0.794 ± 0.245	-1.301 ± 0.316	3.582 ± 0.159
SM495	0.794 ± 0.185	0.000 ± 0.287	3.846 ± 0.218
SM506	0.316 ± 0.139	-0.699 ± 0.772	3.722 ± 0.181
SM514	11.200 ± 3.795	-2.301 ± 0.150	4.900 ± 0.154
SM517	3.550 ± 1.250	-0.071 ± 0.350	4.089 ± 0.444
SM518	1.120 ± 0.259	-2.000 ± 0.301	3.641 ± 0.146
SM519	0.355 ± 0.204	-2.301 ± 0.150	3.702 ± 0.118
SM520	1.780 ± 0.415	-0.022 ± 0.287	3.989 ± 0.178
SM521	11.200 ± 2.760	-1.301 ± 0.301	4.878 ± 0.141
SM522	0.018 ± 0.003	-2.301 ± 0.350	2.467 ± 0.103
SM527	2.510 ± 0.990	-2.301 ± 0.150	4.392 ± 0.248
SM529	3.160 ± 1.115	-2.301 ± 0.150	4.378 ± 0.153
SM535	0.251 ± 0.145	-1.699 ± 0.199	3.419 ± 0.164
SM536	0.022 ± 0.004	-0.699 ± 0.111	2.763 ± 0.139
SM540	2.820 ± 0.460	0.000 ± 0.166	4.484 ± 0.126
SM542	12.600 ± 1.300	0.477 ± 0.040	4.974 ± 0.192
SM546	3.550 ± 1.745	0.000 ± 0.213	4.861 ± 0.413
SM549	0.028 ± 0.012	0.000 ± 0.889	2.652 ± 0.180
SM552	1.780 ± 0.295	0.477 ± 0.088	4.016 ± 0.131
SM554	2.510 ± 0.990	-2.301 ± 0.238	4.423 ± 0.250
SM557	0.316 ± 0.202	-1.301 ± 0.389	4.092 ± 0.302
SM559	0.631 ± 0.146	0.398 ± 0.150	3.990 ± 0.177
SM561	0.631 ± 0.301	-2.301 ± 0.238	3.584 ± 0.168
SM562	0.025 ± 0.004	-0.699 ± 0.111	2.604 ± 0.101
SM569	6.310 ± 2.220	-2.301 ± 0.150	4.462 ± 0.127
SM574	0.501 ± 0.116	0.176 ± 0.199	4.056 ± 0.128
SM575	2.510 ± 0.990	-2.301 ± 0.150	4.337 ± 0.246
SM577	0.631 ± 0.146	0.301 ± 0.238	3.318 ± 0.159
SM578	0.562 ± 0.104	0.176 ± 0.199	3.352 ± 0.110
SM579	1.000 ± 0.233	-2.000 ± 0.238	3.705 ± 0.140
SM583	11.200 ± 3.795	0.477 ± 0.088	...
SM586	0.022 ± 0.005	-1.155 ± 0.228	3.154 ± 0.112
SM591	0.025 ± 0.004	-0.699 ± 0.111	2.801 ± 0.101
SM592	2.510 ± 0.775	-2.301 ± 0.150	4.371 ± 0.213
SM593	1.000 ± 0.233	-0.071 ± 0.287	4.087 ± 0.272
SM595	1.780 ± 0.550	-2.000 ± 0.350	4.173 ± 0.140
SM597	7.080 ± 4.065	-2.301 ± 0.150	4.797 ± 0.168
SM061	11.200 ± 3.145	-1.824 ± 0.350	5.120 ± 0.144
SM071	2.820 ± 0.460	-0.155 ± 0.262	4.735 ± 0.163
SM076	0.020 ± 0.004	0.176 ± 0.238	2.503 ± 0.098
SM083	1.580 ± 0.295	-2.301 ± 0.150	4.158 ± 0.115
SM088	2.820 ± 0.870	-2.301 ± 0.238	4.482 ± 0.153